

**OPTIMUM DESIGN OF CARBON/EPOXY  
COMPOSITE LAMINATES FOR MAXIMUM  
FATIGUE LIFE USING MULTIAXIAL  
PREDICTION MODELS**

**A Thesis Submitted to  
the Graduate School of Engineering and Sciences of  
İzmir Institute of Technology  
in Partial Fulfillment of the Requirements for the Degree of**

**DOCTOR OF PHILOSOPHY**

**in Mechanical Engineering**

**by  
Hamza Arda DEVECİ**

**December 2017  
İZMİR**

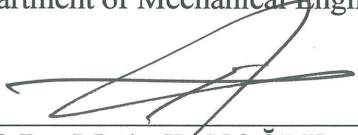
We approve the thesis of **Hamza Arda DEVECİ**

**Examining Committee Members:**



**Assoc. Prof. Dr. H. Seçil ARTEM**

Department of Mechanical Engineering, İzmir Institute of Technology



**Prof. Dr. Metin TANOĞLU**

Department of Mechanical Engineering, İzmir Institute of Technology



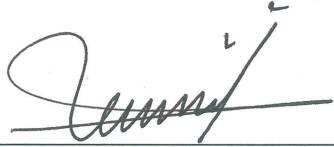
**Prof. Dr. Ramazan KARAKUZU**

Department of Mechanical Engineering, Dokuz Eylül University



**Prof. Dr. Alper TAŞDEMİRCİ**

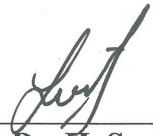
Department of Mechanical Engineering, İzmir Institute of Technology



**Asst. Prof. Dr. Levent AYDIN**

Department of Mechanical Engineering, İzmir Katip Çelebi University

**27 December 2017**



**Assoc. Prof. Dr. H. Seçil ARTEM**

Supervisor, Department of Mechanical Engineering, İzmir Institute of Technology



**Prof. Dr. Metin TANOĞLU**

Head of the Department of Mechanical Engineering

**Prof. Dr. Aysun SOFUOĞLU**

Dean of the Graduate School of Engineering and Sciences

## ACKNOWLEDGMENTS

Firstly, I would like to express my sincere gratitude to my supervisor Assoc. Prof. Dr. H. Seil ARTEM for her advises, guidance, support, encouragement, and inspiration through the thesis. Her patience and kindness are greatly appreciated. I have been fortunate to have her as my advisor and I consider it an honor working with. Also, I need to acknowledge my sincere gratitude to my PhD Thesis Committee and Jury Members, Prof. Dr. Metin TANOĐLU, Prof. Dr. Ramazan KARAKUZU and Prof. Dr. Alper TAŐDEMİRCİ for sharing their experience and knowledge with me.

I would like to thank Asst. Prof. Dr. Levent AYDIN for his “complementary” guidance, support and encouragement, which made my dissertation a better work.

I would like to thank my friends and colleagues; Serkan KANGAL, Kaya MANOĐLU, Mehmet Deniz GÜNEŐ, Bertan BEYLERGİL, Osman KARTAV, Ziya OKUR, Sinan ÜSTÜN and Nahit ÖZTOPRAK for their support whenever I needed.

I especially want to thank my dear friends; Aydın CİHANOĐLU and Gizem CİHANOĐLU for their encouragement and support from the beginning of my career.

I also would like to thank to Serdar GÜMÜŐOĐLU, Ayta AKALAN and Mehmet Umut SÖYLEYİCİ for making PhD easier to me.

Lastly, I would like to thank my dear family for their never-ending love, motivation and support throughout my PhD period.

# **ABSTRACT**

## **OPTIMUM DESIGN OF CARBON/EPOXY COMPOSITE LAMINATES FOR MAXIMUM FATIGUE LIFE USING MULTIAXIAL PREDICTION MODELS**

In this thesis study, the aim is to propose a methodology on the optimum stacking sequence design of carbon/epoxy composite laminates under various cyclic loading conditions for maximum fatigue life. In this respect, first, fatigue life prediction models, Failure Tensor Polynomial in Fatigue (FTPF), Fawaz-Ellyin (FWE), Sims-Brogdon (SB) and Shokrieh-Taheri (ST) are selected to investigate their prediction capabilities in multidirectional laminates and optimization capabilities in laminate design for maximum fatigue life. An experimental correlation study is performed for different multidirectional composite materials to evaluate the prediction capability of the models by comparing to each other. The predictions of the models give accurate and close results for all the composites in many lay-up configurations. Then, the optimum designs for maximum fatigue life are obtained for glass/epoxy composite laminate from the literature using different powerful hybrid algorithms to determine the optimization capability of the models. The results of the optimization imply that FTPF and SB models produce more consistent fatigue-resistant designs than FWE and ST models. After obtaining reasonable theoretical derivations, the methodology for fatigue-resistant design is applied to carbon/epoxy composite laminates under proper cyclic loading conditions. For this, first, quasi-static and fatigue strength properties of the carbon/epoxy laminates are determined by experimental procedure. Then, many problems including different design cases are solved using the FTPF model and hybrid PSA-GPSA algorithm, and multidirectional laminate designs with maximum fatigue life are determined. The results show that fatigue strength of the composite laminates can be seriously increased by appropriate stacking sequence designs.

## ÖZET

### KARBON/EPOKSİ KOMPOZİT PLAKALARIN ÇOK EKSENLİ TAHMİN MODELLERİ KULLANILARAK MAKSİMUM YORULMA ÖMRÜ İÇİN OPTİMUM TASARIMI

Bu tez çalışmasında amaç, maksimum yorulma ömrü için çeşitli çevrimsel yükleme koşulları altında karbon/epoksi kompozit plakaların optimum fiber açılı dizilim tasarımları üzerine bir metodoloji önermektir. Bu bağlamda, ilk olarak, yorulma ömrü tahmini modelleri, FTPF, FWE, SB ve ST, çok yönlü plakalarda tahmin yeteneklerini ve maksimum yorulma ömrü için plaka tasarımında optimizasyon olanaklarını araştırmak amacıyla seçilmiştir. Farklı çok yönlü kompozit malzemeler için deneysel bir korelasyon çalışması yapılarak modellerin tahmin yetenekleri birbirleriyle karşılaştırılarak değerlendirilmiştir. Modellerin tahminleri, birçok dizilim konfigürasyonunda ve kompozit malzemelerin hepsi için doğru ve yakın sonuçlar vermiştir. Daha sonra, modellerin optimizasyon özelliklerini belirlemek üzere maksimum yorulma ömrü için optimum tasarımlar, literatürden cam/epoksi kompozit plaka için güçlü melez algoritmalar kullanarak elde edilmiştir. Optimizasyonun sonuçları, FTPF ve SB modellerinin, FWE ve ST modellerinden daha tutarlı yorulmaya dayanıklı tasarımlar üretebildiğini göstermiştir. Makul teorik sonuçlar elde ettikten sonra, yorulmaya dayanıklı tasarım metodolojisi karbon/epoksi kompozit plakalara uygun çevrimsel yükleme koşulları altında uygulanmıştır. Bunun için önce karbon/epoksi plakaların yarıstatik ve yorulma mukavemeti özellikleri deney prosedürü ile belirlenmiştir. Sonra, FTPF modeli ve melez PSA-GPSA algoritması kullanılarak farklı tasarım durumları içeren pek çok problem çözülmüş ve maksimum yorulma ömrüne sahip çok yönlü plaka tasarımları belirlenmiştir. Sonuçlar, kompozit plakaların yorulma dayanımının uygun fiber açılı dizilimi tasarımlarıyla ciddi bir şekilde artırılabilirliğini göstermektedir.

# TABLE OF CONTENTS

LIST OF FIGURES .....	ix
LIST OF TABLES.....	xi
CHAPTER 1. INTRODUCTION .....	1
1.1. Literature Survey .....	2
1.2. Motivation.....	4
1.3. The Aim of the Study.....	5
1.4. Contributions to the Literature.....	6
CHAPTER 2. COMPOSITE MATERIALS.....	8
2.1. Introduction.....	8
2.2. Classification of Composites .....	10
2.2.1. Polymer Matrix Composites.....	11
2.2.2. Metal Matrix Composites .....	14
2.2.3. Ceramic Matrix Composites.....	15
2.2.4. Carbon - Carbon Composites .....	16
2.3. Common Applications of Composite Materials .....	17
2.4. Mechanics of Composite Materials .....	19
2.4.1. Classical Lamination Theory.....	19
CHAPTER 3. FATIGUE OF FIBER-REINFORCED POLYMER COMPOSITES .....	25
3.1. Introduction.....	25
3.2. Fatigue Test of Composite Materials .....	26
3.2.1. Fundamental Fatigue Terminology .....	28
3.2.2. Fatigue Data Processing .....	30
3.3. Fatigue Life Prediction of Composite Materials.....	32
CHAPTER 4. FATIGUE LIFE PREDICTION MODELS .....	35
4.1. Hashin-Rotem (HR) Model.....	35
4.2. Failure Tensor Polynomial in Fatigue (FTPF) Model .....	37

4.3. Fawaz-Ellyin (FWE) Model .....	39
4.4. Sims-Brogdon (SB) Model .....	41
4.5. Shokrieh-Taheri (ST) Model.....	41
<b>CHAPTER 5. EXPERIMENTAL CORRELATION .....</b>	<b>44</b>
5.1. Off-Axis Angle Predictions .....	45
5.2. Multidirectional Laminate Predictions for Various Materials .....	48
5.2.1. Graphite/Epoxy Composite Laminates.....	48
5.2.2. Carbon/Epoxy Composite Laminates.....	50
5.2.3. E-glass/Epoxy Composite Laminates.....	52
5.2.4. Carbon/PEEK Composite Laminates .....	54
<b>CHAPTER 6. OPTIMIZATION.....</b>	<b>57</b>
6.1. Introduction.....	57
6.2. Basic Definition of an Optimization Problem .....	60
6.3. Metaheuristic Algorithms .....	61
6.3.1. Single Algorithms.....	61
6.3.2. Hybrid Algorithms.....	61
6.4. GA-GPSA Hybrid Algorithm .....	62
6.4.1. Algorithm Performance .....	66
6.5. PSA - GPSA Hybrid Algorithm.....	67
6.5.1. Algorithm Performance .....	70
<b>CHAPTER 7. FATIGUE LIFE MAXIMIZATION .....</b>	<b>72</b>
7.1. Fatigue Life Maximization using FTPF Model .....	72
7.1.1. Problem Definition .....	72
7.1.1.1. Formulation of the Objective Function.....	73
7.1.2. Optimization Problems and Results .....	74
7.2. Fatigue Life Maximization using Different Models .....	80
7.2.1. Validation of the Proposed Fatigue Optimization Strategy.....	80
7.2.2. Optimization Problems and Results .....	83
<b>CHAPTER 8. EXPERIMENTAL STUDIES .....</b>	<b>92</b>
8.1. Background.....	92

8.2. Liquid Composite Molding Processes .....	93
8.2.1. Resin Transfer Molding (RTM) .....	94
8.3. Material Characterization of the Carbon/Epoxy Composites .....	96
8.3.1. Quasi-static Mechanical Properties .....	97
8.3.2. Fatigue Strength Properties .....	101
 CHAPTER 9. OPTIMUM FATIGUE-RESISTANT DESIGN OF CARBON/EPOXY COMPOSITE LAMINATES .....	 104
9.1. Problem Definition.....	104
9.2. Fatigue Optimization and Results.....	106
 CHAPTER 10. CONCLUSION .....	 117
 REFERENCES .....	 120
 APPENDICES	
APPENDIX A. MATLAB PROGRAM CODE FOR EXPERIMENTAL CORRELATION .....	 124
APPENDIX B. MATLAB PROGRAM CODE FOR OPTIMIZATION .....	133



# LIST OF FIGURES

<u>Figure</u>	<u>Page</u>
Figure 2.1. Specific strength as a function of time of use of materials .....	9
Figure 2.2. Types of composites based on reinforcement shape .....	11
Figure 2.3. Comparison of performance of several common matrices used in polymer matrix composites.....	13
Figure 2.4. Stealth aircraft .....	18
Figure 2.5. Use of fiber-reinforced polymer composites in Airbus 380.....	18
Figure 2.6. A thin fiber-reinforced laminated composite subjected to in-plane loading.....	20
Figure 2.7. Coordinate locations of plies in a laminate .....	20
Figure 2.8. Resultant forces (a) and moments (b) on a laminate .....	22
Figure 3.1. Example specimen geometry and stacking sequence.....	27
Figure 3.2. Basic fatigue terminology .....	28
Figure 3.3. Representative constant amplitude loading patterns .....	29
Figure 3.4. Example of an irregular fatigue time series.....	29
Figure 3.5. Schematic representation of S-N curve derivation.....	31
Figure 3.6. Application of different S-N curve formulations for a multidirectional glass/epoxy laminate with a stacking sequence $[(\pm 45 / 0)_4 / \pm 45]$ .....	33
Figure 4. 1. Representative plate geometry showing in-plane cyclic loading and principal coordinates.....	38
Figure 5.1. Predicted S-N curves for 5° off-axis angle .....	45
Figure 5.2. Predicted S-N curves for 10° off-axis angle.....	46
Figure 5.3. Predicted S-N curves for 20° off-axis angle.....	46
Figure 5.4. Predicted S-N curves for 30° off-axis angle.....	47
Figure 5.5. Predicted S-N curves for 60° off-axis angle.....	47
Figure 5.6. Fatigue life predictions for $[0 / 90]_{4s}$ graphite/epoxy laminate .....	49
Figure 5.7. Fatigue life predictions for $[0 / 45 / - 45 / 90]_{2s}$ graphite/epoxy laminate.....	49
Figure 5.8. Fatigue life predictions for $[0 / 90_2]_s$ carbon/epoxy laminate .....	50
Figure 5. 9. Fatigue life predictions for $[0 / 90_4]_s$ carbon/epoxy laminate .....	51
Figure 5.10. Fatigue life predictions for $[0_2 / 90_2]_s$ carbon/epoxy laminate .....	51

Figure 5.11. Fatigue life predictions for $[0/45/-45/90]_s$ carbon/epoxy laminate .....	52
Figure 5.12. Fatigue life predictions for $[0/90/90/0]_s$ E-glass/epoxy laminate .....	53
Figure 5.13. Fatigue life predictions for $[45/90/-45/0]_s$ E-glass/epoxy laminate .....	53
Figure 5.14. Fatigue life predictions for $[45/0/0/-45]_s$ E-glass/epoxy laminate .....	54
Figure 5.15. Fatigue life predictions for $[0/90]_{4s}$ carbon/PEEK laminate .....	55
Figure 5.16. Fatigue life predictions for $[0/45/90/-45]_{2s}$ carbon/PEEK laminate .....	55
Figure 6.1. Minimum and maximum of an objective function ( $f(x)$ ) .....	58
Figure 6.2. Flowchart of the hybrid GA-GPSA optimization.....	65
Figure 6.3. Flowchart of the hybrid PSA-GPSA optimization.....	68
Figure 8.1. General representation of the LCM process .....	93
Figure 8.2. Vacuum-assisted resin transfer molding (VARTM) .....	95
Figure 8.3. VARTM process application in the laboratory .....	96
Figure 8.4. Shimadzu AG1 250 kN mechanical testing machine.....	98
Figure 8.5. Specimen geometry and dimensions for longitudinal properties in test .....	98
Figure 8.6. Specimen geometry and dimensions for transverse properties in test.....	98
Figure 8.7. Specimen geometry and dimensions for shear properties in test .....	99
Figure 8.8. The specimen for Poisson's ratio test.....	99
Figure 8.9. The representation of the Poisson's ratio test.....	100
Figure 8.10. Fatigue test specimens for the (a) $[0_4]$ , (b) $[90_6]$ and (c) $[\pm 45]_{2s}$ laminates.....	101
Figure 8.11. S-N curve of the $[0_4]$ laminate .....	102
Figure 8.12. S-N curve of the $[90_6]$ laminate.....	102
Figure 8.13. S-N curve of the $[\pm 45]_{2s}$ laminate .....	103

## LIST OF TABLES

<b><u>Table</u></b>	<b><u>Page</u></b>
Table 2.1. Specific modulus and specific strength of typical fibers, composites, and bulk metals.....	10
Table 2.2. Differences between thermosets and thermoplastics .....	14
Table 2.3. Typical properties of metal matrix composites .....	15
Table 2.4. Typical mechanical properties of some ceramic matrix composites .....	16
Table 2.5. Typical mechanical properties of carbon - carbon matrix composites .....	17
Table 3.1. Number of specimens required for standard fatigue test.....	27
Table 6.1. Methods of operations research .....	58
Table 6.2. Load cases for test problem .....	66
Table 6.3. Performance results of the GA-GPSA hybrid algorithm.....	66
Table 6.4. Performance results of the PSA-GPSA hybrid algorithm .....	70
Table 7.1. Properties of the laminates used in the study [5] .....	72
Table 7.2. Fatigue life prediction and optimization using different experimental data from the literature .....	75
Table 7.3. Optimum stacking sequence designs and the corresponding fatigue lives for various in-plane tension cyclic loads .....	76
Table 7.4. Optimum stacking sequence designs and the corresponding fatigue lives for various in-plane tension and shear cyclic loads .....	77
Table 7.5. Optimum stacking sequence designs and the corresponding fatigue lives for various in-plane tension and compression cyclic loads .....	77
Table 7.6. Comparison of conventional (Con.) and non-conventional (Non-con.) fiber angle optimizations for various in-plane cyclic loadings .....	78
Table 7.7. Fatigue life prediction and optimization using different models for various experimental data.....	82
Table 7.8. Properties of the laminates used in the study [5].....	83
Table 7.9. Optimum stacking sequence designs and the corresponding fatigue lives for various in-plane tension cyclic loads .....	85
Table 7.10. Optimum stacking sequence designs and the corresponding fatigue lives for various in-plane tension-compression cyclic loads .....	86

Table 7.11. Optimum stacking sequence designs and the corresponding fatigue lives for various in-plane tension and shear cyclic loads.....	87
Table 7.12. Optimum stacking sequence designs and the corresponding fatigue lives for various in-plane tension-compression-shear cyclic loads.....	89
Table 8.1. Quasi-static material properties of carbon/epoxy composite .....	101
Table 9.1. Properties of the carbon/epoxy composite .....	104
Table 9.2. Performance results of the PSA-GPSA algorithm in fatigue optimization .	106
Table 9.3. Optimum 8-ply design results for various in-plane tension cyclic loads.....	107
Table 9.4. Optimum 8-ply design results for various in-plane tension and compression cyclic loads.....	108
Table 9.5. Optimum 8-ply design results for various in-plane tension, compression and shear cyclic loads .....	108
Table 9.6. Optimum 16-ply design results for various in-plane tension cyclic loads...	109
Table 9.7. Optimum 16-ply design results for various in-plane tension and compression cyclic loads.....	110
Table 9.8. Optimum 16-ply design results for various in-plane tension, compression and shear cyclic loads .....	110
Table 9.9. Optimum 32-ply stacking sequence design results for various in-plane cyclic loads .....	112
Table 9.10. Optimum 8-ply design results with 5° incremental fiber angles for the low fatigue life cases .....	113
Table 9.11. Optimum 16-ply stacking sequence design results with 5° incremental fiber angles for the low fatigue life cases .....	114
Table 9.12. Optimum 32-ply stacking sequence design results with 5° incremental fiber angles for the low fatigue life cases .....	115

# CHAPTER 1

## INTRODUCTION

In general terms, a composite is a structural material that comprises of two or more components that are combined at macroscopic level and are not soluble in each other. One of the components is called the reinforcement and the other component in which the reinforcement is embedded is called the matrix. The reinforcement material may be in the form of fibers, particles, or flakes. The matrix materials are usually in continuous nature. Concrete reinforced with steel and epoxy reinforced with glass fibers, etc. are some of the most known examples of composite systems [1]. Among several composite forms, fiber reinforced composites are the most used materials for decades in the industrial applications. Many fiber reinforced materials enable a better combination of strength and modulus as compared with many traditional metallic materials. Due to their properties such as low density, high strength-weight ratio, modulus-weight ratio, corrosion resistance and high durability, fiber reinforced composite materials are significantly superior to metallic materials. Accordingly, fiber reinforced materials have become a major class of structural materials and began to be considered in use more than metals in many weight-critical components in the industries such as aerospace, automotive and marine [2]. Besides the inherent advantages of composites, the nature of fiber-reinforced composites enables the unique opportunity of tailoring their properties according to design requirements for a given application. The full potential of laminated composite plates can be achieved by searching the optimum stacking sequence designs.

Composite materials are designated as being fatigue-insensitive, especially when compared to metallic materials. However, they are also affected from fatigue loads. Composite materials are used in a wide range of applications. This situation obliged researchers and engineers to consider fatigue as a critical failure mode while investigating a composite material and to realize that fatigue is an important parameter that must be considered in calculations during design processes. Fatigue damage is especially an important issue to be considered in composite structures subjected to complex multiaxial stress states during service. Therefore, fatigue requires durability investigation and

special lay-up design in the composite structure components that must bear significant cyclic fatigue loads during operation, such as airplanes and wind turbine rotor blades [3].

## 1.1. Literature Survey

In order to maximize the fatigue life of a composite laminate, first, it should be able to calculate the fatigue life of this composite laminate accurately for any arbitrary lay-up configuration. This requires a reliable fatigue life prediction model.

Numerous fatigue theories and methodologies have been developed so far to investigate the fatigue behavior of composite materials and structures. The fatigue life prediction models in the literature can be classified into five categories: empirical, phenomenological modelling; specific damage metrics such as the residual strength and/or stiffness of the examined material; probabilistic; artificial neural network based; and micromechanics. Moreover, the investigation of fatigue behavior of composite structures under multiaxial loadings is more important for the applications subjected to real complex loading conditions as the fatigue damage under uniaxial loading has been clarified in many studies [4]. Among these models, only some of them are suitable to address the problem of fatigue life prediction of composite materials under multiaxial stress states. In this respect, it is reported that empirical models which estimate the fatigue life due to constant amplitude loading based on experimental data without making any assumption regarding the micro mechanisms leading to fatigue failure have also practical application potential in fatigue design of composite structures [3].

Hashin and Rotem [5] presented a fatigue life prediction model based on the different failure modes for unidirectional materials considering the fiber and matrix failure modes independently. The authors then reported that an interlaminar failure mode is encountered when multidirectional composite laminates are considered [6]. Sims and Brogdon [7] proposed a model modified the Tsai-Hill failure criterion to a fatigue criterion by replacing the static strengths with the corresponding fatigue strengths taking the number of cycles to failure into consideration. This was the first attempt to use a static failure criterion to constitute a fatigue failure criterion. Similarly, Fawaz and Ellyin [8] proposed a multiaxial fatigue life prediction model based on Tsai-Hill static strength failure criterion. The model requires only an experimental S-N curve of a reference off-axis specimen to make estimations. They showed that the model accurately predicts

fatigue failure of different unidirectional and bidirectional fiber reinforced composite materials subjected to uniaxial and multiaxial stresses and different cyclic stress ratios. Philippidis and Vassilopoulos [9] introduced a model which is an extension of the quadratic version of the Failure Tensor Polynomial for the prediction of fatigue life under complex stress states. It is reported that the model yields reliable predictions for both unidirectional and multidirectional laminated composites when compared to experimental data, and can be used in design of composite structures subjected to multiaxial fatigue loadings. Kawai [10] developed a phenomenological fatigue damage mechanics based model that could take into account the off-axis angle and stress ratio effect under any constant amplitude loading with non-negative mean stresses in order to predict the off-axis fatigue behavior of unidirectional composites. It is shown that the model is capable of adequately predicting the off-axis behavior over a range of non-negative mean stresses. Shokrieh and Taheri-Behrooz [11] developed a model based on strain energy method and Sandhu static failure criterion for predicting fatigue life of unidirectional composite laminates in various fiber orientation angles.

In the optimization point of view, composite materials provide great design possibility by allowing material tailoring to meet preferred design requirements. Fatigue strength is one of the most important requirements to ensure in composite laminate design. This can be possible through an optimum selection of fiber orientations in a laminate. Nevertheless, there are few published studies on the optimum design of laminated composites for maximum fatigue life [12-16]. As the first attempt in this area, Adali [12] introduced a study to obtain the optimum symmetric angle-ply laminate under in-plane tensile fatigue loads for maximum failure load by employing a fatigue failure criterion, and determined optimum fiber orientations, thickness ratio and fiber content for constant cyclic lives. Then, Walker [13] proposed a procedure to minimize the thickness of laminated composite plates subjected to cyclic bending loads for specific fatigue lives under a cumulative damage constraint. In these earlier studies on fatigue design optimization, the researchers used fatigue models that were valid only for limited laminate configurations and specific loading conditions. Essentially, more general stacking sequences and loading conditions are supposed to be considered in design optimization for typical applications. In this regard, Ertas and Sonmez [14] showed in their study that the optimum designs of laminated composite plates under in-plane cyclic loading for maximum fatigue life can theoretically be obtained for more general stacking sequences using Fawaz-Ellyin model. Muc and Wierzgoń [15] proposed a design

methodology to find the optimum stacking sequences having three different fiber orientations for maximum buckling load of composite plates by introducing a new type of discrete design variables. Recently, Deveci and Artem have presented a design methodology to investigate optimum multidirectional stacking sequence design of laminated composites under various in-plane cyclic loads for maximum fatigue life by using another model, Failure Tensor Polynomial in Fatigue model [16].

## 1.2. Motivation

It is clear that long fatigue life has increasingly become a structural requirement for composite materials in typical applications such as aircraft components, wind turbine blades and helicopter rotor blades to provide dynamic control and stability. Also, it has started to be understood that the fatigue failure is very critical. The importance of fatigue for composite materials and/or structures can be listed as:

- The use of composites in the structures that must bear significant fatigue loads during operation, such as airplanes, wind turbine rotor blades, boats, bridges etc. provides to experience the sensitivity of each structure to fatigue.
- Unidirectional fiber-reinforced composites are brittle and behave linearly under loading. The failure of them comes sudden without any prior notice. Therefore, to understand their fatigue behavior and prediction of their fatigue life are very important.
- The understanding and prediction of fatigue behavior of composite materials are also significant for the product development procedure improvement. Previous product development practice was mostly based on an iterative process in which a prototype was produced and tested under realistic loading patterns. However, this process is costly and takes much time. The fatigue life prediction ability of composite materials or structures reduces the cost and allows a product development in a wider range without any need for increasing the number of physical prototypes.
- The critical effect of cyclic loads on durability may be disregarded when it is evaluated based on static strength calculations. The introduction of fatigue life prediction methods into durability simulation procedures allows the assessment



of durability performance early in the product development process and the establishment of clear recommendations for guiding major design choices.

Besides these important points about fatigue phenomena, the motivation of this PhD thesis can be summarized as

- In the last few decades, fiber-reinforced composite materials are increasingly demanded by the industry due to their advantageous properties such as high stiffness, high strength and lightweight.
- The anisotropic nature of composites provides engineers the opportunity of structure tailoring according to design requirements.
- 50 to 90 percent of the general material failures are caused by fatigue.
- Since mechanical components, especially in the structures such as airplanes, wind turbine blades, leisure boats, bridges etc. usually experience cyclic loading during their operation, fatigue failure prevention is the most crucial design requirement.
- Fatigue life of a laminated composite structure and thus its durability can be significantly increased by an optimal selection of several parameters such as fiber and matrix materials, fiber orientations, stacking sequence, and lamina thickness.
- There are not adequate number of researches in the literature on the optimum design of laminated composites to extend the fatigue life, and very few of them support the realistic multidirectional laminate design.

### **1.3. The Aim of the Study**

The main objective of this PhD study is to obtain optimum stacking sequence designs of balanced-symmetric carbon/epoxy composite laminates under various loading conditions for maximum fatigue life.

In this manner, firstly in the thesis study, multidirectional laminate design methodology for maximum fatigue life is applied on glass/epoxy composite material from the literature using the “Failure Tensor Polynomial in Fatigue” prediction model in order to test the accuracy of the methodology. A powerful hybrid algorithm is used to solve the optimization problems for several design cases with different loading conditions. Secondly, using the same composite material, fatigue life prediction models, “Failure

Tensor Polynomial in Fatigue”, “Fawaz-Ellyin”, “Sims-Brogdon” and “Shokrieh-Taheri” are selected to investigate their prediction capabilities in multidirectional laminates and optimization capabilities in laminate design for maximum fatigue life. A comprehensive experimental correlation is performed for different multidirectional composite materials to evaluate the prediction capabilities of the models by comparing to each other. Each model is used to constitute the objective function of its own, and a different hybrid algorithm is used in the optimization process. Before the optimization, the effective performance of the proposed hybrid algorithm is shown by comparative results using a test problem with different design cases from the literature. A pre-optimization study is then performed to justify the theoretical derivation procedure to be followed using experimental data from the literature. After these investigations, a number of problems including many design cases are solved for each model separately and the optimum results are presented to discuss.

As the concluding and essential part of the thesis study, the Failure Tensor Polynomial in Fatigue (Philippidis and Vassilopoulos [9]) is selected as the fatigue life prediction model and it is applied to the optimum stacking sequence design of carbon/epoxy composite laminates under various in-plane cyclic loadings to obtain maximum fatigue life. Before the optimization, quasi-static and fatigue strength properties of the carbon/epoxy laminates are determined by experimental procedure to define in the model. The hybrid algorithm combining particle swarm and generalized patterns search algorithms is selected to use as search algorithm in the optimization. A number of problems including different design cases are solved, and the multidirectional laminate designs with maximum fatigue life are determined.

#### **1.4. Contributions to the Literature**

In the literature, as known, there are many studies dealing with the derivation of fatigue life prediction models and their applications for fiber-reinforced composite laminates. However, except few studies [3,4,17] the literature is deficient in studies considering the fatigue life prediction models together to make an evaluation about their estimation capabilities on multidirectional laminates. Moreover, few studies [12-16] have conducted on the optimization of composites for fatigue life maximization. In this regard, our study fulfils this gap in the literature and reveals the potential of the selected suitable

models for modeling and improvement of fatigue life of laminated composites. This is the first contribution of my thesis study to the literature.

The second contribution of this thesis study to the literature is the application of the proposed fatigue-resistant composite design methodology on carbon/epoxy composite laminates. This design practice does not require many fatigue tests to determine the best fiber lay-up configuration for a given loading condition. Such a study, which offers the opportunity of the optimum composite laminate design for maximum fatigue strength with low experimental cost, is the first attempt in the literature.

## CHAPTER 2

### COMPOSITE MATERIALS

#### 2.1. Introduction

The combining of materials to create a new material system with improved material properties was continually practiced in history. For instance, the ancient Egyptian workers included chopped straw in bricks during the construction of pyramids with the intent of improving their structural integrity. The Japanese Samurai warriors used laminated metals in the forging of their swords to provide desirable material properties. More recently, in the 20th century civil engineers put construction iron into cement and produced a well-known composite material, i.e., reinforced concrete. It can easily be said that the modern times of composite materials began with fiberglass polymer matrix composites during World War II [18].

In general terms, a composite is a structural material that comprises of two or more components that are combined at macroscopic level and are not soluble in each other. One of the components is called the reinforcement and the other one in which it is embedded is called the matrix. The reinforcement material may be in the form of fibers, particles, or flakes. The matrix materials are usually in continuous nature. Concrete reinforced with steel and epoxy reinforced with glass fibers, etc. are some of the principal examples of composite systems [1].

Many fiber-reinforced materials enable a better combination of strength and modulus as compared with many traditional metallic materials. Due to their low density, high strength-weight and modulus-weight ratios, these composite materials are significantly superior to those of metallic materials. Furthermore, fatigue strength as well as fatigue damage tolerance of many laminated composites are pretty good. Therefore, fiber reinforced materials have come up as a major class of structural materials and they are preferred instead of metals in many weight-critical components in aerospace, automotive, and other industries [2].

Figure 2.1 shows the comparison of composites and fibers with the other traditional materials in terms of specific strength on yearly basis.

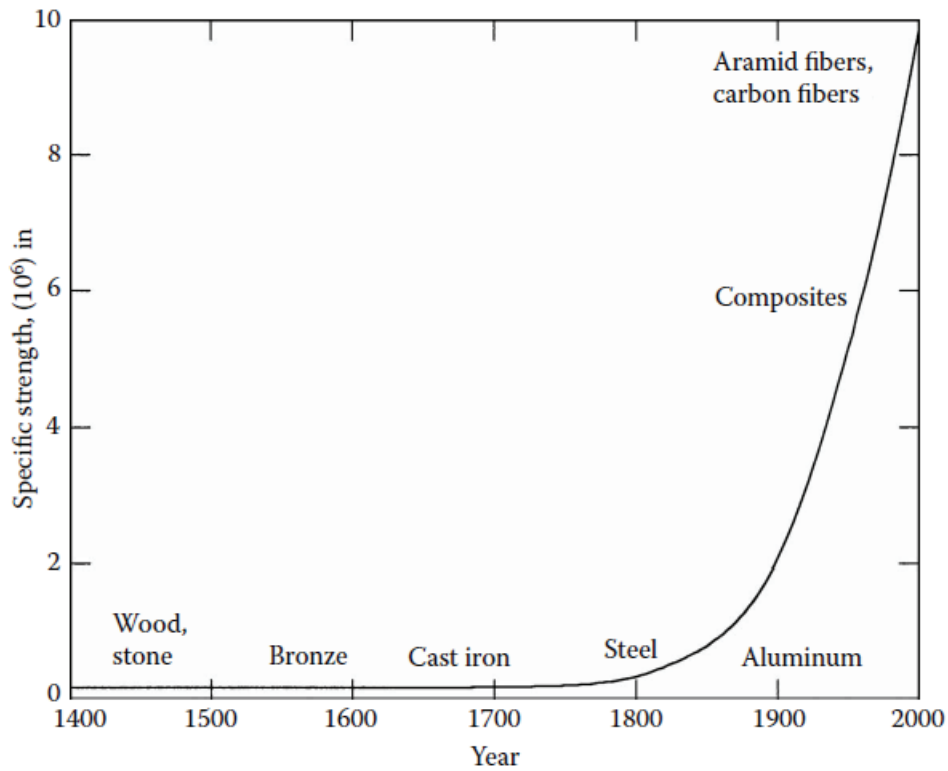


Figure 2.1. Specific strength as a function of time of use of materials  
(Source: Kaw, 2006)

It is seen from the figure that composites reinforced with the fibers such as carbon and aramid fibers show so much greater specific strength than the traditional materials as iron, steel and aluminum have.

Specific modulus and specific strength properties for commonly used composite fibers, unidirectional composites, cross-ply and quasi-isotropic laminated composites and monolithic metals are given in Table 2.1 [1].

Table 2.1. Specific modulus and specific strength of typical fibers, composites, and bulk metals (Source: Kaw, 2006)

Material	Specific gravity	Young's modulus (GPa)	Ultimate strength (MPa)	Specific modulus (GPa-m <sup>3</sup> /kg)	Specific strength (MPa-m <sup>3</sup> /kg)
Graphite fiber	1.8	230.00	2067	0.1278	1.148
Aramid fiber	1.4	124.00	1379	0.08857	0.9850
Glass fiber	2.5	85.00	1550	0.0340	0.6200
Unidirectional graphite/epoxy	1.6	181.00	1500	0.1131	0.9377
Unidirectional glass/epoxy	1.8	38.60	1062	0.02144	0.5900
Cross-ply graphite/epoxy	1.6	95.98	373.0	0.06000	0.2331
Cross-ply glass/epoxy	1.8	23.58	88.25	0.01310	0.0490
Quasi-isotropic graphite/epoxy	1.6	69.64	276.48	0.04353	0.1728
Quasi-isotropic glass/epoxy	1.8	18.96	73.08	0.01053	0.0406
Steel	7.8	206.84	648.1	0.02652	0.08309
Aluminum	2.6	68.95	275.8	0.02652	0.1061

## 2.2. Classification of Composites

Composites can be classified by the geometry of the reinforcement such as particulate, flake, and fibers (Figure 2.2) or by the type of matrix such as polymer, metal, ceramic and carbon.

Particulate composites include particles embedded in matrices such as alloys and ceramics. The use of aluminum particles in rubber; silicon carbide particles in aluminum; and gravel, sand and cement to make concrete are common examples of particulate composites. Flake composites contain flat reinforcements in matrices. Typical flakes are glass, mica, aluminum, and silver. Fiber reinforced composite materials consist of matrices reinforced by short (discontinuous) or long (continuous) fibers. Fibers are usually anisotropic; carbon, glass and aramids are the most used examples of fibers. Matrices include resins such as epoxy, metals such as aluminum, and ceramics such as calcium-alumina silicate. Continuous fiber matrix composites consist of unidirectional or woven fiber laminas. Laminas are stacked on top of each other at various angles to form a multidirectional laminate [1].

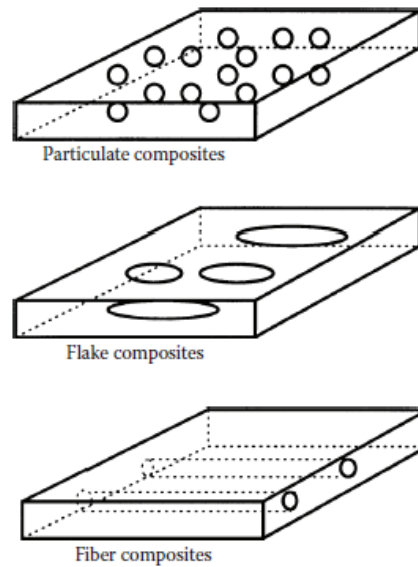


Figure 2.2. Types of composites based on reinforcement shape  
(Source: Kaw, 2006)

Another type of composite material is the nanocomposites with a big potential of becoming an important material in the future. Although nanocomposites are in the early stages of development, they now attract considerable attention of academia as much as a wide range of industries, including aerospace, automotive, and biomedical industries. The reinforcement in nanocomposites is ensured by either nanoparticles, nanofibers, or carbon nanotubes [2].

In the following, the composite materials classified by the type of matrix are explained in detail.

### 2.2.1. Polymer Matrix Composites

Common advanced composites are polymer matrix composites (PMCs) consisting of a polymer such as epoxy, polyester and urethane, reinforced by thin diameter fibers such as graphite, aramids and boron. PMCs are mostly preferred due to their low cost, high strength, and simple manufacturing principles. Some disadvantages of PMCs are

low operating temperatures, high coefficients of thermal and moisture expansion and low elastic properties in certain directions.

The most common fibers used are glass, graphite, and Kevlar. Glass is the most common fiber used in polymer matrix composites. Its advantages are its high strength, low cost, high chemical resistance and good insulating properties. The disadvantages are low elastic modulus, poor adhesion to polymers, high specific gravity, sensitivity to abrasion (reduces tensile strength) and low fatigue strength. The main types of glass fibers are E-glass (fiberglass) and S-glass. The “E” in E-glass corresponds to electrical since it was designed for electrical applications. Besides, it is used for many other purposes now, such as decoration and structural applications. The “S” in S-glass corresponds to higher content of silica. S-glass fibers hold their strength at high temperatures compared to E-glass and have higher fatigue strength. They are used principally for aerospace applications. Other types available commercially are C-glass (Corrosion) used in chemical environments, such as storage tanks; R-glass used in structural applications such as construction; D-glass (Dielectric) used for applications requiring low dielectric constants, such as radomes; and A-glass (Appearance) used to improve surface appearance. Some combinational types such as E-CR glass (Electrical and Corrosion resistance) and AR glass (Alkali Resistant) also exist.

Graphite fibers are more often used in high-modulus and high-strength applications such as aircraft components, etc. The advantages of graphite fibers are high specific strength and modulus, low coefficient of thermal expansion, and high fatigue strength. The disadvantages are high cost, low impact resistance, and high electrical conductivity.

An aramid fiber is an aromatic organic compound made of carbon, hydrogen, oxygen, and nitrogen. The advantages of using aramid fiber are low density, high tensile strength, low cost, and high impact resistance. Its disadvantages are low compressive properties and degradation in sunlight. Kevlar 29® and Kevlar 49® are the two main types of aramid fibers. Both types of Kevlar fibers have similar specific strengths, but Kevlar 49 has a higher specific stiffness. Kevlar 29 is principally used in bulletproof vests, ropes, and cables. Kevlar 49 is used in high performance applications by the aircraft industry.

Various polymers are used in advanced polymer composites. These polymers are such as epoxy, phenolics, acrylic, urethane, and polyamide and each polymer holds its advantages and disadvantages in its use.



Besides, each of the resin systems has its some advantages and disadvantages. The use of a particular resin system depends on the application. These considerations involve mechanical strength, cost, smoke emission, temperature excursions, etc. The comparison of five common resins based on smoke emission, strength, service temperature, and cost are given in Figure 2.3.

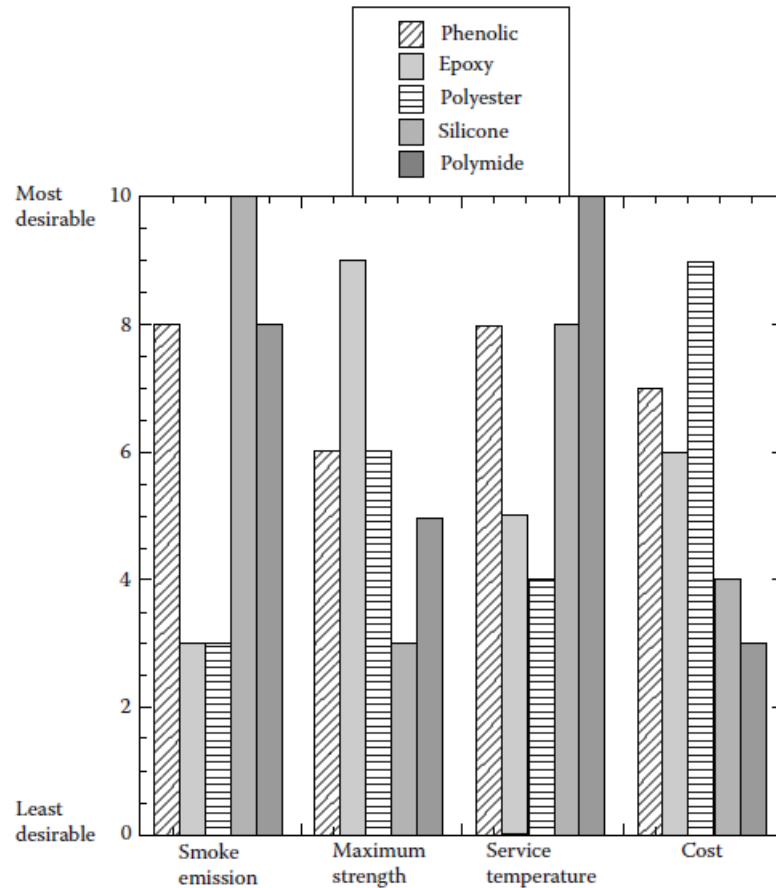


Figure 2.3. Comparison of performance of several common matrices used in polymer matrix composites (Source: Kaw, 2006)

Epoxy resins are the most preferred resins. They are low molecular weight organic liquids containing epoxide groups. Epoxide comprises of three members in its molecule ring: one oxygen and two carbon atoms. Epoxy is the most commonly used PMC matrix; however, it is costlier than other polymer matrices. More than two-thirds of the polymer matrices used in aerospace applications is epoxy based. Because of their some advantages such as high strength, low viscosity and low flow rates, which allow good wetting of

fibers and prevent misalignment of fibers during processing, low volatility during cure, low shrink rates, which reduce the tendency of gaining large shear stresses of the bond between epoxy and its reinforcement, epoxy resins are the most widely held PMC matrix and existing in more than 20 grades to meet specific property and processing requirements.

Polymers are categorized as thermosets and thermoplastics. Thermoset polymers are insoluble and infusible after cure because its molecular chains are rigidly joined with strong covalent bonds; thermoplastics are formable at high pressure and high temperatures because their molecular bonds are weak and of the van der Waals type. Typical examples of thermosets are epoxies, polyesters, phenolics, and polyamide; typical examples of thermoplastics are polyethylene, polystyrene, polyether–ether–ketone (PEEK), and polyphenylene sulfide (PPS). The differences between thermosets and thermoplastics are indicated in Table 2.2 [1].

Table 2.2. Differences between thermosets and thermoplastics  
(Source: Kaw, 2006)

<b>Thermoplastics</b>	<b>Thermoset</b>
Soften on heating and pressure, and thus easy to repair	Decompose on heating
High strains to failure	Definite shelf life
Can be processed	Cannot be processed
Not tacky and easy to handle	Tacky
Short cure cycles	Long cure cycles
Higher fabrication temperature and viscosities have made it difficult to process	Lower fabrication temperature
Excellent solvent resistance	Fair solvent resistance

### **2.2.2. Metal Matrix Composites**

Metal matrix composites (MMCs), as the name refers, have a metal matrix. Examples of metal matrices in such composites are aluminum, magnesium, and titanium. Typical fibers used in MMCs are carbon and silicon carbide. Metals are chiefly reinforced to increase or decrease their properties to provide the needs of design. For instance, the

stiffness and strength of metals can be increased, and large coefficients of thermal expansion and thermal and electric conductivities of metals can be reduced, by the addition of fibers such as silicon carbide.

Metal matrix composites are principally used to get more advantageous than monolithic metals such as steel and aluminum. The advantages of MMCs can be counted as higher specific strength and modulus by reinforcing low-density metals, such as aluminum and titanium; lower coefficients of thermal expansion by reinforcing with fibers with low coefficients of thermal expansion, such as graphite; and maintaining properties such as strength at high temperatures. Metal matrix composites have several superiorities in comparison to polymer matrix composites. These advantages are better elastic properties; higher service temperature; insensitivity to moisture; higher electric and thermal conductivities; and better wear, fatigue, and flaw resistances. The disadvantages of MMCs over PMCs are higher processing temperatures and higher densities. Typical mechanical properties of MMCs are shown in Table 2.3 [1].

Table 2.3. Typical properties of metal matrix composites  
(Source: Kaw, 2006)

Material	Specific gravity	Young's modulus (GPa)	Ultimate tensile strength (MPa)	Coefficient of thermal expansion ( $\mu\text{m}/\text{m}/^\circ\text{C}$ )
SiC/ aluminum	2.6	117.2	1206	12.4
Graphite/ aluminum	2.2	124.1	448.2	18
Steel	7.8	206.8	648.1	11.7
Aluminum	2.6	68.95	234.40	23

### 2.2.3. Ceramic Matrix Composites

Ceramic matrix composites (CMCs) contain ceramic matrix such as alumina calcium alumina silicate reinforced by fibers such as carbon or silicon carbide. The main advantages of CMCs are high strength, hardness, high service temperature limits for ceramics, chemical inertness, and low density. On the other hand, ceramics by themselves have low fracture toughness. Ceramics fail disastrously under tensile or impact loading. The fracture strength of ceramics increases by reinforcing ceramics with fibers, such as

silicon carbide or carbon thereby the failure of the composite occurs gradually. The combination of fiber and ceramic matrix makes CMCs more attractive for applications in which high mechanical properties and extreme service temperatures are desired. In Table 2.4, typical mechanical properties of ceramic matrix composites are presented [1].

Table 2.4. Typical mechanical properties of some ceramic matrix composites  
(Source: Kaw, 2006)

Material	Specific gravity	Young's modulus (GPa)	Ultimate tensile strength (MPa)	Coefficient of thermal expansion ( $\mu\text{m}/\text{m}/^\circ\text{C}$ )
SiC/LAS	2.1	89.63	496.4	3.6
SiC/CAS	2.5	121	400	4.5
Steel	7.8	206.8	648.1	11.7
Aluminum	2.6	68.95	234.4	23

#### 2.2.4. Carbon - Carbon Composites

Carbon-carbon composite (C/C) is a material consisting of carbon fiber reinforcement in a matrix of graphite. Carbon fibers are used in a carbon matrix such as graphite to create carbon-carbon composites. This type of composites can be used in very high-temperature environments of up to  $3315^\circ\text{C}$  and are 20 times stronger and 30% lighter than graphite fibers. Carbon is inherently brittle and flaw sensitive like ceramics. Reinforcement of carbon matrix allows the composite to fail gradually and also ensures some better properties such as ability to withstand high temperatures, low creep at high temperatures, low density, good tensile and compressive strengths, high fatigue resistance, high thermal conductivity, and high coefficient of friction. Main disadvantages of C/C composites are their high cost, low shear strength, and susceptibility to oxidations at high temperatures. Typical properties of carbon-carbon composites are given as comparative with some metals in Table 2.5 below [1].

Table 2.5. Typical mechanical properties of carbon - carbon matrix composites  
(Source: Kaw, 2006)

Material	Specific gravity	Young's modulus (GPa)	Ultimate tensile strength (MPa)	Coefficient of thermal expansion ( $\mu\text{m}/\text{m}/^\circ\text{C}$ )
C-C	1.68	13.5	35.7	2.0
Steel	7.8	206.8	648.1	234.4
Aluminum	2.6	68.95	234.4	23

### 2.3. Common Applications of Composite Materials

There are so various commercial and industrial applications of fiber-reinforced polymer composites so that it is impossible to list them all. In this section, the major structural application areas such as aircraft, space, automotive, sporting goods, marine, and infrastructure are highlighted. Besides these common application fields, fiber-reinforced polymer composites are also used in electronics (e.g., printed circuit boards), building construction (e.g., floor beams), furniture (e.g., chair springs), power industry (e.g., transformer housing), oil industry (e.g., offshore oil platforms and oil sucker rods used in lifting underground oil), medical industry (e.g., bone plates for fracture fixation, implants, and prosthetics), and in many industrial products such as step ladders, oxygen tanks, and power transmission shafts. Potential use of fiber-reinforced composites can be seen in many engineering fields today. A careful design practice and appropriate process development based on the understanding of their unique mechanical, physical, and thermal characteristics are required to put them to actual use.

The main structural applications for fiber-reinforced composites are in the field of military and commercial aircrafts, for which weight reduction is critical for higher speeds and increased loads. The use of fiber-reinforced polymers has experienced a steady growth in the aircraft industry since the production application of boron fiber -reinforced epoxy skins for F-14 horizontal stabilizers in 1969. Carbon fibers are introduced to industry in the 1970s and carbon fiber-reinforced epoxy has become the indispensable material in many wing, fuselage, and empennage components.

For instance, the outer skin of B-2 (Figure 2.4) and other stealth aircrafts is almost all made of carbon fiber-reinforced polymers. Figure 2.5 schematically illustrates the

composite usage in Airbus A380 introduced in 2006. About 25% of its weight is made of composites [2].



Figure 2.4. Stealth aircraft  
(Source: Mallick, 2007)

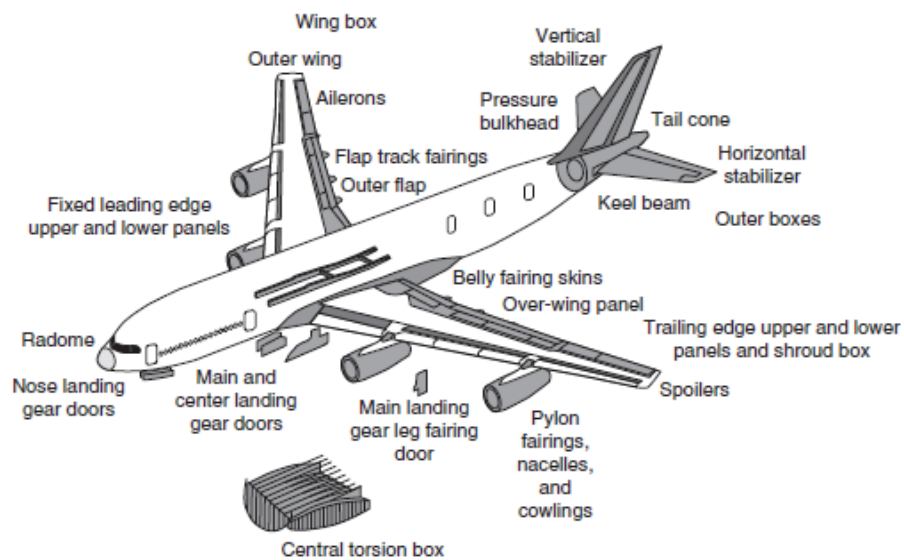


Figure 2.5. Use of fiber-reinforced polymer composites in Airbus 380  
(Source: Mallick, 2007)

## 2.4. Mechanics of Composite Materials

Many engineers and material scientists have adequate knowledge of the behavior and design of isotropic materials, which include the family of most metals and pure polymers. The rapidly increasing use of anisotropic materials such as composite materials has ended up with a materials revolution and it requires a new knowledge base of anisotropic material behavior.

The use of fiber-reinforced composite materials is different compared to conventional materials in application because the use of long fibers results in a material which has a higher strength-to-density ratio and/or stiffness-to-density ratio than any other material system at moderate temperature, and there exists the opportunity to uniquely tailor the fiber orientations to a given geometry, applied load and environment. For this reason, with the use of composite materials, an engineer is not only a material selector, but is also a material designer [18]. On the other hand, fiber-reinforced composites are microscopically inhomogeneous and orthotropic. Consequently, the mechanics of fiber-reinforced composites are more complicated than that of conventional materials [2].

### 2.4.1. Classical Lamination Theory

Classical lamination theory is an extension of the classical plate theory (Kirchoff and Love plate theory) to take into account the inhomogeneity in thickness direction and orthotropy of the laminate. Classical lamination theory is only valid for thin laminates and used to analyze the infinitesimal deformation of laminated structures. In this theory, it is assumed that laminate is thin and wide, perfect bonding exists between laminas, there exist a linear strain distribution through the thickness, all laminas are macroscopically homogeneous and behave in a linearly elastic manner, and the through the thickness strains and the transverse shear strains are zero [1]. Thin laminated composite structure subjected to mechanical in-plane loading ( $N_x, N_y$ ) is shown in Figure 2.6. Cartesian coordinate system  $x, y$  and  $z$  defines global coordinates of the layered material. A layer-wise principal material coordinate system is denoted by 1, 2, 3 and fiber direction is oriented at angle  $\theta$  to the  $x$  axis. Representation of laminate convention for the  $n$ -layered structure with total thickness  $h$  is given in Figure 2.7.

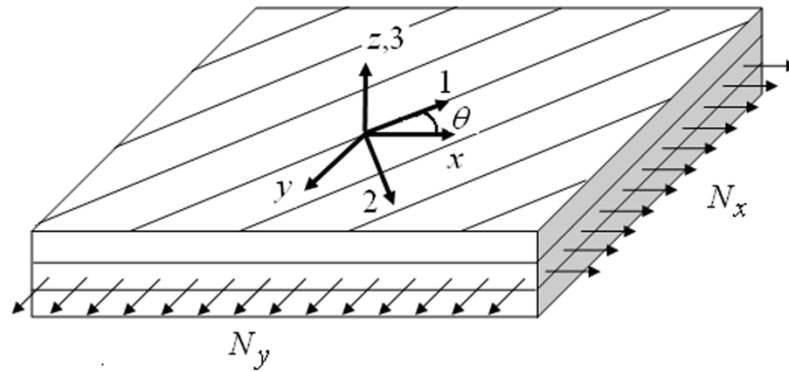


Figure 2.6. A thin fiber-reinforced laminated composite subjected to in-plane loading

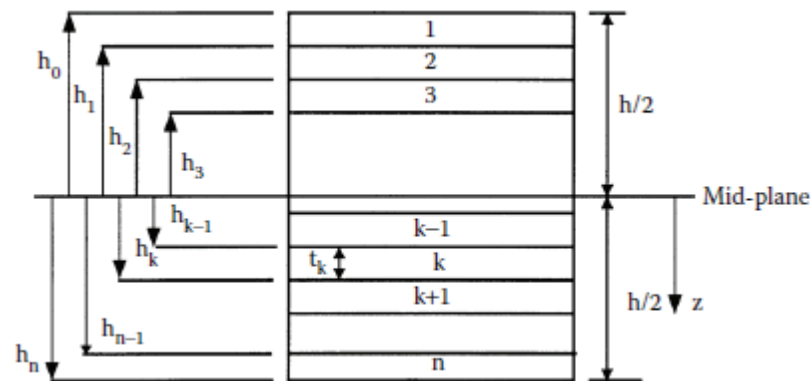


Figure 2.7. Coordinate locations of plies in a laminate  
(Source: Kaw, 2006)

In most structural applications, composite materials are used in the form of thin laminates loaded in the plane of the laminate. Consequently, composite laminates can be considered to be under a condition of plane stress with all stress components in the out-of-plane direction (3-direction) being zero.

The stress-strain relation for the  $k$ -th layer of a composite plate based on the classical lamination theory can be written in the following form



$$\begin{bmatrix} \sigma_x \\ \sigma_y \\ \sigma_{xy} \end{bmatrix}_k = \begin{bmatrix} \bar{Q}_{11} & \bar{Q}_{12} & \bar{Q}_{16} \\ \bar{Q}_{12} & \bar{Q}_{22} & \bar{Q}_{26} \\ \bar{Q}_{16} & \bar{Q}_{26} & \bar{Q}_{66} \end{bmatrix}_k \left( \begin{bmatrix} \varepsilon_x^o \\ \varepsilon_y^o \\ \varepsilon_{xy}^o \end{bmatrix} + z \begin{bmatrix} \kappa_x \\ \kappa_y \\ \kappa_{xy} \end{bmatrix} \right) \quad (2.1)$$

where  $[\bar{Q}_{ij}]_k$  are the elements of the transformed reduced stiffness matrix,  $[\varepsilon^o]$  is the mid-plane strains,  $[\kappa]$  is curvatures, respectively.

The elements of transformed reduced stiffness matrix  $[\bar{Q}_{ij}]$  given in Equation 2.1 can be expressed as in the following form

$$\bar{Q}_{11} = Q_{11}c^4 + Q_{22}s^4 + 2(Q_{12} + 2Q_{66})s^2c^2 \quad (2.2)$$

$$\bar{Q}_{12} = (Q_{11} + Q_{22} - 4Q_{66})s^2c^2 + Q_{12}(c^4 + s^4) \quad (2.3)$$

$$\bar{Q}_{22} = Q_{11}s^4 + Q_{22}c^4 + 2(Q_{12} + 2Q_{66})s^2c^2 \quad (2.4)$$

$$\bar{Q}_{16} = (Q_{11} - Q_{12} - 2Q_{66})sc^3 - (Q_{22} - Q_{12} - 2Q_{66})s^3c \quad (2.5)$$

$$\bar{Q}_{26} = (Q_{11} - Q_{12} - 2Q_{66})cs^3 - (Q_{22} - Q_{12} - 2Q_{66})sc^3 \quad (2.6)$$

$$\bar{Q}_{66} = (Q_{11} + Q_{22} - 2Q_{12} - 2Q_{66})s^2c^2 + Q_{66}(c^4 + s^4) \quad (2.7)$$

where stiffness matrix quantities  $[Q_{ij}]$  are

$$Q_{11} = \frac{E_1}{1 - \nu_{21}\nu_{12}} \quad (2.8)$$

$$Q_{12} = \frac{\nu_{12}E_2}{1 - \nu_{21}\nu_{12}} \quad (2.9)$$

$$Q_{22} = \frac{E_2}{1 - \nu_{21}\nu_{12}} \quad (2.10)$$

$$Q_{66} = G_{12} \quad (2.11)$$

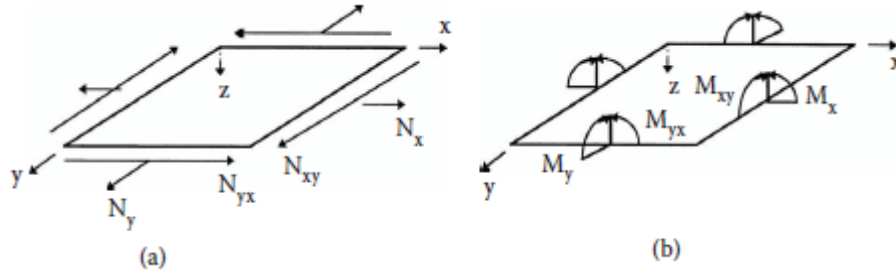


Figure 2.8. Resultant forces (a) and moments (b) on a laminate  
(Source: Kaw, 2006)

Applied normal force resultants  $N_x$ ,  $N_y$ , shear force resultant  $N_{xy}$  (per unit width) and moment resultants  $M_x$ ,  $M_y$  and  $M_{xy}$  on a laminate (Figure 2.8) have the following relations:

$$\begin{bmatrix} N_x \\ N_y \\ N_{xy} \end{bmatrix} = \begin{bmatrix} A_{11} & A_{12} & A_{16} \\ A_{12} & A_{22} & A_{26} \\ A_{16} & A_{26} & A_{66} \end{bmatrix} \begin{bmatrix} \varepsilon_x^0 \\ \varepsilon_y^0 \\ \gamma_{xy}^0 \end{bmatrix} + \begin{bmatrix} B_{11} & B_{12} & B_{16} \\ B_{12} & B_{22} & B_{26} \\ B_{16} & B_{26} & B_{66} \end{bmatrix} \begin{bmatrix} \kappa_x \\ \kappa_y \\ \kappa_{xy} \end{bmatrix} \quad (2.12)$$

$$\begin{bmatrix} M_x \\ M_y \\ M_{xy} \end{bmatrix} = \begin{bmatrix} B_{11} & B_{12} & B_{16} \\ B_{12} & B_{22} & B_{26} \\ B_{16} & B_{26} & B_{66} \end{bmatrix} \begin{bmatrix} \varepsilon_x^0 \\ \varepsilon_y^0 \\ \gamma_{xy}^0 \end{bmatrix} + \begin{bmatrix} D_{11} & D_{12} & D_{16} \\ D_{12} & D_{22} & D_{26} \\ D_{16} & D_{26} & D_{66} \end{bmatrix} \begin{bmatrix} \kappa_x \\ \kappa_y \\ \kappa_{xy} \end{bmatrix} \quad (2.13)$$

The matrices  $[A]$ ,  $[B]$  and  $[D]$  can be defined as in Equations 2.14, 2.15, 2.16 below:

$$A_{ij} = \sum_{k=1}^n [(\bar{Q}_{ij})]_k (h_k - h_{k-1}), \quad i, j = 1, 2, 6 \quad (2.14)$$

$$B_{ij} = \frac{1}{2} \sum_{k=1}^n [(\bar{Q}_{ij})]_k (h_k^2 - h_{k-1}^2), \quad i, j = 1, 2, 6 \quad (2.15)$$

$$D_{ij} = \frac{1}{3} \sum_{k=1}^n [(\bar{Q}_{ij})]_k (h_k^3 - h_{k-1}^3), \quad i, j = 1, 2, 6 \quad (2.16)$$

The  $[A]$ ,  $[B]$ , and  $[D]$  matrices are called the extensional, coupling, and bending stiffness matrices, respectively. Combining Equation 2.12 and Equation 2.13 gives six simultaneous linear equations and six unknowns as:

$$\begin{bmatrix} N_x \\ N_y \\ N_{xy} \\ M_x \\ M_y \\ M_{xy} \end{bmatrix} = \begin{bmatrix} A_{11} & A_{12} & A_{16} & B_{11} & B_{12} & B_{16} \\ A_{12} & A_{22} & A_{26} & B_{12} & B_{22} & B_{26} \\ A_{16} & A_{26} & A_{66} & B_{16} & B_{26} & B_{66} \\ B_{11} & B_{12} & B_{16} & D_{11} & D_{12} & D_{16} \\ B_{12} & B_{22} & B_{26} & D_{12} & D_{22} & D_{26} \\ B_{16} & B_{26} & B_{66} & D_{16} & D_{26} & D_{66} \end{bmatrix} \begin{bmatrix} \varepsilon_x^0 \\ \varepsilon_y^0 \\ \gamma_{xy}^0 \\ \kappa_x \\ \kappa_y \\ \kappa_{xy} \end{bmatrix} \quad (2.17)$$

The extensional stiffness matrix  $[A]$  relates the resultant in-plane forces to the in-plane strains, and the bending stiffness matrix  $[D]$  relates the resultant bending moments to the plate curvatures. The coupling stiffness matrix  $[B]$  couples the force and moment terms to the mid-plane strains and mid-plane curvatures [1].

Now, stresses and strain expressions based on classical lamination theory can be expressed by local coordinate system (1, 2). The relation between the local and global stresses in an angled lamina can be written as in the following form:

$$\begin{bmatrix} \sigma_1 \\ \sigma_2 \\ \sigma_{12} \end{bmatrix} = [T] \begin{bmatrix} \sigma_x \\ \sigma_y \\ \sigma_{xy} \end{bmatrix} \quad (2.18)$$

Similarly, the local and global strains are also related as follows

$$\begin{bmatrix} \varepsilon_1 \\ \varepsilon_2 \\ \varepsilon_{12} \end{bmatrix} = [R][T][R]^{-1} \begin{bmatrix} \varepsilon_x \\ \varepsilon_y \\ \varepsilon_{xy} \end{bmatrix} \quad (2.19)$$

where

$$[R] = \begin{bmatrix} 1 & 0 & 0 \\ 0 & 1 & 0 \\ 0 & 0 & 2 \end{bmatrix} \quad (2.20)$$

and  $[T]$  transform matrix,

$$[T] = \begin{bmatrix} c^2 & s^2 & 2sc \\ s^2 & c^2 & -2sc \\ -sc & sc & c^2 - s^2 \end{bmatrix} \quad c = \cos \theta, \quad s = \sin \theta \quad (2.21)$$

## CHAPTER 3

# FATIGUE OF FIBER-REINFORCED POLYMER COMPOSITES

### 3.1. Introduction

As human beings, we are aware of the fact that nothing lasts forever. Life involves a finite period and will eventually come to an end. This case is related to reduction in efficiency, which is known as aging. This human life experience is also valid in materials science. A structure or a component can fail under a high loading. However, it can sustain lower loads. On the other hand, if the loads are applied over longer time in a constant (creep) or cyclic (fatigue) way periodically to the same structure or component, it can also fail. The phenomenon of the degradation of mechanical properties of a material due to applied loads that fluctuate over time is named as fatigue and the resulting failure is named as fatigue failure.

From the 1850s, engineers noticed that fatigue is a critical loading pattern and could be responsible for a large percentage of structural failures. Thereafter, it was widely accepted that fatigue should not be neglected. The fatigue term was incorporated in the dictionary of the American Society for Testing and Materials (ASTM) not before 1946 and then, the E9 committee was founded to promote the development of fatigue test methods. Recently, it is reported that most of structural failures occur by a fatigue mechanism. Approximately 60% of 230 examined failures were associated with fatigue according to an extensive study by the US National Institute of Standards and Technology. This percentage was found a higher value between 80% and 90% in another study carried out by the Battelle Institution [17].

During the following years, with the development of material technologies and the emergence of composite materials, numerous experiments were conducted on several structural fiber-reinforced polymer (FRP) composite materials for the characterization of the fatigue behavior. As technology developed and new test frames and measuring devices were invented, it became more straightforward to conduct complex fatigue experiments and measure properties and characteristics, which would not have been

possible in earlier years. Eventually, almost all failure modes of FRP composites were identified and many theoretical failure criteria were proposed for modelling and predicting the fatigue life of various composite material systems [3].

As seen, experimental study is a beginning stage of any investigation to describe the behavior of a composite material, model the failure mechanisms and predict its fatigue behavior under different loading patterns. In the following section, the basic considerations for the design of an experimental program are explained in more detail [17].

### **3.2. Fatigue Test of Composite Materials**

Extensive experimental studies concerning composite materials are carried out for several purposes on standardized specimens. These studies are performed to (i) investigate material behavior and characterization of the damage development process, (ii) characterize the material and develop theoretical models for the description of its behavior, (iii) test predetermined standardized specimens of different materials and/ or different specimen configurations aimed at material selection and optimization of specimen configuration, (iv) develop analytical models for the modeling and subsequent prediction of the fatigue life of the examined components, and (v) validate the design of a structure, normally based on quasi-static load cases [17].

In the literature, there are limited information related to standards concerning the fatigue investigation of FRP composites. In this context, a referenced method, ASTM D3479 [19] denotes to the tension-tension fatigue of polymer matrix composites. It includes only basic guidelines without describing clamping procedures, loading frequency and methods for data reduction. Besides, ISO 13003 [20] defines general procedures for the tension-tension fatigue investigation involving all modes of testing machines. However, it also gives limited information regarding data evaluation procedures [3]. An example multidirectional specimen geometry for a standard fatigue test and number of specimens required to obtain each applied stress (or strain) - cycles to failure (S-N or  $\epsilon$ -N) curve (ASTM D3479) are given in Figure 3.1 and Table 3.1, respectively.

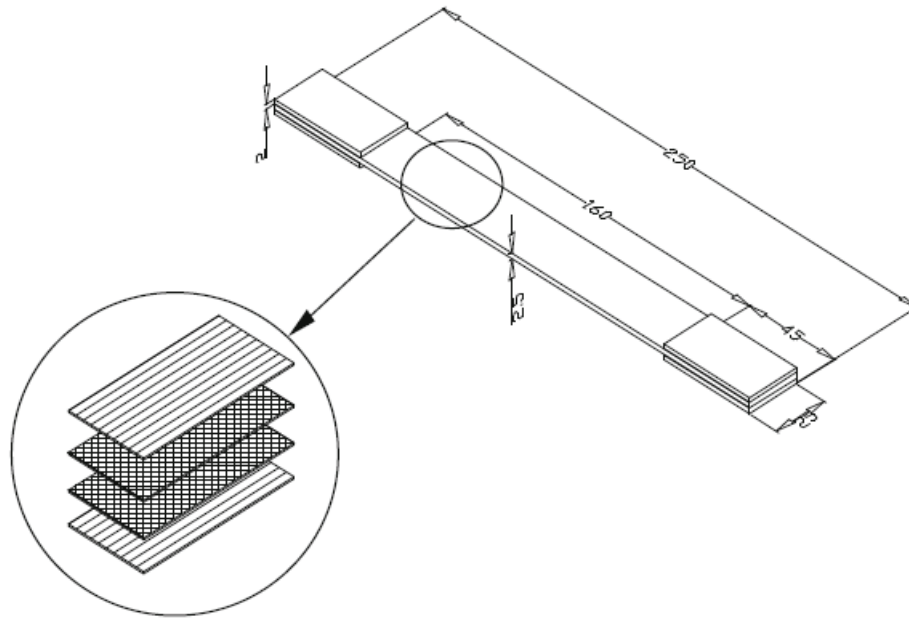


Figure 3.1. Example specimen geometry and stacking sequence  
(Source: Vassilopoulos and Keller, 2011)

Table 3.1. Number of specimens required for standard fatigue test

Type of Test	Minimum Number of Specimens
Preliminary and exploratory	6
Research and development testing of components and structures	12
Design allowable data	24
Reliability data	24

Several steps exist to follow for the design of a fatigue-testing program. There are different parameters which affect the test results to a degree. Therefore, the right decisions should be taken during the test. The outstanding parameters among them can be specified as the loading pattern, loading frequency, control mode, stress ratio, waveform type, temperature and humidity of the testing environment etc. Detailed information of the effects of each parameter is given in [17].

### 3.2.1. Fundamental Fatigue Terminology

The basic general terms used in fatigue is described here. The basic terminology is given schematically together with representative constant amplitude and variable amplitude loading patterns in Figures 3.2 – 3.4.

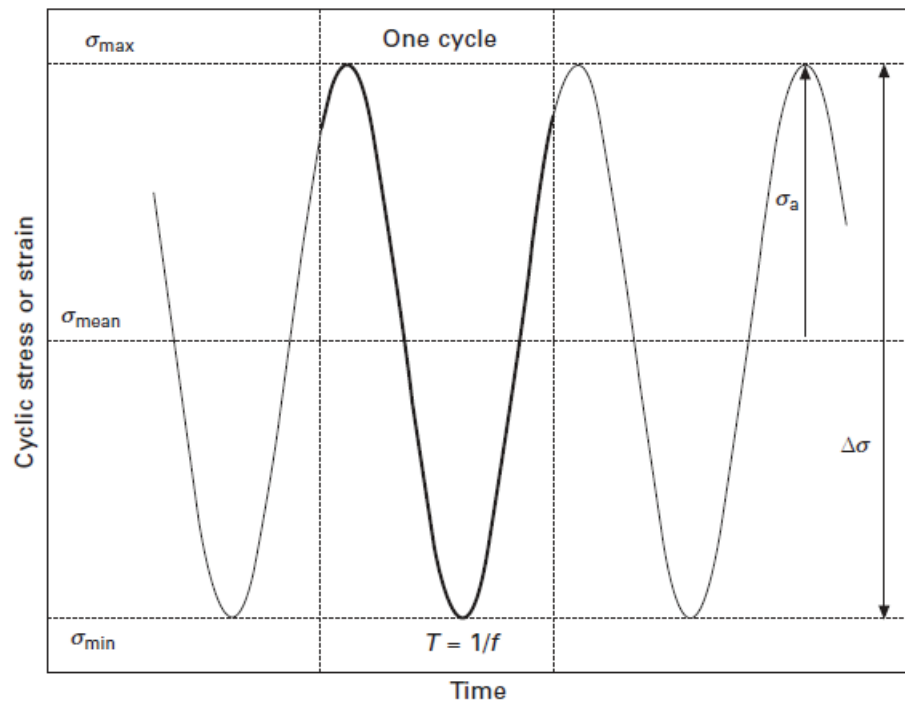


Figure 3.2. Basic fatigue terminology  
(Source: Vassilopoulos, 2010)



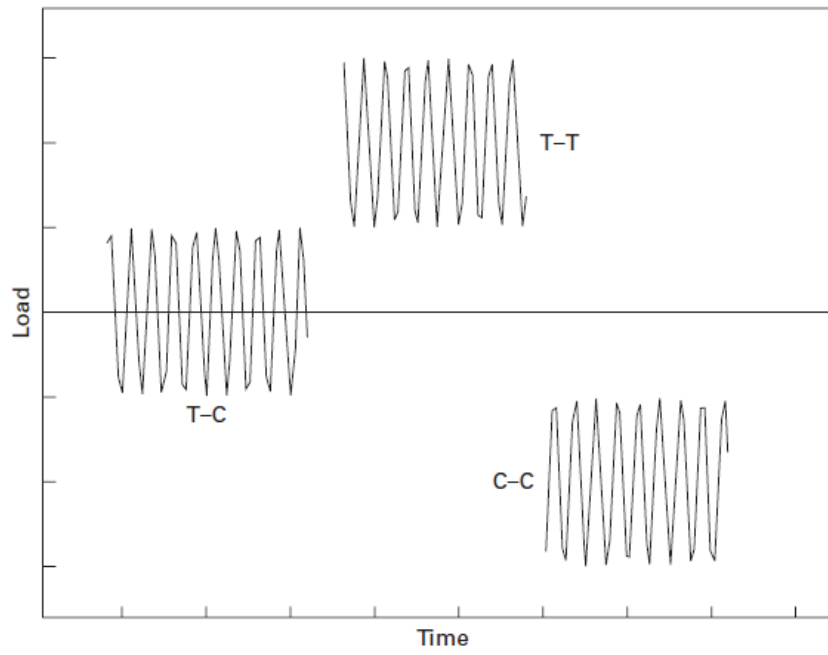


Figure 3.3. Representative constant amplitude loading patterns  
(Source: Vassilopoulos, 2010)

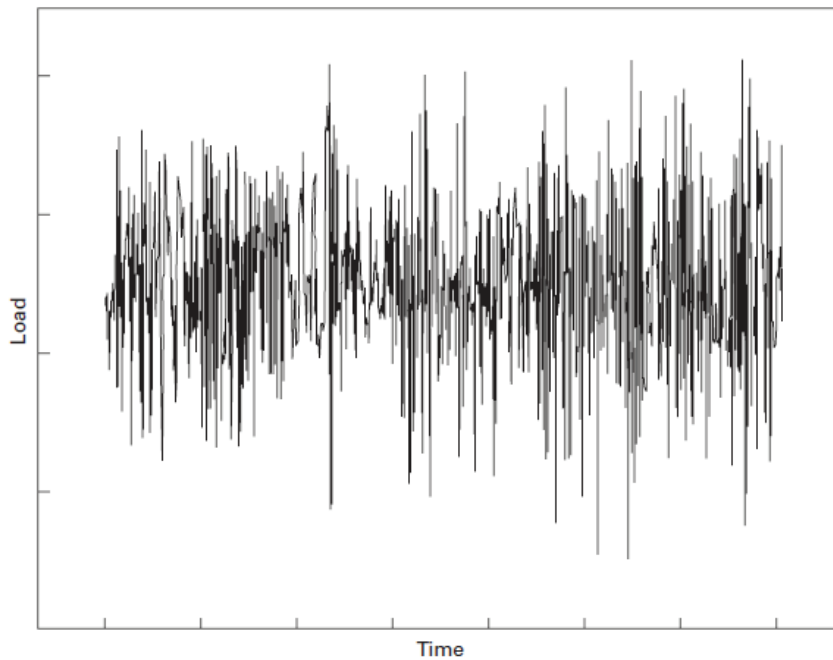


Figure 3.4. Example of an irregular fatigue time series  
(Source: Vassilopoulos, 2010)

Figure 3.2 shows cyclic stress versus time. Conventional abbreviations used in fatigue are specified in the figure and given as follows:

$\sigma_{\max}$  = maximum applied cyclic stress

$\sigma_{\min}$  = minimum applied cyclic stress

$\sigma_{\text{mean}}$  = mean stress

$\sigma_a$  = cyclic stress amplitude

$\Delta\sigma$  = cyclic stress range

f = test frequency measured in Hz that is loading cycles per second (1/s).

In Figure 3.3, fatigue loading types are shown.  $R$  is the ratio of minimum over maximum cyclic stress and can be expressed as  $R = \frac{\sigma_{\min}}{\sigma_{\max}}$ . This ratio defines the loading patterns that might be of:

T – T: tension–tension loading, when  $0 \leq R < 1$

C – C: compression–compression loading, when  $1 < R < +\infty$

T – C or C – T: combined tension – compression loading when  $-\infty < R < 0$

$R = -1$  when the compressive stress amplitude is the same as the tensile stress amplitude. This is known as reversed loading. [17].

### 3.2.2. Fatigue Data Processing

It is a difficult task to adapt methods for the interpretation of static and fatigue data to interpolate among experimental data (modeling) and extrapolate beyond that for the prediction of the expected material behavior. This procedure depends on the examined material and thermo-mechanical loading conditions. For this purpose, deterministic or stochastic theoretical models can be used. The use of the selected models including S–N curves, constant life diagrams, residual strength models, residual stiffness models, etc. allow to process the fatigue data and estimate the fatigue life of the materials theoretically under any applied loading pattern.

The first mathematical model to describe the relationship between the applied cyclic stress ( $\sigma$  or  $S$ ) and the number of cycles to failure ( $N$ ) is proposed by Basquin in 1910. It is stated that material increases as a power law when the external load amplitude decreases. The Basquin relationship can be in the form of the following equations:

$$N\sigma^m = C \quad \text{or} \quad \sigma = \sigma_0 N^{-1/k} \quad (3.1)$$

where  $\sigma$  can be any stress variable such as cyclic stress amplitude  $\sigma_a$ , maximum cyclic stress  $\sigma_{\max}$  or cyclic stress range  $\Delta\sigma$ , and  $N$  is the number of cycles the material can sustain until failure under the corresponding stress value.  $C$ ,  $\sigma_0$ ,  $m$  and  $k$  are model parameters. They can be easily estimated by linear regression of the above relationships to the experimental data.

The procedure to derive S-N curves belongs to constant amplitude fatigue data is schematically shown in Figure 3.5. Three different maximum cyclic stress levels from three fatigue tests are presented as  $\sigma_{\max 1}$ ,  $\sigma_{\max 2}$  and  $\sigma_{\max 3}$  in the figure. The tests end with different numbers of cycles to failure. It is seen that longer fatigue life is obtained when the stress level is less. Thus, the S-N curve of the examined material is obtained by interpolation between the collected fatigue data for the selected fatigue conditions - R-ratio, frequency, environment, etc. [3].

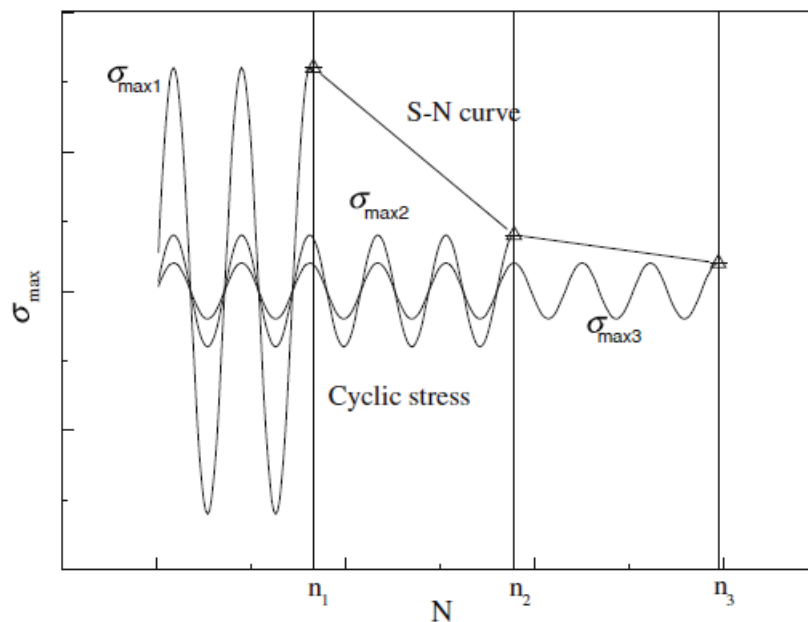


Figure 3.5. Schematic representation of S-N curve derivation (Source: Keller and Vassilopoulos, 2011)

### **3.3. Fatigue Life Prediction of Composite Materials**

Fiber reinforced polymer composites are used instead of traditional metallic materials in many structural applications such as airplanes that must bear critical fatigue loads during operation. This situation emerges that accurate fatigue life modeling is necessary. To simulate the fatigue behavior of composite structures lowers the cost and allows the development of a wider range of products with less need of physical prototypes. The use of fatigue life prediction methods makes possible to assess the durability performance of the composites early in the product development process and guide engineers to proper design choices. Furthermore, composite materials generally behave in a brittle manner and their failure caused from fatigue is abrupt without any prior notice. Therefore, the proper modeling of behavior of composite structures and prediction of their fatigue lives are significant.

To meet all these requirements, many theoretical models have been developed to define fatigue damage analytically and eventually predict the fatigue life of composite materials. Previous experience of fatigue life prediction for metallic materials led to select similar measurable material characteristics with metallic materials for composite materials to form the fatigue damage metric. Then, material damage was measured by the degradation of that quantity with loading cycles. Several approaches based on different damage metrics for measuring fatigue damage accumulation have been adapted. The expectation from these prediction models is that it provides a process requiring minimum experimental data while reliably predicting the condition of the material [17].

Theoretical models mainly can be classified into five categories: empirical, phenomenological modelling; specific damage metrics such as the residual strength and/or stiffness of the examined material; probabilistic; artificial neural network based; and micromechanics. Phenomenological fatigue failure models are in one of the broadest groups of theoretical models representing damage-tolerant design concepts. Models in this group use the definition of reliable S-N curves and constant life diagram formulations. Allowable numbers of cycles to failure under any given loading pattern from constant to variable amplitude can be estimated with these definitions. Fatigue tests are normally performed under the uniaxial stress states during laboratory experiments. However, in most practical cases, designers need fatigue models in which behavior failure can be predicted under realistic load combinations that yield realistic combinations of

stresses. For this purpose, multiaxial fatigue failure criteria have emerged to take multiaxial fatigue into account. In the literature, most of these fatigue life prediction models mainly focus on the introduction and validation of the models suitable for constant amplitude multiaxial proportional stress fields without addressing the problem of life prediction under irregular load spectra [3].

The S-N curve is fitted to experimental data traditionally by a semi-logarithmic or logarithmic equation. There are other types of S-N curve formulations usually applied to consider the statistical nature of fatigue data. It can be said that the best S-N curve type is the one that can best fit the available fatigue data. Currently, it is accepted that the S-N curve equations in power curve type can be better adapted than linear equations for composite material fatigue data.

Example S-N curves for the fatigue life prediction of a multidirectional glass/epoxy laminate using different theoretical models are shown in Figure 3.6.

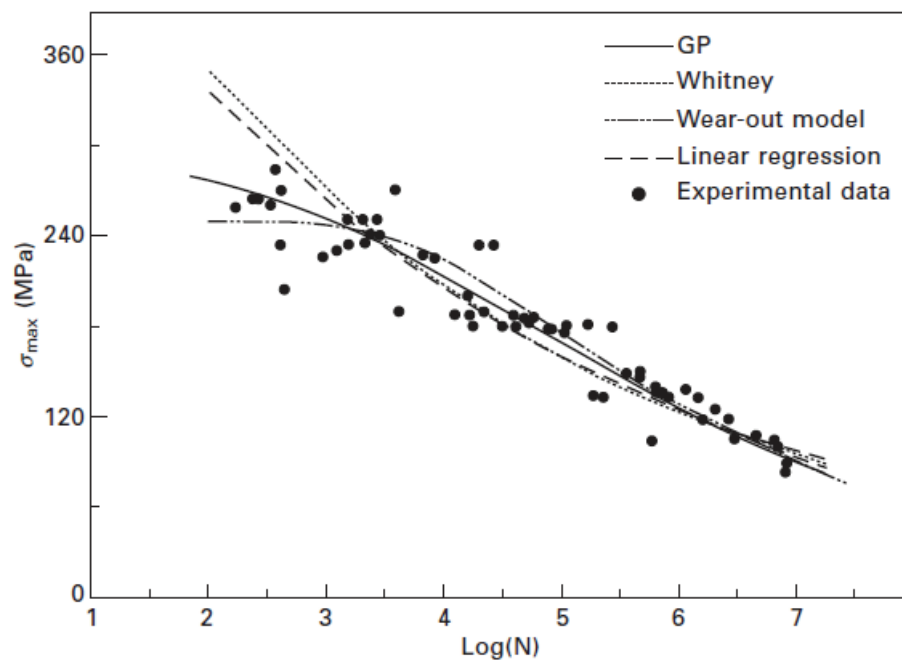


Figure 3.6. Application of different S-N curve formulations for a multidirectional glass/epoxy laminate with a stacking sequence  $[(\pm 45/0)_4/\pm 45]$  (Source: Vassilopoulos, 2010)

It is seen from Figure 3.6 that the application of different methods for derivation of the S-N curve of the examined composite material leads to different types of curves. When compared to each other, the model proposed by Sendeckyj (the wear-out model) and the curve estimated using genetic programming (GP) seem to be more accurate than the linear regression and Whitney models.

As previously mentioned, most of fatigue life prediction models are limited with the application of uniaxial loading and do not take the effect of other stress components into account on fatigue life. This assumption can be accepted as reasonable for the highly anisotropic composite materials and has even been adopted by the scientific community. However, multiaxial fatigue theories are necessary for the estimation and design procedures considering the complexity of real loading conditions [3,17].

## CHAPTER 4

### FATIGUE LIFE PREDICTION MODELS

#### 4.1. Hashin-Rotem (HR) Model

It was one of the first attempts that Hashin and Rotem extended a static failure theory to consider factors relevant to fatigue [5]. The authors proposed a fatigue failure theory including different damage modes. Two main failure modes in the case of unidirectional materials are reported: the fiber failure mode and the matrix failure mode. The off-axis angle of the reinforcement with respect to the loading direction specifies the difference between these two modes. This angle, called as the critical fiber angle, defines the transition from one failure mode to another, and related to the static strengths of the material. It is expressed by the following equation:

$$\tan \theta_c = \frac{\tau^s f_\tau(R, N, fr)}{\sigma_A^s f_A(R, N, fr)} \quad (4.1)$$

where  $\tau^s$  and  $\sigma_A^s$  are the static shear and longitudinal strengths, respectively; the functions  $f_\tau(R, N, fr)$  and  $f_A(R, N, fr)$  are the fatigue functions of the composite material along the shear and longitudinal directions, respectively. The functions depend on the stress ratio  $R$ , number of cycles  $N$  and fatigue frequency  $fr$ .

The S-N curves of the material under shear ( $\tau$ ), longitudinal ( $\sigma_A$ ) or transverse ( $\sigma_T$ ), directions are given as the product of the static strengths along any direction and the corresponding fatigue function. If the fiber forms an angle of less than  $\theta$  with respect to the loading direction, the fiber mode is the main failure mode. Otherwise the matrix failure mode leads to fatigue failure. Thus, the failure theory has two expressions:

$$\sigma_A = \sigma_A^u \quad (4.2)$$

$$\left(\frac{\sigma_T}{\sigma_T^u}\right)^2 + \left(\frac{\tau}{\tau^u}\right)^2 = 1 \quad (4.3)$$

where superscript  $u$  denotes fatigue failure stress (or the S-N curve) of the material in the related direction and subscript  $T$  corresponds to transverse to the fiber direction.

It is shown that any off-axis fatigue function in matrix failure mode can be expressed as a function of  $f_\tau$ ,  $f_T$ ,  $\tau^s$ ,  $\sigma_T^s$  and the angle  $\theta$  as follows:

$$f''(R, N, f_r) = f_\tau \sqrt{\frac{1 + \left(\frac{\tau^s}{\sigma_T^s}\right)^2 \tan^2 \theta}{1 + \left(\frac{\tau^s f_\tau}{\sigma_T^s f_T}\right)^2 \tan^2 \theta}} \quad (4.4)$$

Equation (4.4) can also be used to calculate fatigue functions  $f_\tau$  and  $f_T$  through two different experimentally obtained off-axis fatigue functions. HR model can be applied over the entire range of off-axis directions by defining three S-N curves in axial, shear and transverse directions experimentally along with the corresponding static strengths of the material.

HR fatigue failure model is also applicable for multidirectional laminates, but then, the case is more complicated. In this case, since each lamina is under a different stress field, failure may occur in some laminae after a specific cycle life whereas the other laminae does not fail yet. These different stress fields developed in each lamina cause interlaminar stresses and they may lead to failure. An interlaminar failure mode is proposed to take the interlaminar stresses into account. The expression of this mode is given below:

$$\left(\frac{\sigma_d}{\sigma_d^u}\right)^2 + \left(\frac{\tau_d}{\tau_d^u}\right)^2 = 1 \quad (4.5)$$

where subscript  $d$  represents the interlaminar stress components.

The HR failure criterion model can be used to estimate the fatigue behavior of unidirectional (UD) or multidirectional (MD) laminates subjected to uniaxial or



multiaxial cyclic loads. However, the type of failure mode should be distinguished during fatigue failure. It is not recommended the use of the model in woven or stitched fabrics composites [3].

## 4.2. Failure Tensor Polynomial in Fatigue (FTPF) Model

A modification of the quadratic version of the failure tensor polynomial for the prediction of fatigue strength under complex stress states was introduced by Philippidis and Vassilopoulos [9] and termed as Failure Tensor Polynomial in Fatigue (FTPF) criterion. The FTPF criterion is based on Tsai-Hahn tensor polynomial [21] and adapted for fatigue.

For a fiber-reinforced composite plate subjected to in-plane loading (Figure 2.6), Tsai-Hahn tensor polynomial criterion is expressed in the material coordinates by

$$F_{11}\sigma_1^2 + F_{22}\sigma_2^2 + 2F_{12}\sigma_1\sigma_2 + F_1\sigma_1 + F_2\sigma_2 + F_{66}\sigma_6^2 - 1 \leq 0 \quad (4.6)$$

Here, the components of the failure tensors can be given by

$$F_{11} = \frac{1}{XX'}, \quad F_{22} = \frac{1}{YY'}, \quad F_{66} = \frac{1}{S^2}, \quad F_1 = \frac{1}{X} - \frac{1}{X'}, \quad F_2 = \frac{1}{Y} - \frac{1}{Y'}, \quad (4.7)$$

$$F_{12} = -\frac{1}{2}\sqrt{F_{11}F_{22}}$$

where  $X$  and  $Y$  represent the failure strengths of the material along the longitudinal and the transverse directions, respectively, and  $S$  represents shear failure strength. The prime (') is used for compressive strengths.

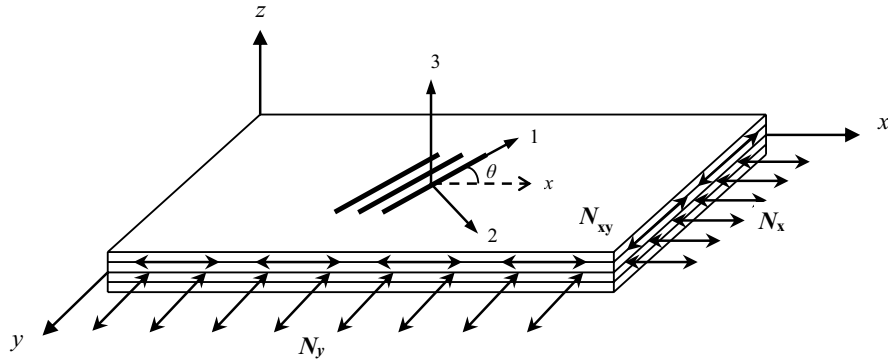


Figure 4.1. Representative plate geometry showing in-plane cyclic loading and principal coordinates

For cyclic in-plane fatigue loading as in Figure 4.1, the components of failure tensors are functions of the number of cycles  $N$ , stress ratio,  $R = \sigma_{\min} / \sigma_{\max}$ , and the frequency  $\nu$ , of the loading as

$$F_{ij} = F_{ij}(N, R, \nu), F_i = F_i(N, R, \nu), i, j = 1, 2, 6 \quad (4.8)$$

and the expressions in Equation (4.7) are still valid for the calculation of tensor components but the failure stresses  $X$ ,  $X'$ ,  $Y$ ,  $Y'$ , and  $S$  are replaced by the S–N curves of the material along the same directions and under the same conditions. Thus, the failure stresses  $X$ ,  $X'$ ,  $Y$ ,  $Y'$ ,  $S$  can be expressed as functions of number of cycles, stress ratio and frequency. If the S–N curves of the material are assumed in the general semi-logarithmic form

$$S = A + B \log N \quad (4.9)$$

then, the expressions of the fatigue failure stresses can be written as

$$\begin{aligned}
X(N, R, \nu) &= A_X + B_X \log N \\
X'(N, R, \nu) &= A_{X'} + B_{X'} \log N \\
Y(N, R, \nu) &= A_Y + B_Y \log N \\
Y'(N, R, \nu) &= A_{Y'} + B_{Y'} \log N \\
S(N, R, \nu) &= A_S + B_S \log N
\end{aligned} \tag{4.10}$$

For the composite materials in which static tensile strengths are equal or close to static compressive strengths, it is assumed that  $X' = X$  and  $Y' = Y$ , and only  $X(N, R, \nu)$ ,  $Y(N, R, \nu)$  and  $S(N, R, \nu)$  from the above fatigue failure stresses are sufficient for the FTPF criterion to yield satisfactory predictions. When only these three S–N curves are used, the fatigue failure tensor components can be given by

$$F_{11} = \frac{1}{X^2(N, R, \nu)}, F_{22} = \frac{1}{Y^2(N, R, \nu)}, F_{66} = \frac{1}{S^2(N, R, \nu)}, F_1 = F_2 = 0 \tag{4.11}$$

and by substituting these tensors into Equation (4.6), the criterion finally takes the form

$$\frac{\sigma_1^2}{X^2(N)} + \frac{\sigma_2^2}{Y^2(N)} - \frac{\sigma_1 \sigma_2}{X(N)Y(N)} + \frac{\sigma_6^2}{S^2(N)} - 1 \leq 0 \tag{4.12}$$

where the fatigue failure stresses are shown only as functions of the number of cycles  $N$ . The criterion can be used in the form of Equation (4.12) for any stress ratio  $R$ , and frequency  $\nu$ , provided the basic S–N curves are also known for the same  $R$  and  $\nu$  values.

### 4.3. Fawaz-Ellyin (FWE) Model

Fawaz and Ellyin [8] presented a fatigue life prediction model to simulate the fatigue behavior of unidirectional and multidirectional composite laminates under multiaxial cyclic stress states as presented in Figure 4.1. The model requires only one experimentally obtained S–N curve and the static strengths of the laminate along different directions. The FWE model assumes that all the on- and off-axis S–N curves of the laminate can be found lying in a narrow band on the S–N plane when they are normalized by the corresponding static strengths.

If a reference S-N curve is expressed by the following semi-log linear relationship,

$$S_r = m_r \log(N) + b_r \quad (4.13)$$

the S-N curve under any off-axis angle can be calculated by

$$S(a_1, a_2, \theta, R, N) = f(a_1, a_2, \theta)[g(R)m_r \log(N) + b_r] \quad (4.14)$$

as a function of the reference S-N curve.

In Eqs. (4.13) and (4.14), subscript  $r$  denotes the reference direction and  $a_1$  and  $a_2$  are the first and second biaxial stress ratios, transverse stress over normal stress ( $\sigma_y / \sigma_x$ ) and shear stress over normal stress ( $\tau_{xy} / \sigma_x$ ), respectively.  $m_r$  and  $b_r$  are the parameters derived after fitting to the experimental data of the reference S-N curve.  $f$  and  $g$  are non-dimensional entities defined by

$$f(a_1, a_2, \theta) = \frac{\sigma_x(a_1, a_2, \theta)}{X_r} \quad (4.15)$$

$$g(R) = \frac{\sigma_{\max}(1-R)}{\sigma_{(\max)r} - \sigma_{(\min)r}} \quad (4.16)$$

where  $\sigma_x(a_1, a_2, \theta)$  is the static strength along the longitudinal direction,  $X_r$  is the static strength along the reference direction and  $\sigma_{(\max)r} - \sigma_{(\min)r}$  is the stress range applied to obtain the reference line.

The off-axis static strengths of the examined material can be estimated using any reliable multiaxial static failure criterion. While defining the model, Fawaz and Ellyin uses Tsai-Hill static failure criterion to determine  $\sigma_x(a_1, a_2, \theta)$ , thus  $f(a_1, a_2, \theta)$ . Function  $g$  is introduced to consider different stress ratios,  $R$  as seen in Equation (4.16). Note that  $g$  is equal to 1 when the stress ratio of the reference S-N curve is the same as that of the S-N curve being predicted ( $R = R_r$ ), and for  $R = 1$  (quasi-static loading),  $g = 0$ . The FWE criterion has the advantage of requiring only one S-N curve data. However, the predictions are very dependent to the selection of the reference curve [3].

#### 4.4. Sims-Brogdon (SB) Model

Sims-Brogdon (SB) [7] extended the Tsai-Hill static failure criterion to a fatigue criterion (fatigue life prediction model) by replacing the static strengths with corresponding fatigue functions. The expression of the model can be written as

$$\left(\frac{K_1}{\sigma_L}\right)^2 - \frac{K_1 K_2}{\sigma_L^2} + \left(\frac{K_2}{\sigma_T}\right)^2 + \left(\frac{K_{12}}{\sigma_S}\right)^2 = \frac{1}{\sigma_F^2} \quad (4.17)$$

where  $\sigma_L$ ,  $\sigma_T$  and  $\sigma_S$  denotes the fatigue functions (the corresponding S–N curve equations) along the longitudinal, the transverse directions and shear, respectively. The  $\sigma_F$  is laminate fatigue strength at any off-axis angle. The parameters  $K_1$ ,  $K_2$  and  $K_{12}$  are the ratios of the stresses along the principal material system over the lamina stress in the direction of the load,  $K_1 = \sigma_1 / \sigma$ ,  $K_2 = \sigma_2 / \sigma$  and  $K_{12} = \tau_{12} / \sigma$  in which  $\sigma$  is lamina stress in the direction of applied load.

The SB model refers to lamina fatigue strength and can be extended to laminates of any orientation using laminated plate theory and knowledge of the stresses in the individual lamina to predict first-ply fatigue failure (the number of cycles). However, the SB model has the same drawback as the Tsai-Hill criterion, which it does not take the different strengths of the material under tension and compression into account [3].

#### 4.5. Shokrieh-Taheri (ST) Model

Shokrieh and Taheri [11] proposed a strain energy-based model for predicting the fatigue life of unidirectional composite laminates at various fiber angles and stress ratios subjected to constant amplitude, tension-tension or compression-compression cyclic loading ( $R \geq 0$ ). They derived the ST model from the static failure criterion by Sandhu et al. [22]. They also adopted the assumption of El Kadi and Ellyin [23] that the relationship between fatigue life and total input energy can be described by the power law type of equation,

$$\Delta W^t = kN^\alpha + C \quad (4.18)$$

where  $k$ ,  $\alpha$  and  $C$  are material constants. Letting  $C = 0$ , and  $k$  and  $\alpha$  are independent of the stress ratio and fiber orientation, the total input energy is defined as

$$\Delta W^* = kN^\alpha \quad (4.19)$$

The proposed model in the on-axis coordinate system is given by the following equation:

$$\Delta W^* = \Delta W_I^* + \Delta W_{II}^* + \Delta W_{III}^* = \frac{\Delta \sigma_1 \Delta \varepsilon_1}{X \varepsilon_{u1}} + \frac{\Delta \sigma_2 \Delta \varepsilon_2}{Y \varepsilon_{u2}} + \frac{\Delta \sigma_6 \Delta \varepsilon_6}{S \varepsilon_{u6}} \quad (4.20)$$

where  $\Delta$  before a symbol indicates its range and  $\Delta W^*$  represents the sum of strain energy densities contributed by all stress components in material directions.  $\Delta W_I^*$ ,  $\Delta W_{II}^*$  and  $\Delta W_{III}^*$  denote the strain energy densities in the longitudinal, transverse and shear directions, respectively and can be expressed by the set of Eqs. (4.21):

$$\begin{aligned} \Delta W_I^* &= \frac{1}{X^2} \frac{(1+R)}{(1-R)} (\Delta \sigma_x)^2 (\cos^4 \theta) \\ \Delta W_{II}^* &= \frac{1}{Y^2} \frac{(1+R)}{(1-R)} (\Delta \sigma_x)^2 (\sin^4 \theta) \\ \Delta W_{III}^* &= \frac{1}{S^2} \frac{(1+R)}{(1-R)} (\Delta \sigma_x)^2 (\sin^2 \theta \cos^2 \theta) \end{aligned} \quad (4.21)$$

where  $X$ ,  $Y$  and  $S$  are the material static strengths;  $\sigma_1$ ,  $\sigma_2$ ,  $\sigma_6$ , and  $\varepsilon_1$ ,  $\varepsilon_2$ ,  $\varepsilon_6$  are stress and strain tensor components;  $\varepsilon_{u1}$ ,  $\varepsilon_{u2}$  and  $\varepsilon_{u6}$  are the maximum strains in the principal material directions.

Assuming a linear stress-strain response along the material directions, the conversion of off-axis stresses into the on-axis coordinate (Equation (4.20)) takes the form:

$$\Delta W^* = \frac{(1+R)}{(1-R)} (\Delta \sigma_x)^2 \left( \frac{\cos^4 \theta}{X^2} + \frac{\sin^4 \theta}{Y^2} + \frac{\sin^2 \theta \cos^2 \theta}{S^2} \right) \quad (4.22)$$

where  $\theta$  is the fiber orientation angle. Equation (4.22) is valid as long as  $R \geq 0$ .

The ST model uses both stress and strain to predict failure and only one set of data is required (and used as the reference set) for calibration of the model parameters. However, it seems that the model is only applicable to unidirectional laminates [3].

## CHAPTER 5

### EXPERIMENTAL CORRELATION

In this thesis, fatigue life prediction models will be applied to find optimum multidirectional laminates consisting of different fiber alignments. Hence, first of all, it is important to understand whether the related models can perform accurate fatigue life estimations of multidirectional laminates. In this regard, first, off-axis angle laminate predictions of E-glass/epoxy composite samples are obtained using the proposed models. Then, multidirectional laminate predictions of four different composite materials, graphite/epoxy, carbon/epoxy, E-glass/epoxy and carbon/PEEK are achieved using the proposed models.

All the estimations except off-axis laminates are performed by following a specific procedure. This procedure consists of two parts. The first part is related to the determination of the fatigue load range to be applied for the prediction. For this purpose, first, logarithmic fatigue lives ( $\log N$ ) corresponding to minimum and maximum stress amplitudes ( $\sigma_a$ ) are determined from the experimental data for the related laminate. Then, minimum and maximum cyclic load values corresponding to these fatigue lives are found by solving the related model equation (of which model we are using) for the outmost layer of the laminate. The outmost layer is considered in calculations since measurements in the experiments are taken from the outmost layer. Note that the principal stresses appear in the related model equation are calculated using the classical lamination theory (CLT). In the second part of the procedure, fatigue life of the laminate is simulated between the stress amplitude range using a formula including  $\log N$  parameter. This formula is shown in closed form below

$$f(\sigma_1, \sigma_2, \sigma_6, \log N) - 1 \leq 0 \quad (5.1)$$

For the related laminate, first, based on the outermost layer, stress amplitude range are calculated from the minimum and maximum loads determined in the first part using the CLT. Afterwards,  $\log N$  values corresponding to these principal stresses are obtained



by solving the relevant model equations. Thus, fatigue life for a given laminate is estimated.

Programming codes for off-axis and multidirectional predictions of composite laminates are given in Appendix A.

### 5.1. Off-Axis Angle Predictions

The fatigue behavior of unidirectional E-glass/epoxy laminae [5] is predicted using the proposed models for various fiber off-axis angle specimens, and the predictions of all models are shown in the same figure to compare their estimation capabilities with the experimental data. Input data for theoretical derivations are taken directly from reference [5]. The prediction curves (solid or dashed lines) of the various off-axis angles with the experimental data (Exp. data) specified with black circles are presented as stress amplitude ( $\sigma_a$ ) versus logarithmic fatigue life ( $\log N$ ) in Figures 5.1 - 5.5.

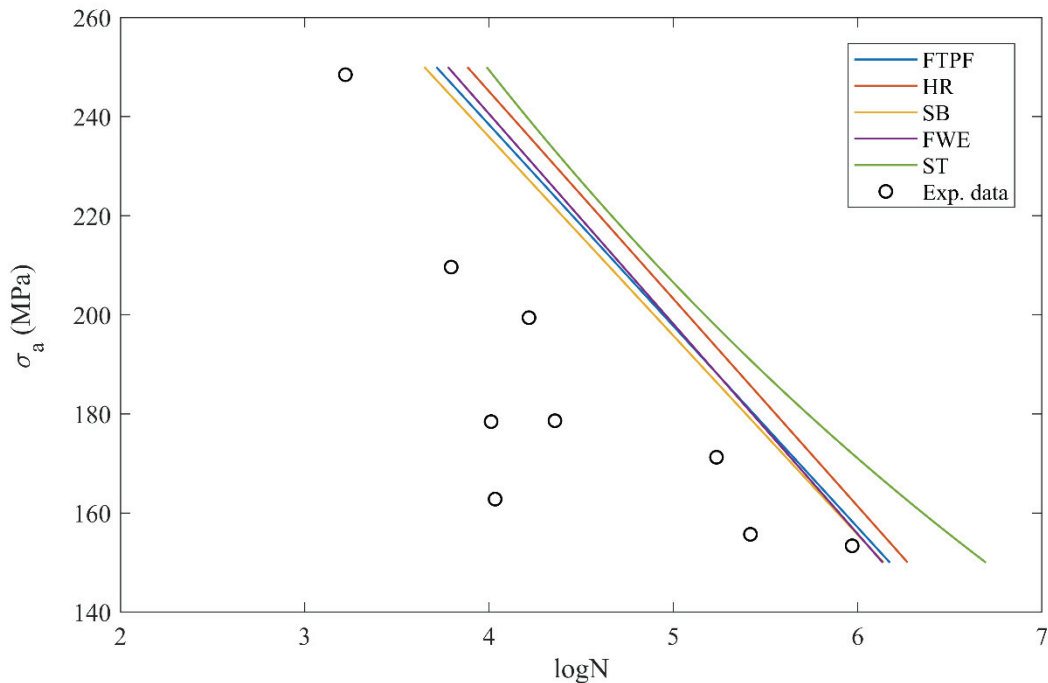


Figure 5.1. Predicted S-N curves for 5° off-axis angle

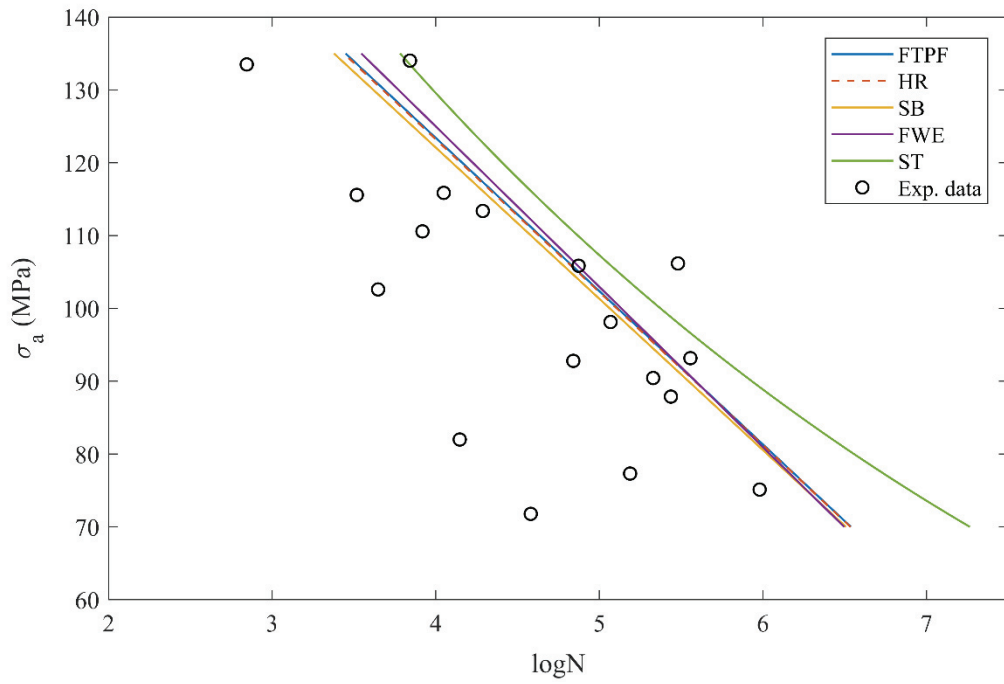


Figure 5.2. Predicted S-N curves for 10° off-axis angle

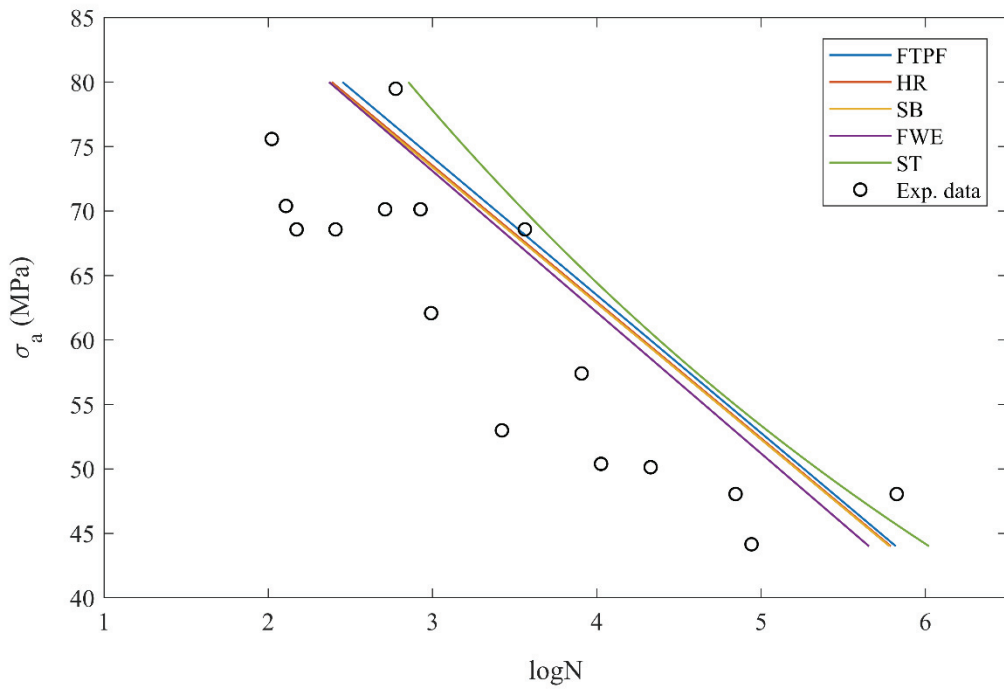


Figure 5.3. Predicted S-N curves for 20° off-axis angle

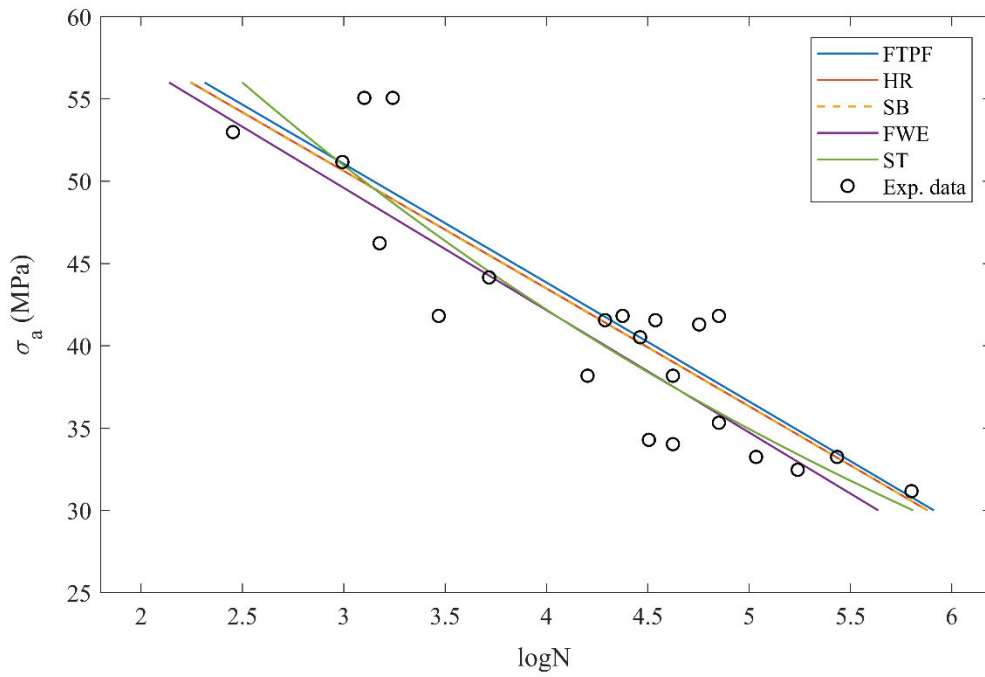


Figure 5.4. Predicted S-N curves for 30° off-axis angle

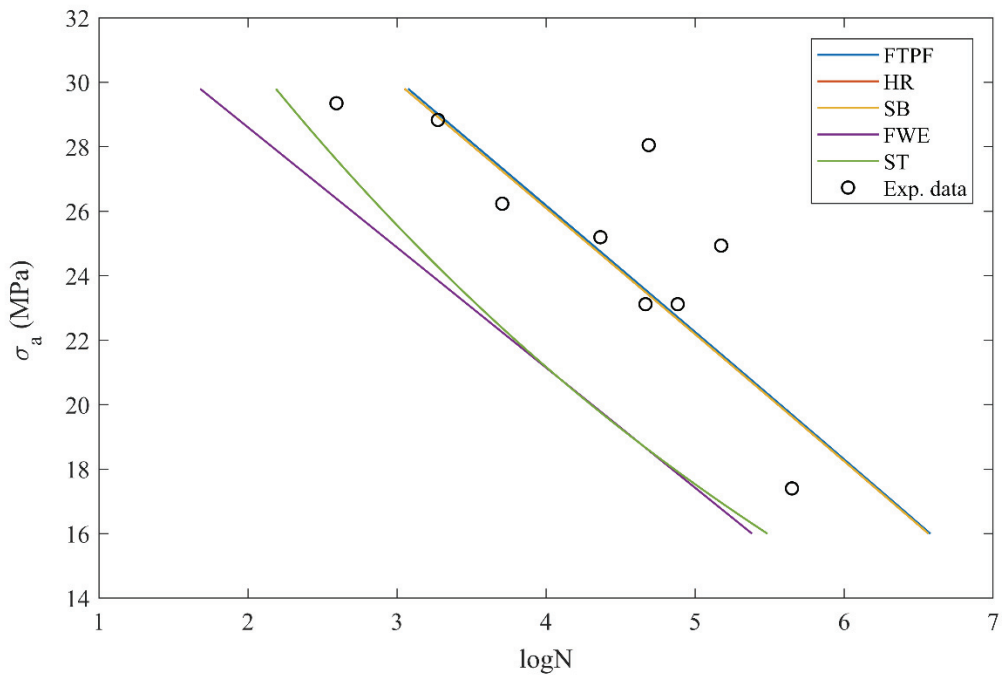


Figure 5.5. Predicted S-N curves for 60° off-axis angle

It is seen from the figures that the predictions of the models for unidirectional laminated composites are usually close to each other and in a good agreement with the experimental data. Particularly, the prediction curves for the off-axis 30° (Figure 5.4) simulate the fatigue behavior very well and for the off-axis 60° angle, FTFP, HR, and SB models predict the fatigue behavior good; however, FWE and ST models slightly underestimate the fatigue life.

## **5.2. Multidirectional Laminate Predictions for Various Materials**

The fatigue life predictions of different multidirectional composite laminates that include graphite/epoxy laminates [24], carbon/epoxy laminates [25], E-glass/epoxy laminates [26], and carbon/PEEK [27] are made by using the proposed models. Predictions of all the models are shown in the same figure for the related laminate configuration to make a comparison of their estimation capabilities. The fatigue life prediction curves are presented in Figures 5.6 – 5.16.

### **5.2.1. Graphite/Epoxy Composite Laminates**

Fatigue life predictions for multidirectional  $[0/90]_{4s}$  and  $[0/45/-45/90]_{2s}$  graphite/epoxy laminates ( $R = -1$ ) [24] are shown in Figures 5.6 and 5.7. ST model predictions could not be performed since the method restricts the use for negative  $R$  values. In the figures, also, first ply and final failure predictions of Ertas and Sonmez [14] obtained by FWE method are included to give an idea about our prediction performance. It is noted that the reference curve of  $[\pm 45]_{4s}$  laminate is selected for the predictions of FWE method. The programming code to obtain the S-N curve in Figure 5.6 is presented in the Appendix A.

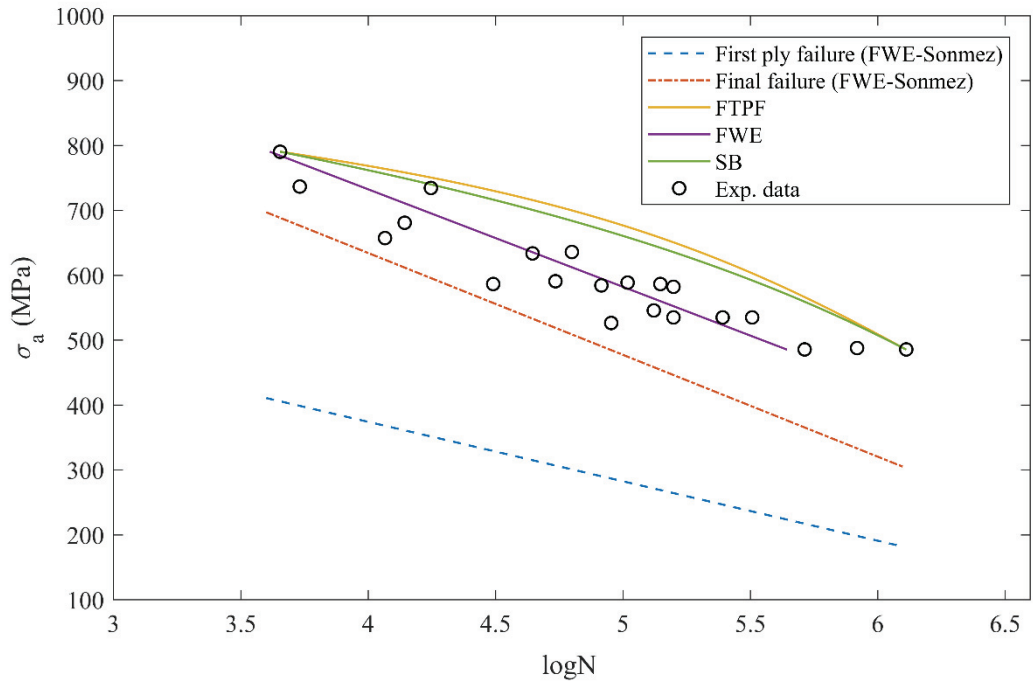


Figure 5.6. Fatigue life predictions for  $[0/90]_{4s}$  graphite/epoxy laminate

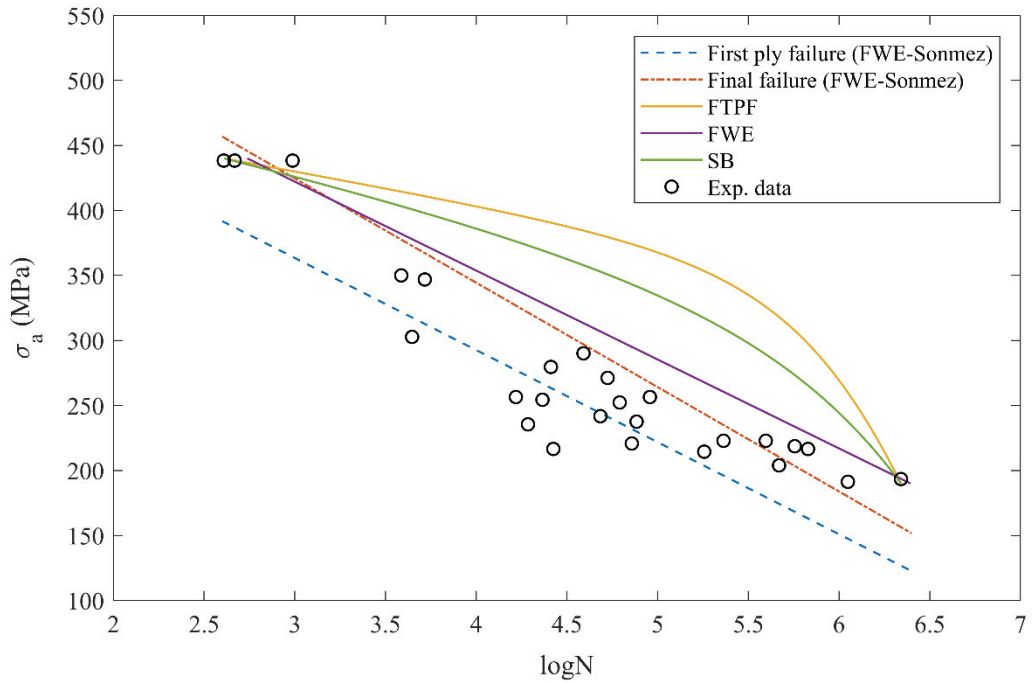


Figure 5.7. Fatigue life predictions for  $[0/45/-45/90]_{2s}$  graphite/epoxy laminate

It is seen from Figure 5.6 that the prediction of FWE on the  $[0/90]_{4s}$  laminate is better than the predictions of Ertas and Sonmez [14], and the related curve is in a good agreement with the experimental data. However, FTPF and SB slightly overestimate the experimental data.

Figure 5.7 shows the fatigue life predictions for  $[0/45/-45/90]_{2s}$  laminate. As seen in the figure, the prediction of FWE is in good agreement with the experimental data. Nevertheless, FTPF and SB methods overestimate the data to some degree.

### 5.2.2. Carbon/Epoxy Composite Laminates

Fatigue life predictions for  $[0/90_2]_s$ ,  $[0/90_4]_s$ ,  $[0_2/90_2]_s$  and  $[0/45/-45/90]_s$  carbon/epoxy laminates under tension-tension fatigue testing (stress ratio,  $R = 0.1$ ) [25] are shown in Figures 5.8 – 5.11, respectively. It is noted that the reference curve of  $[\pm 45]_{2s}$  laminate is selected for the predictions of FWE and ST methods.

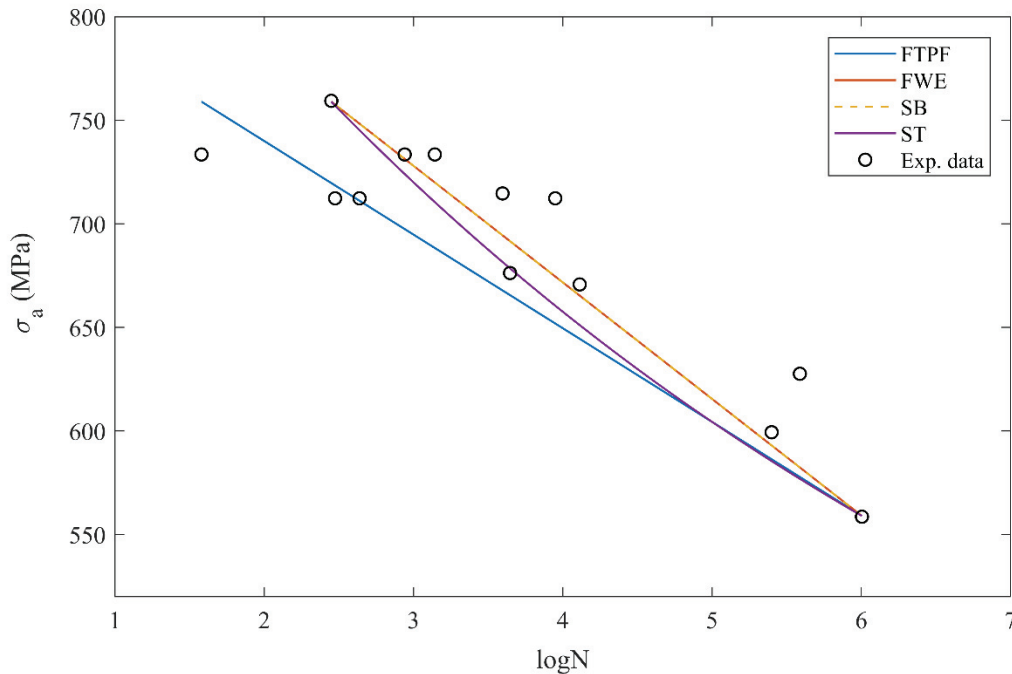


Figure 5.8. Fatigue life predictions for  $[0/90_2]_s$  carbon/epoxy laminate

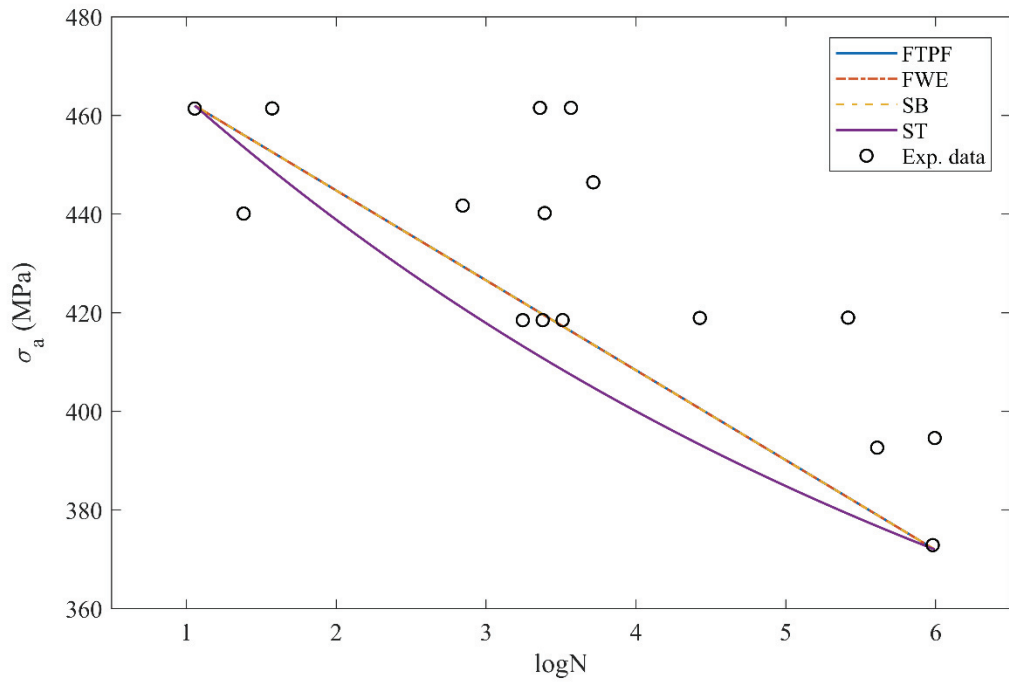


Figure 5.9. Fatigue life predictions for  $[0/90_4]_s$  carbon/epoxy laminate

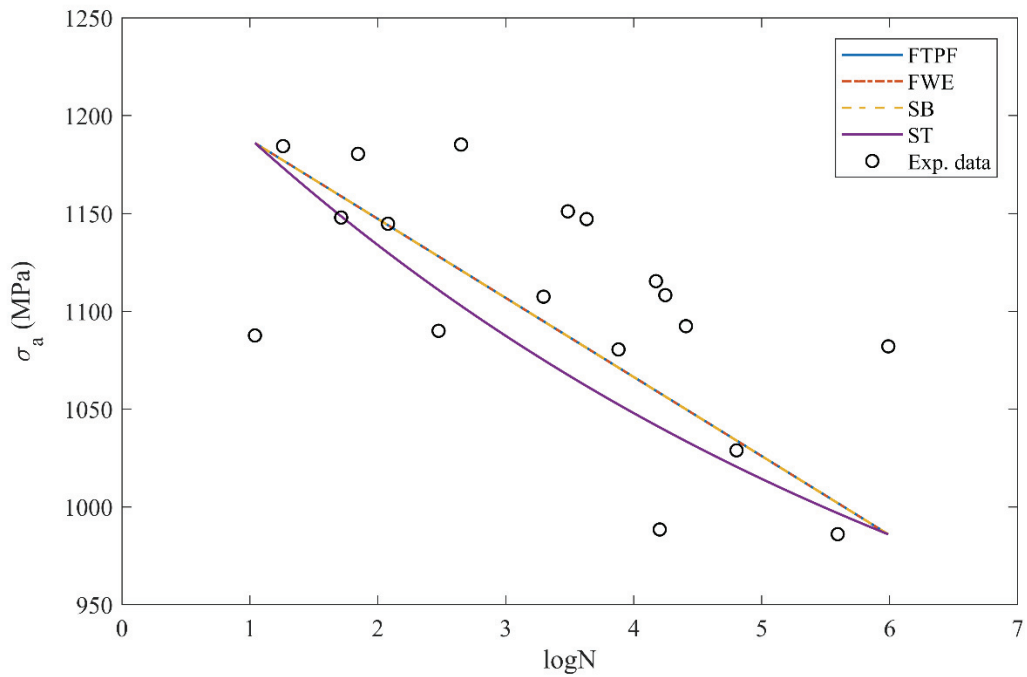


Figure 5.10. Fatigue life predictions for  $[0_2/90_2]_s$  carbon/epoxy laminate

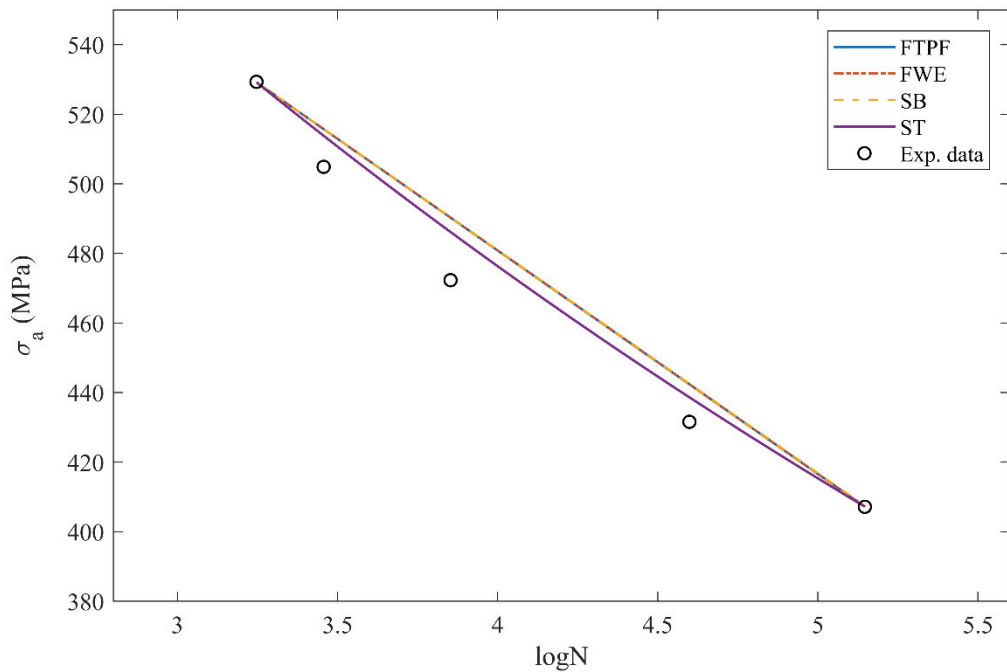


Figure 5.11. Fatigue life predictions for  $[0/45/-45/90]_s$  carbon/epoxy laminate

It can be said that all the predictions obtained from the models are very close to each other or the same except the predictions of ST model, and the predictions are in good agreement with the experimental data considering the slope of the curves and dispersion range of the experimental data.

### 5.2.3. E-glass/Epoxy Composite Laminates

In Figures 5.12 – 5.14, fatigue life predictions for  $[0/90/90/0]_s$ ,  $[45/90/-45/0]_s$  and  $[45/0/0/-45]_s$  E-glass/epoxy laminates under zero-tension fatigue testing ( $R = 0$ ) [26] are presented, respectively. It can be noted that the reference curve of  $[\pm 45]_{2s}$  laminate is selected for the predictions of FWE and ST methods.



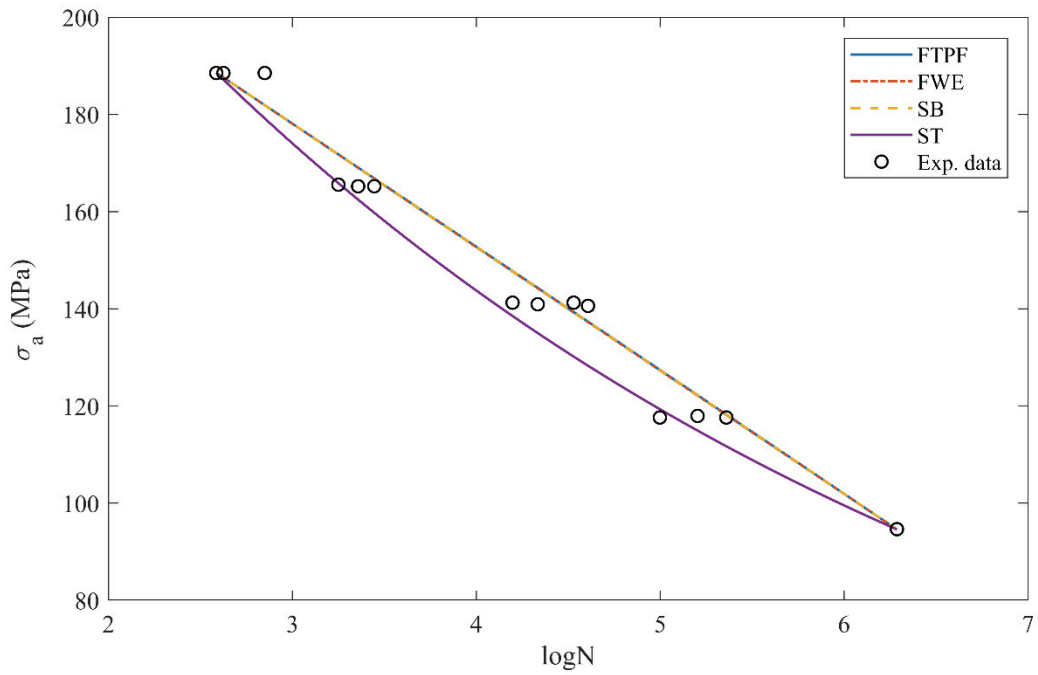


Figure 5.12. Fatigue life predictions for  $[0/90/90/0]_s$  E-glass/epoxy laminate

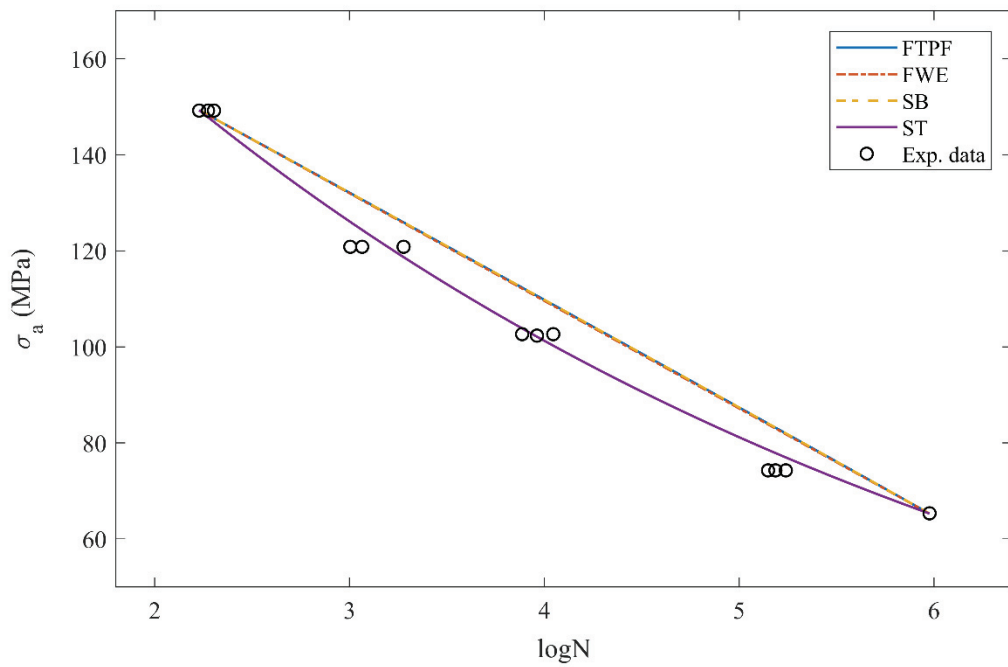


Figure 5.13. Fatigue life predictions for  $[45/90/-45/0]_s$  E-glass/epoxy laminate

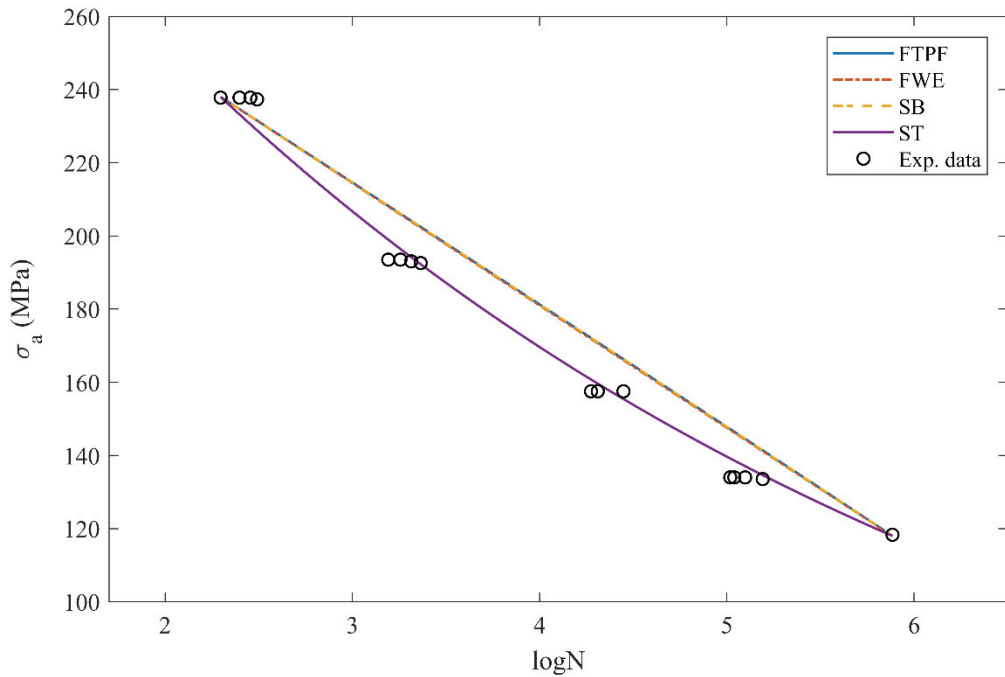


Figure 5.14. Fatigue life predictions for  $[45/0/0/-45]_s$  E-glass/epoxy laminate

It is seen from the figures that the estimations of the models except the ST model are exactly the same and in general all the predictions are in good agreement with the experimental data. The predictions of the ST model fit the data very well for the  $[45/90/-45/0]_s$  and  $[45/0/0/-45]_s$  laminates. This situation can be related to the selection of  $[\pm 45]_{2s}$  laminate as the reference curve.

#### 5.2.4. Carbon/PEEK Composite Laminates

Fatigue life predictions for  $[0/90]_{4s}$  and  $[0/45/90/-45]_{2s}$  carbon/PEEK laminates under zero-tension fatigue testing (stress ratio,  $R = 0$ ) [27] are shown in Figures 5.15 and 5.16, respectively. It is noted that the reference curve of  $[\pm 45]_{4s}$  laminate is selected for the predictions of FWE and ST methods.

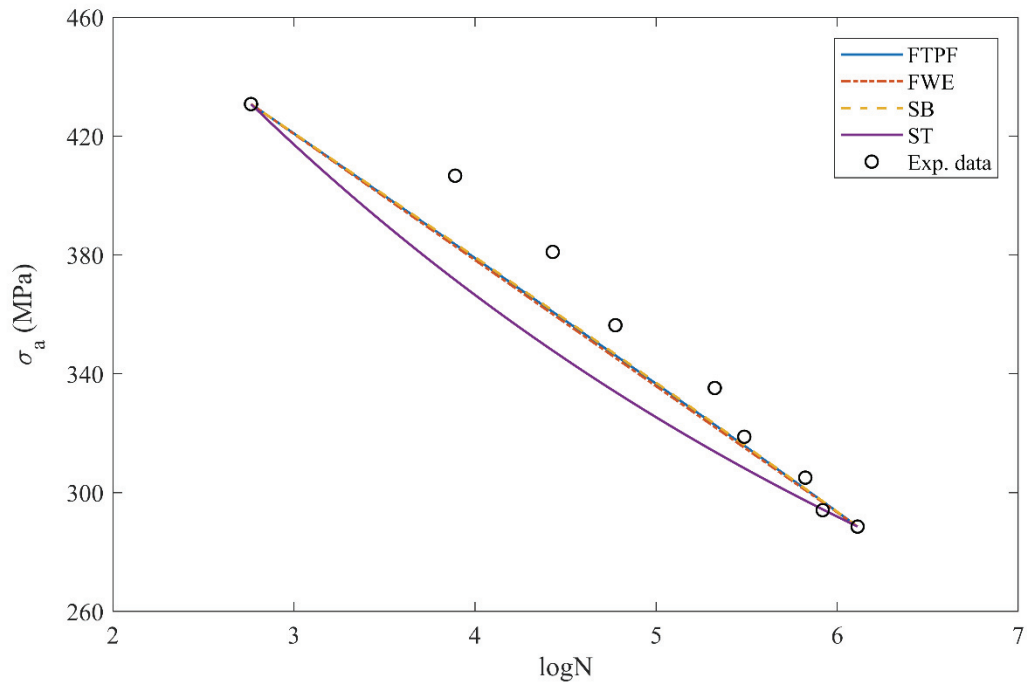


Figure 5.15. Fatigue life predictions for  $[0/90]_{4s}$  carbon/PEEK laminate

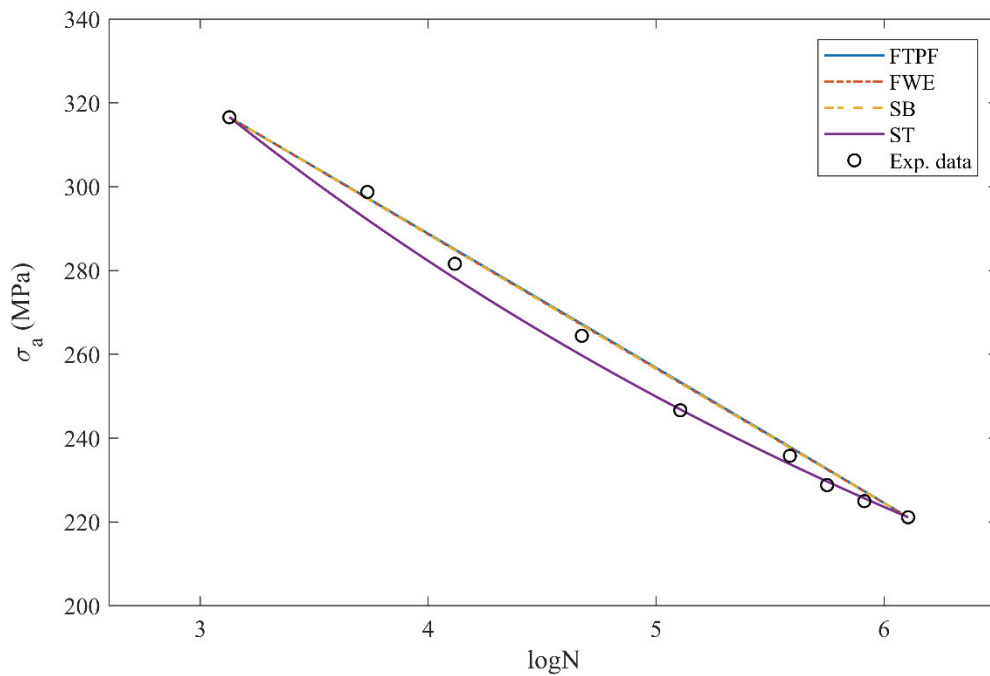


Figure 5.16. Fatigue life predictions for  $[0/45/90/-45]_{2s}$  carbon/PEEK laminate

From the figures, it is seen in general that the predictions of FTPF, FWE and SB models are the same. For the  $[0/90]_{4s}$  laminate, the predictions of FTPF, FWE and SB are in better agreement with the experimental data than the one of ST. For the  $[0/45/90/-45]_{2s}$  laminate, all the predictions are closely estimate the experimental data.

It can be inferred from this correlation study that all the predictions show that any method is not obviously superior to the other. Besides, the predictions of FTPF, SB and FWE models are mostly the same and reliable when all the predictions are evaluated together.

## CHAPTER 6

### OPTIMIZATION

#### 6.1. Introduction

Optimization is commonly used, from engineering design to financial markets, from our daily activity to planning our holidays, and computer sciences to industrial applications. People always tend to maximize or minimize something. In fact, we are continuously searching for the optimal solutions to every problem we face even if it is not necessary to find such solutions [28].

In a mathematical manner, optimization is the act of obtaining the best result under given conditions. The ultimate purpose in design of any engineering system is either to minimize the effort required or to maximize the desired benefit. Since the effort required or the benefit anticipated in any practical situation can be expressed as a function of certain decision variables, optimization can be defined as the process of finding the conditions that give the maximum or minimum value of a function. As an example, Figure 6.1 shows how a maxima and minima of an objective function can be expressed. Accordingly, if a point  $x^*$  corresponds to the minimum value of function  $f(x)$ , the same point also corresponds to the maximum value of the negative of the function,  $-f(x)$ . Consequently, without loss of generality, optimization can be taken to mean minimization because the maximum of a function can be found by searching for the minimum of the negative of the same function [29].

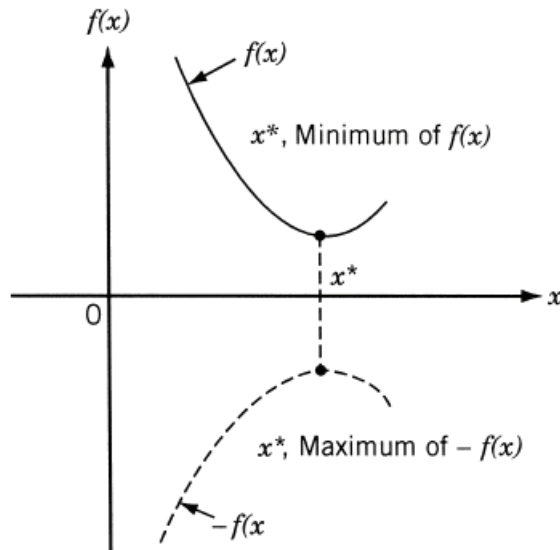


Figure 6.1. Minimum and maximum of an objective function ( $f(x)$ )  
(Source: Rao, 2009)

In Table 6.1, optimization techniques are generally classified by listing various many mathematical programming methods together with other well-defined areas of operations research.

Table 6.1. Methods of operations research  
(Source: Rao, 2009)

<b>Mathematical programming (optimization) methods</b>	<b>Stochastic process methods</b>	<b>Statistical methods</b>
Calculus methods	Statistical decision theory	Regression analysis
Calculus of variations	Markov processes	Cluster analysis, pattern recognition
Nonlinear programming	Queueing theory	Design of experiments
Geometric programming	Renewal theory	Discriminate analysis
Quadratic programming	Simulation methods	
Linear programming	Reliability theory	
Dynamic programming		
Integer programming		
Stochastic programming		
Separable programming		
Multiobjective programming		
Network methods: CPM and PERT		
Game theory		

(Cont. on next page)

Table 6.2 (Cont.)

---

<b>Modern optimization methods</b>
Genetic algorithm
Simulated annealing
Ant colony optimization
Particle swarm optimization
Neural networks
Fuzzy optimization

---

As seen from Table 6.1, optimization methods can be divided into two major categories. These are deterministic algorithms and stochastic algorithms. Deterministic algorithms use a complicated procedure. They are based on mathematical programming whose path and values of both design variables and the functions are repeatable. However, stochastic algorithms always have randomness and apply approximate procedures to find global optima.

In general, there are two types for stochastic algorithms: heuristic and metaheuristic. The difference between them is minor. Heuristic's word meaning is 'to find' or 'to discover by trial and error'. In the operations performed using heuristic algorithms, quality solutions for tough optimization problems can be found in reasonable amount of time, though optimal solutions are not guaranteed. Stochastic algorithms typically perform well for many problems. Nevertheless, they sometimes stuck to local solutions. This is good enough when decent solutions easily reachable are preferable instead of the best solutions.

The stochastic algorithms further improved are called as metaheuristic algorithms. "Meta" prefix means 'beyond' or 'higher level'. Metaheuristic algorithms usually work better than simple heuristics. They basically use processes as specific adjustment of randomization and local search. It should be noted in this point that there are not agreed definitions of heuristics and metaheuristics in literature. Both can be used alternately, however all stochastic algorithms with randomization and local search are lately started to name as metaheuristic. Randomization provides a good way to escape from local search to the global search. Consequently, it can be said that almost all metaheuristic algorithms are suitable for global optimization [28].

The mathematical programming methods represented in Table 6.1 are capable in finding the minimum of a function with several variables under a described set of constraints. The other class, stochastic search methods are suitable to analyze problems defined by a set of random variables which include known probability distributions. Statistical methods firstly analyze the experimental data and then build empirical models to achieve the most accurate representation of the physical situation. On the other hand, the modern optimization methods have been developed in last few decades as powerful and popular methods for solving complex engineering optimization problems. Outstanding examples of these optimization methods are genetic algorithm, simulated annealing, particle swarm optimization, ant colony optimization, neural network-based optimization, and fuzzy optimization [29].

## 6.2. Basic Definition of an Optimization Problem

An optimization or a mathematical programming problem can be defined as follows

$$\text{Find } X = \begin{Bmatrix} x_1 \\ x_2 \\ \vdots \\ x_n \end{Bmatrix} \text{ which minimizes } f(x) \quad (6.1)$$

subject to the constraints

$$\begin{aligned} g_i(X) &\leq 0, & i = 1, 2, \dots, m \\ l_i(X) &= 0, & i = 1, 2, \dots, p \end{aligned}$$

where  $X$  is an  $n$ -dimensional vector called the design vector,  $f(X)$  is termed the objective function, and  $g_i(X)$  and  $l_i(X)$  are known as inequality and equality constraints, respectively. The number of variables  $n$  and the number of constraints  $m$  and/or  $p$  are not necessary to be related in any way. The optimization problem stated in Equation (6.1) is called a constrained optimization problem. There are not any constraints in some optimization problems and they are called as unconstrained optimization problems [29].



## **6.3. Metaheuristic Algorithms**

Metaheuristic algorithms emerged in the 1970s as a new class of general approximate algorithms. They are basically constituted to combine constructive heuristics and/or local search methods with other ideas in higher-level frameworks. Thus, they can effectively explore a search space to find an optimal or near-optimal solution. The significant point of metaheuristics is that they all have solution mechanisms for escaping from local minima. They are extensions of constructive heuristics and local search methods, exploring the search spaces of the tackled problems in less limited ways [30].

In general, metaheuristic algorithms apply approximate solutions to optimization problems that are not specifically expressed for a problem. We can address these algorithms as single and hybrid algorithms separately.

### **6.3.1. Single Algorithms**

Single algorithms are the individual metaheuristic algorithms having good capability to solve complicated problems involving many variables alone. Ant colony optimization, artificial bee colony, evolutionary algorithms, greedy heuristics, local search, pattern search, particle swarm optimization, simulated annealing and tabu search are the outstanding examples of the class of metaheuristic algorithms. Each of these metaheuristic algorithms has its own phenomenological background. While some metaheuristics are inspired by natural processes such as evolution or the shortest-path-finding behavior of ant colonies, others are the extensions of less sophisticated algorithms such as greedy heuristics, local search and pattern search.

### **6.3.2. Hybrid Algorithms**

Hybrid methods combining two different metaheuristic approaches have been used by the researchers to take advantages of each powerful side of the optimization algorithms to be used [31-32]. For this purpose, first, the initial algorithm is applied to obtain a point close to the global minimum, and then the other chosen algorithm is applied to refine and improve the result obtained by the initial algorithm, thus, global convergence can be more guaranteed depending on the nature of the problem.

The main motivation of the hybridization of different algorithms is to utilize the complementary characteristics of different optimization processes. In other words, hybrids can benefit from synergy of different algorithms. Many complex optimization problems can be solved in the best possible way by choosing an accurate combination of complementary algorithms. However, developing an effective hybrid approach is generally a difficult task and requires expertise from different areas of optimization. Furthermore, it is shown in the literature that while a certain hybridization might work well for some type of problems, it might perform poorly for others. Nevertheless, the literature covers the hybridization types which that have been shown to be successful for many applications. These hybrid algorithms can lead up to new improvements.

Hybrid algorithm studies are relatively current. In the first two decades of metaheuristics research area, different research communities working on metaheuristic models studied together without much interaction among themselves and the Operations Research community, because studying on pure metaheuristics provided considerable success for many problems. However, the attempt to be different from the traditional operations research caused the ignorance of the valuable optimization expertise collected over the years. Only after pure metaheuristics had reached their limits, a growing number of researchers turned towards the advance of hybrid metaheuristics [30].

#### **6.4. GA-GPSA Hybrid Algorithm**

As a modern evolutionary algorithm technique, genetic algorithm (GA) provides important advantages against traditional optimization algorithms, such as robustness to problem complexity and the ability to easily discover global optimum rather than local stationary optima. Nevertheless, standard GA has the disadvantages of slow convergence rates when they work with complicated or time-consuming objective functions, being stuck with local optima, and the lack of cooperation between populations. In order to overcome these weak points, some hybrid methods combining two different metaheuristic approaches have been used by the researchers to take advantages of each powerful side of these approaches [31-32]. For this purpose, first, GA is applied to obtain a point close to the global minimum, and then the other chosen algorithm is applied to refine and improve the result obtained by GA, thus, global convergence can be more guaranteed depending on the nature of the problem [33]. Accordingly, in this study, the combination

of GA and generalized pattern search algorithm (GPSA) is considered as the hybrid algorithm to achieve a high accuracy rate in our results. In the following sections, brief information about each algorithm is given.

GA is a widely-used heuristic algorithm developed by John Holland [34] in the solution of laminated composite problems. GA utilizes the natural selection process which ends up with the evolution of organisms best adapted to the environment. GA begins its search with a population of random individuals, and the process is carried out by applying operators similar to natural genetic processes, which are called as selection, crossover, mutation and replacement. The process is iterated over many generations until final optimal designs are obtained [29].

GPSA on the other hand is a derivative-free optimization method developed by Torczon [35] for unconstrained optimization of functions and later extended to cover nonlinear constrained optimization problems. As opposed to the traditional local optimization methods that use information about the gradient or partial derivatives to search for an optimal solution, GPSA is a direct search method which finds a sequence of points  $x_i$  that approach the global optimal point through many iterations. Each iteration consists of two phases: the search phase and the poll phase. In the search phase, the objective function is evaluated at a finite number of points on a mesh to find a new point with a lower objective function value than the best current solution. In the poll phase, the objective function is evaluated at the neighboring mesh points to see if a lower objective function value can be obtained [36].

The optimization procedure which describes how GPSA works and interacts with GA in the hybrid algorithm is given in Figure 6.2 and explained step by step as follows:

**Step 1.** GA runs until either the maximum number of iterations is reached or there is no improvement in the fitness value.

**Step 2.** When GA terminates, the reached optimal solution is used as an initial point for GPSA to search.

**Step 3.** GPSA starts its search with an initial solution  $x_0$  and an initial mesh size  $\Delta_0^m$ .

**Step 4.** If the search phase satisfies a solution with a lower objective function value than the best current solution, the algorithm stops.

**Step 5.** If termination criteria not satisfied, the algorithm goes to the poll phase and generates a set of neighboring mesh points  $x_i^m$  by multiplying the current mesh size by each pattern vector  $\{d_i\}$ . The fixed-direction pattern vectors are used to determine the

points to search at each iteration and defined by the independent variables in the objective function; commonly the maximal basis with  $2N$  vectors consisting of  $N$  positive and  $N$  negative vectors, and the minimal basis with  $N + 1$  vectors.

**Step 6.** In the polling step at  $k$ th iteration, GPSA polls all the mesh points by computing their objective function values  $f(x_i^m)$  in order to find an improved point.

**Step 7.** If the poll is successful, which means an improved point is found, the current mesh size is multiplied as  $\Delta_{i+1}^m = 2\Delta_i^m$ , and the current point is updated by the new mesh size for the next iteration  $k + 1$ . If the polling fails to find an improved point, the mesh size is reduced by  $\Delta_{i+1}^m = 0.5\Delta_i^m$ , and this current point is used for the next iteration.

This process continues through many iterations until global optimum is reached.

In the first fatigue optimization study, this hybrid GA-GPSA algorithm is used in fatigue optimization problems. MATLAB R2016a Optimization Toolbox is used to constitute the hybrid algorithm [37]. In the literature, different (single or hybrid) approaches have already been used for the modeling of the fatigue life of composite materials. For example, a genetic programming method that finally evolves a computer program is used in [38] for modeling the fatigue life of various laminated composite materials. Also, artificial neural networks based methods are commonly used for fatigue life modeling of different unidirectional and multidirectional laminated composites [39-42]. Furthermore, some hybrid methods are used to predict the fatigue life of glass fiber reinforced composites. For example, a hybrid method combining artificial neural networks and fuzzy logic is used for modeling fatigue behavior of unidirectional glass/epoxy composites in [43]. However, there is not any study in the literature on fatigue life modeling and/or optimization study by hybridization of heuristic algorithms. In this regard, the proposed hybrid GA-GPSA algorithm brings a novel approach to the solution of optimization problems for fatigue life advance of laminated composites.

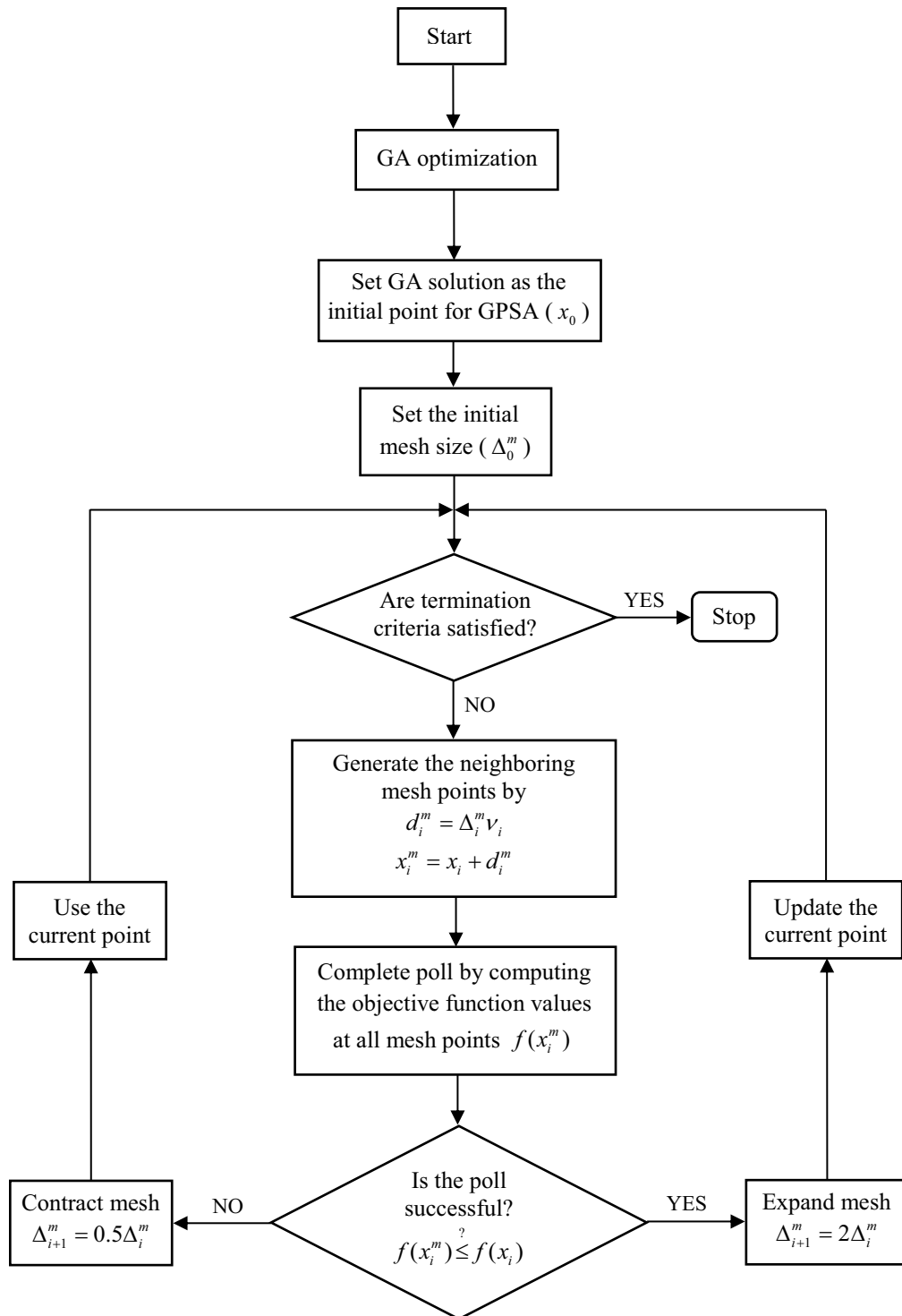


Figure 6.2. Flowchart of the hybrid GA-GPSA optimization

### 6.4.1. Algorithm Performance

A buckling optimization problem previously studied [44-45] was considered as a test problem and solved with the selected options to evaluate the performance of the hybrid algorithm in terms of best stacking sequences giving maximum critical buckling load factor. The results of the hybrid algorithm are compared with the known best results studied by different hybrid algorithms in the literature [46-49]. Table 6.2 shows the details of composite plate dimensions  $a$  and  $b$ , and in-plane loads  $N_{xx}$  and  $N_{yy}$  for the load cases. The optimum critical buckling load factors for all the load cases are compiled from the literature and presented together with the present critical buckling load factor and stacking sequence results in Table 6.3.

Table 6.2. Load cases for test problem

Load case	Number of plies	$a$ (mm)	$b$ (mm)	$N_{xx}$ (N/mm)	$N_{yy}$ (N/mm)
1	48	508	127	17.5	2.2
2	48	508	127	17.5	4.4
3	48	508	127	17.5	8.8
4	64	508	254	17.5	17.5

Table 6.3. Performance results of the GA-GPSA hybrid algorithm

Load Case	$\lambda_{cb}^{[46-49]}$ ([lbf/in <sup>3</sup> ]/[lbf/in <sup>3</sup> ])	$\lambda_{cb}^{present}$ ([lbf/in <sup>3</sup> ]/[lbf/in <sup>3</sup> ])	Stacking sequence <sup>present</sup>
1	16120.38	20950.55	$[90_4 / (\pm 45_2 / 90_2)_2 / \pm 45_3 / 90_2]_s$
	16119.48	20920.39	$[90_2 / (90_2 / \pm 45)_2 / \pm 45_5 / 90_2 / \pm 45]_s$
	16087.83	20894.53	$[90_4 / \pm 45_3 / 90_4 / \pm 45_5]_s$
2	13442.04	15961.75	$[90_4 / \pm 45 / (90_2 / \pm 45_2)_2 / \pm 45_3]_s$
	13441.28	15729.07	$[90_2 / (90_2 / \pm 45)_2 / \pm 45_4 / 90_2 / \pm 45_2]_s$
	13435.94	15512.55	$[90_4 / \pm 45_2 / 90_2 / \pm 45_7]_s$
3	10003.53	10591.61	$[90_2 / \pm 45 / 90_2 / (90_2 / \pm 45)_2 / \pm 45_4 / 90_2]_s$
	10002.95	10460.19	$[90_2 / (90_2 / \pm 45)_2 / \pm 45_5 / 90_2 / \pm 45]_s$
	9999.45	10343.85	$[(90_2 / \pm 45)_3 / \pm 45 / 90_2 / \pm 45_4]_s$
4	3973.01*	3973.01	$[90_{10} / \pm 45 / 90_2 / \pm 45_7 / 90_2 / \pm 45]_s$
	3973.00*	3973.00	$[90_4 / (90_2 / \pm 45)_3 / 90_8 / \pm 45 / 90_6]_s$

\* The optimum values calculated from the reference stacking sequences.

In Table 6.3, the critical buckling load factor ( $\lambda_{cb}$ ) results are given in British units to provide consistency with the literature. Ply contiguity constraint for stacking sequences is applied to the first three load cases. Besides, stacking sequences are subjected to symmetry and balance constraints. In order to provide an average quality of solutions, each load case is performed 100 times with different starting points. It can be seen from the table that  $\lambda_{cb}$  values for the test problem are found superior to the results given in the literature for load cases 1, 2 and 3. In load case 4, the same results are obtained for the first and second optima.  $\lambda_{cb}$  values denoted with asterisk sign are the real optimum values calculated from the stacking sequence designs given by the related references. It can be noted that  $\lambda_{cb}$  values found by [46-49] are possibly misrepresented due to round of error in their optimization procedures. This test study implies that the hybrid algorithm shows very good performance in searching the design space for laminated composite optimization and has capability to yield the best possible results for the fatigue optimization studies.

## 6.5. PSA - GPSA Hybrid Algorithm

In the second optimization study, a different hybrid algorithm is constituted using MATLAB R2016b Optimization Toolbox [50]. Generalized pattern search algorithm (GPSA) is hybridized with particle swarm algorithm (PSA). The combination of GPSA and PSA is considered to achieve a high accuracy rate in our results. The initial algorithm is PSA, and the GPSA runs after the PSA terminates in each iteration. Since information about GPSA is provided previously, only brief information about particle swarm algorithm is given in the following part.

Particle swarm is a population-based algorithm. In this respect, it is similar to the genetic algorithm. A collection of individuals called particles move in steps throughout a region. At each step, the algorithm evaluates the objective function at each particle. After this evaluation, the algorithm decides on the new velocity of each particle. The particles move, then the algorithm reevaluates. The inspiration for the algorithm is flocks of birds or insects swarming. Each particle is attracted to some degree to the best location it has found so far, and also to the best location any member of the swarm has found. After some steps, the population can coalesce around one location, or can coalesce around a few locations, or can continue to move [51].

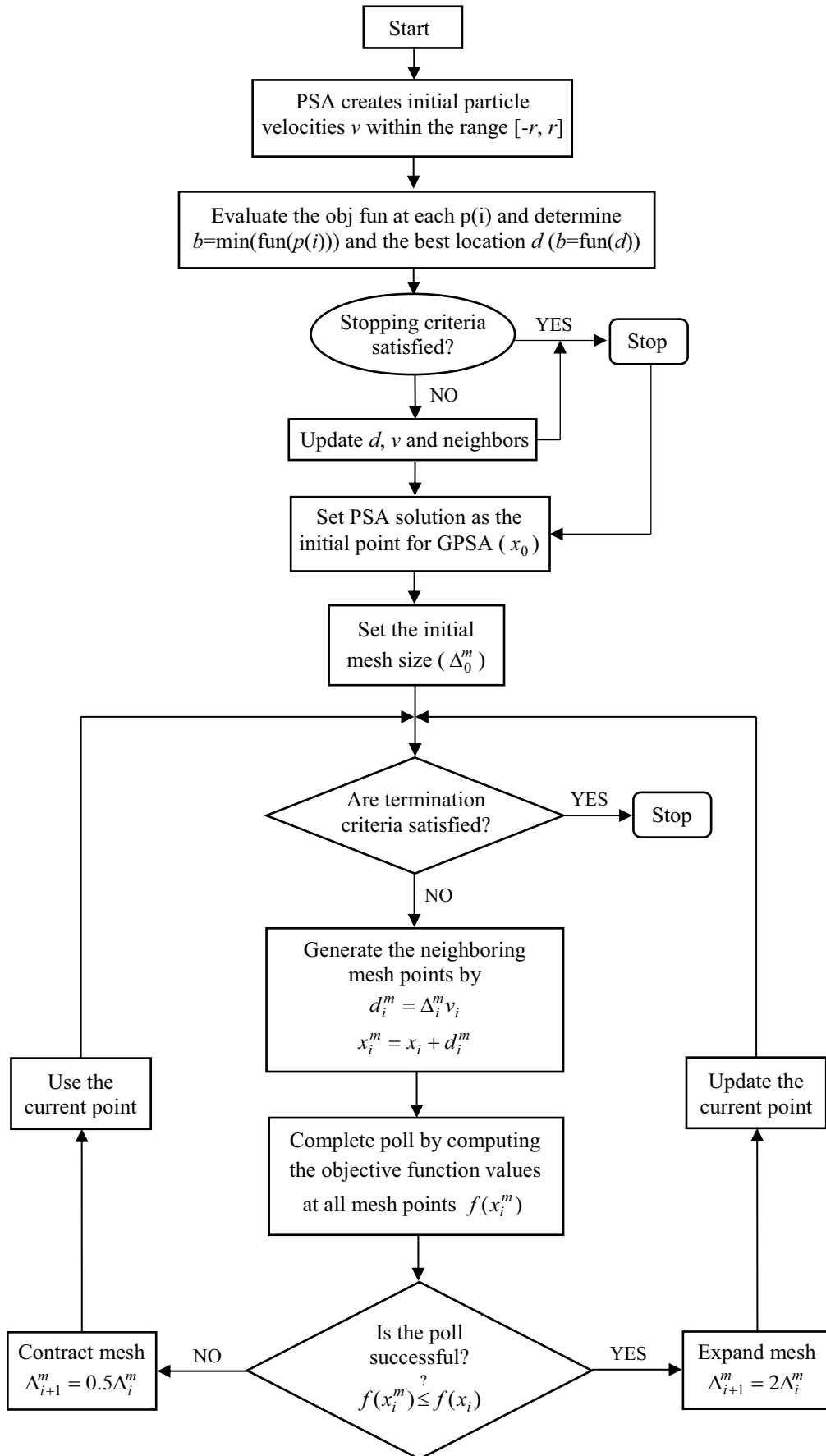


Figure 6.3. Flowchart of the hybrid PSA-GPSA optimization



The optimization procedure which describes how PSA works and interacts with GPSA in the hybrid algorithm is given in Figure 6.3 and explained step by step as follows:

**Step 1.** PSA begins by creating the initial particles, and assigning them initial velocities  $v$  uniformly within the range  $[-r, r]$ , where  $r$  is the vector of initial ranges.

**Step 2.** It evaluates the objective function at each particle location  $p(i)$  of each particle  $i$ , and determines the best (lowest) function value  $b = \min(\text{fun}(p(i)))$  and the best location  $d$ .

**Step 3.** It chooses new velocities, based on the current velocity, the particles' individual best locations, and the best locations of their neighbors.

**Step 4.** It then iteratively updates the particle locations (the new location is the old one plus the velocity, modified to keep particles within bounds), velocities, and neighbors.

**Step 5.** Iterations proceed until the algorithm reaches a stopping criterion.

**Step 6.** When the PSA terminates, the reached optimal solution is used as an initial point for GPSA to search.

**Step 7.** GPSA starts its search with the initial solution  $x_0$  and an initial mesh size  $\Delta_0^m$ .

**Step 8.** If the search phase satisfies a solution with a lower objective function value than the best current solution, the algorithm stops.

**Step 9.** If termination criteria not satisfied, the algorithm goes to the poll phase and generates a set of neighboring mesh points  $x_i^m$  by multiplying the current mesh size by each pattern vector  $\{d_i\}$ . The fixed-direction pattern vectors are used to determine the points to search at each iteration and defined by the independent variables in the objective function; commonly the maximal basis with  $2N$  vectors consisting of  $N$  positive and  $N$  negative vectors, and the minimal basis with  $N + 1$  vectors.

**Step 10.** In the polling step at  $k$ th iteration, GPSA polls all the mesh points by computing their objective function values  $f(x_i^m)$  in order to find an improved point.

**Step 11.** If the poll is successful, which means an improved point is found, the current mesh size is multiplied as  $\Delta_{i+1}^m = 2\Delta_i^m$ , and the current point is updated by the new mesh size for the next iteration  $k + 1$ . If the polling fails to find an improved point, the mesh size is reduced by  $\Delta_{i+1}^m = 0.5\Delta_i^m$ , and this current point is used for the next iteration.

This process continues through many iterations until global optimum is reached.

There is not any other study except [16] in the literature on fatigue life modeling and/or optimization study by hybridization of heuristic algorithms. In this regard, the proposed hybrid PSA-GPSA algorithm brings a new approach to the solution of optimization problems for fatigue life advance of laminated composites.

### 6.5.1. Algorithm Performance

The buckling optimization problem [44-45] previously mentioned was considered as a test problem again and solved with the selected options to evaluate the performance of the hybrid algorithm in terms of best stacking sequences giving maximum critical buckling load factor. The results of the hybrid algorithm are compared with the best-known results studied by different hybrid algorithms in the literature [46-49]. The details of composite plate dimensions  $a$  and  $b$ , and in-plane loads  $N_{xx}$  and  $N_{yy}$  for the load cases were given in Table 6.2.

The optimum critical buckling load factors for all the load cases are compiled from the literature and presented together with the present critical buckling load factor and stacking sequence results in Table 6.4.

Table 6.4. Performance results of the PSA-GPSA hybrid algorithm

Load Case	$\lambda_{cb}^{[46-49]}$ ([lbf/in <sup>3</sup> ]/ [lbf/in <sup>3</sup> ])	$\lambda_{cb}^{[16]}$ ([lbf/in <sup>3</sup> ]/ [lbf/in <sup>3</sup> ])	$\lambda_{cb}^{present}$ ([lbf/in <sup>3</sup> ]/ [lbf/in <sup>3</sup> ])	Stacking sequence <sup>present</sup>
1	16120.38	20950.55	22385.40	$[90_4 / \pm 45]_{4s}$
	16119.48	20920.39	22303.53	$[(90_4 / \pm 45)_3 / \pm 45 / 90_2 / \pm 45]_s$
	16087.83	20894.53	22273.37	$[(90_4 / \pm 45)_3 / \pm 45]_s$
2	13442.04	15961.75	16769.66	$[(90_4 / \pm 45)_3 / 90_2 / \pm 45 / 90_2]_s$
	13441.28	15729.07	16766.43	$[(90_4 / \pm 45)_3 / 90_2 / \pm 45]_s$
	13435.94	15512.55	16727.65	$[(90_4 / \pm 45)_3 / \pm 45 / 90_2 / \pm 45]_s$
3	10003.53	10591.61	11192.70	$[90_4 / \pm 45]_{4s}$
	10002.95	10460.19	11151.77	$[(90_4 / \pm 45)_3 / \pm 45 / 90_2 / \pm 45]_s$
	9999.45	10343.85	11136.69	$[(90_4 / \pm 45)_3 / \pm 45]_s$
4	3973.01*	3973.01	3973.01	$[\pm 45 / 90_{10} / (\pm 45 / 90_8)_2]_s$
	3973.00*	3973.00	3973.00	$[90_4 / (90_2 / \pm 45)_3 / 90_8 / \pm 45 / 90_6]_s$

\* The optimum values calculated from the stacking sequences of the references.

In Table 6.4, the critical buckling load factor ( $\lambda_{cb}$ ) results are given in British units to provide consistency with the literature. Ply contiguity constraint for stacking sequences is applied to the first three load cases. Besides, stacking sequences are subjected to symmetry and balance constraints. In order to provide an average quality of solutions, each load case is performed 100 times with different starting points.

It can be seen from the table that  $\lambda_{cb}$  values for the test problem are found superior to the results given in the literature for load cases 1, 2 and 3. It should be noted that  $\lambda_{cb}^{[16]}$  represents the results of our previous published study obtained from the hybrid algorithm combining GA and GPSA, and the present proposed PSA-GPSA algorithm finds greater  $\lambda_{cb}$  values than the GA-GPSA hybrid algorithm. In load case 4, the same results are obtained for the first and second optima.  $\lambda_{cb}$  values denoted with asterisk sign are the real optimum values calculated from the stacking sequence designs given by the related references. It can be noted that  $\lambda_{cb}$  values found by [46-49] are possibly misrepresented due to round of error in their optimization procedures. This test study implies that the proposed novel hybrid algorithm shows very good performance in searching the design space for laminated composite optimization, and has capability to yield the best possible results for the fatigue optimization studies.

# CHAPTER 7

## FATIGUE LIFE MAXIMIZATION

### 7.1. Fatigue Life Maximization using FTFP Model

#### 7.1.1. Problem Definition

In this study, the main objective is to investigate optimum fiber stacking sequences of laminated composites subjected to in-plane cyclic loads for maximum fatigue life using FTFP model. The orientation angles in each lamina  $\theta_k$ , thus stacking sequences of the laminates, and fatigue life  $N$  are determined in design process. The number of distinct laminae  $n$  and the thickness of the laminae  $t_0$  of the laminates are predefined in the design. The orientation angles are considered as the discrete values of  $0^\circ$ ,  $45^\circ$ ,  $-45^\circ$ ,  $90^\circ$  which are conventional in industry. The material parameters and experimental fatigue parameters are taken from the study of Hashin and Rotem [5]. The considered laminated composite material is a unidirectional 32-layer E-glass/epoxy. The ply thickness  $t_0$  is 0.127 mm. Stress ratio ( $R$ ) is 0.1 and frequency ( $\nu$ ) is 19 Hz. The material and strength properties are presented in Table 7.1.

Table 7.1. Properties of the laminates used in the study [5]

Material Properties	Strength Properties
$E_{11} = 181 \text{ GPa}$	$X_t = -X_c = 1235.64 \text{ MPa}$
$E_{22} = 10.3 \text{ GPa}$	$Y_t = -Y_c = 28.44 \text{ MPa}$
$G_{12} = 7.17 \text{ GPa}$	$S = 37.95 \text{ MPa}$
$\nu_{12} = 0.28$	

In the study, we have considered several problems including cyclic  $N_{xx}$ ,  $N_{yy}$ ,  $N_{xy}$  loadings applied in combinations of tension-tension, tension-compression, compression-

compression, and tension-tension-shear. These loading cases are given in result tables. The hybrid GA-GPSA algorithm is used to solve the optimization problems.

### 7.1.1.1. Formulation of the Objective Function

Derivation of the objective function and the applied optimization strategy will be addressed here. The expressions of the fatigue failure stresses ( $X, Y, S$ ) directly taken from [5] and given with Equation (4.10) are substituted into the expression of the FTPF criterion defined in Equation (4.12). Afterwards, the fatigue life,  $\log N$ , is obtained in polynomial form through mathematical calculations. Hence, the objective function can be formulated as

$$f(n, \theta_k) = -\log N \quad | \quad \{k = 1, \dots, n = 32\} \quad (7.1)$$

where  $n$  is the number of plies, and  $\theta_k$  is the fiber orientation angle of each ply. Since the search algorithm is normally constructed to minimize the objective function, the logarithmic fatigue life of the laminate,  $\log N$  is taken as negative in the objective function to be able to maximize. The laminates are subjected to symmetry and balance geometric constraints to avoid undesirable stiffness coupling effects. Apart from that, in order to decrease the probability of large scale matrix cracking and to provide damage tolerant structures [44], ply contiguity constraint is applied to the laminates by constraining the maximum number of contiguous plies of the same orientation to four. In addition, Hashin-Rotem (HR) failure criterion [5-6] is used to check whether or not the first ply failure occurs in the laminates until the final fatigue failure.

Consequently, the optimization problem can be defined as

Maximize:  $\log N(\theta_k)$ ,  $\theta_k \in \{0_2, \pm 45, 90_2\}$ ,  $k = 1, \dots, 32$

Constraints: HR failure criterion  $\{FI_{fiber} \leq 1, FI_{matrix} \leq 1\}$

Symmetry

Balance

Ply contiguity

Tool: MATLAB Optimization Toolbox

where the number of design variables  $\theta_k$  becomes 8 due to balance and symmetry. Hence, composite plates are to be arranged in the sequence of  $[\pm\theta_1 / \pm\theta_2 / \pm\theta_3 / \pm\theta_4 / \pm\theta_5 / \pm\theta_6 / \pm\theta_7 / \pm\theta_8]_s$ . The fiber angles will be used as ply stacks of  $0_2, \pm 45, 90_2$  for the design cases.  $FI_{fiber}$  and  $FI_{matrix}$  represent fiber and matrix failure indexes of the laminate, respectively, and they must be smaller than 1 to avoid any ply or matrix failure. MATLAB Optimization Toolbox [37] is used to constitute the hybrid GPSA embedded GA with predefined operators.

In order to determine  $\log N$ , as in the experimental correlation previously, fatigue life of each lamina is calculated using Equation (7.1) and the smallest one of the obtained fatigue lives is chosen as the fatigue life of the laminate,  $\log N$ . Thus, the first-ply failure approach is inherently involved in this study. A laminate configuration is considered to be more fatigue-resistant than another if the fatigue life estimated by the fatigue model is longer than that of the other even if the applied cyclic stress is less than their endurance limits and actually they both have infinite fatigue life.

### 7.1.2. Optimization Problems and Results

In the fatigue optimization study, multidirectional laminate derivations are produced to increase the fatigue life theoretically using the FTPF model and hybrid algorithm. It is obvious that the optimum stacking sequences giving maximum fatigue lives require a validation supporting the proposed fatigue optimization strategy. In this regard, a pre-optimization study is performed to justify the theoretical derivation procedure using experimental data from the literature. The prediction and optimization procedures are applied to different multidirectional composite laminates [24-26]. For each laminate, first, estimated fatigue life is determined. Then, the optimum laminate configurations to be replaced with the tested laminate are investigated and the stacking sequences with increased fatigue lives are obtained. The results are presented with the stacking sequences and experimental fatigue lives of the reference materials in Table 7.2. In the table, first two optimum results for each case are shown, and the fatigue life values are given as logarithmic.

Table 7.2. Fatigue life prediction and optimization using different experimental data from the literature

Stacking sequence <sup>[24-26]</sup>	Experimental fatigue life <sup>[24-26]</sup>	Predicted fatigue life	Optimum stacking sequence	Maximum fatigue life
[0/90/90/0] <sub>s</sub>	6.2871	6.2809	[0 <sub>3</sub> /90] <sub>s</sub>	7.4888
			[0/90] <sub>2s</sub>	6.2809
[45/0/0/-45] <sub>s</sub>	5.8845	5.8831	[0 <sub>3</sub> /45] <sub>s</sub>	7.9712
			[0/45] <sub>2s</sub>	7.8077
[45/90/-45/0] <sub>s</sub>	5.9772	5.9745	[45/0 <sub>3</sub> ] <sub>s</sub>	6.9939
			[45/0] <sub>2s</sub>	6.4057
[0/90 <sub>4</sub> ] <sub>s</sub>	5.9804	5.9939	[0 <sub>4</sub> /90] <sub>s</sub>	7.4419
			[0 <sub>4</sub> /45] <sub>s</sub>	6.7113
[0 <sub>2</sub> /90 <sub>2</sub> ] <sub>s</sub>	5.5941	5.9900	[0 <sub>3</sub> /45] <sub>s</sub>	5.9974
			[0/90] <sub>2s</sub>	5.9900
[0/90] <sub>4s</sub>	6.1121	6.1299	[0 <sub>3</sub> /90] <sub>2s</sub>	6.5118
			[0 <sub>2</sub> /90 <sub>2</sub> ] <sub>2s</sub>	6.1299
[0/±45/90] <sub>2s</sub>	6.0486	6.3835	[0 <sub>3</sub> /90] <sub>2s</sub>	6.4213
			[0/90/±45] <sub>2s</sub>	6.3835

As seen in Table 7.2, the predicted fatigue life values are found to be very close to the experimental fatigue life values, especially for E-glass/epoxy laminates [26]. The optimization results show that longer fatigue lives can be obtained with different stacking sequences of the laminates. For example, while an approximated fatigue life of 5.97 is reached experimentally and predictively for the [45/90/-45/0]<sub>s</sub> sequence [25], fatigue lives of 6.9939 and 6.4057 can be achieved by [45/0<sub>3</sub>]<sub>s</sub> and [45/0]<sub>2s</sub> sequences, respectively. Considering that the fatigue lives of the laminates in [24-26] are accurately predicted by the FTPF model, it can be concluded that the optimum results obtained theoretically will be acceptable.

The fatigue optimization study consists of two parts. As the main part, optimization problems are solved using the discrete fiber angles. As the complementary part, an optimization study is performed using integer fiber angle values between -90° and 90° for some selected design cases and the results are compared with conventional stacking sequence designs containing the discrete fiber angles. In order to increase the efficiency and reliability of the algorithm, at least 50 independent searches are performed for each case. Different load levels and combinations which allow feasible designs are

investigated. The optimum stacking sequences of laminates, the corresponding fatigue lives, and the number of global optima found for various in-plane cyclic loads ( $N_{xx}/N_{yy}/N_{xy}$ ) are presented in Tables 7.3 – 7.5. Since multiple global optima exist in many loading cases, only one stacking sequence is shown for each loading in the tables. Failure indexes of the laminates determined according to HR failure criterion are indicated separately as  $FI_{fiber}$  and  $FI_{matrix}$  for fiber and matrix in the tables. Finally, the results of the comparison study between the optimization with discrete fiber angles and the optimization with integer fiber angles are given in Table 7.6.

Table 7.3. Optimum stacking sequence designs and the corresponding fatigue lives for various in-plane tension cyclic loads

Loading $N_{xx}/N_{yy}/N_{xy}$ ( $\times 10^2$ N/mm)	Stacking sequence	No. of global optima	Fatigue life (cycles)	$FI_{fiber}$	$FI_{matrix}$
5/0/0	$[0_4 / 90_2 / 0_4 / 90_2 / 0_4]_s$	8	$1.283 \times 10^8$	0.0170	0.1009
5/2.5/0	$[0_4 / \pm 45_3 / 0_2 / \pm 45_2]_s$	25	$5.503 \times 10^7$	0.1420	0.1849
5/5/0	$[(0_2 / 90_2)_2 / 90_2 / 0_4 / 90_2]_s$	20	$4.660 \times 10^6$	0.1858	0.3350
5/7.5/0	$[90_2 / 0_2 / (0_2 / 90_4)_2]_s$	32	$2.979 \times 10^5$	0.2374	0.5387
5/10/0	$[90_2 / \pm 45 / 90_4 / \pm 45_4]_s$	22	$3.175 \times 10^4$	0.2839	0.7398
7.5/0/0	$[0_4 / 90_2 / 0_4 / \pm 45 / 0_4]_s$	10	$3.229 \times 10^6$	0.1900	0.1953
7.5/2.5/0	$[0_2 / (0_2 / \pm 45_2)_2 / 0_2]_s$	23	$6.667 \times 10^6$	0.2067	0.2794
7.5/5/0	$[(90_2 / 0_2)_2 / 0_2 / 90_2 / 0_4]_s$	29	$2.979 \times 10^5$	0.2374	0.5387
7.5/7.5/0	$[\pm 45 / 0_2 / \pm 45 / 90_2 / 0_2 / 90_2 / \pm 45_2]_s$	67	$2.826 \times 10^4$	0.2787	0.7538
7.5/10/0	$[\pm 45_5 / 90_2 / \pm 45_2]_s$	8	$2.058 \times 10^3$	0.3823	0.9882
10/0/0	$[0_4 / \pm 45 / 0_4 / 90_2 / 0_4]_s$	3	$2.224 \times 10^5$	0.2533	0.3472
10/2.5/0	$[(0_4 / \pm 45)_2 / 0_2 / \pm 45]_s$	25	$7.752 \times 10^5$	0.2503	0.4284
10/5/0	$[(\pm 45_2 / 0_2)_2 / 0_2 / \pm 45]_s$	22	$3.175 \times 10^4$	0.2839	0.7398
10/7.5/0	$[\pm 45_6 / 0_2 / \pm 45]_s$	6	$2.058 \times 10^3$	0.3823	0.9882



Table 7.4. Optimum stacking sequence designs and the corresponding fatigue lives for various in-plane tension and shear cyclic loads

Loading $N_{xx}/N_{yy}/N_{xy}$ ( $\times 10^2$ N/mm)	Stacking sequence	No. of global optima	Fatigue life (cycles)	$FI_{fiber}$	$FI_{matrix}$
0/0/5	$[\pm 45_8]_s$	1	$3.987 \times 10^6$	0.1912	0.1196
0/5/2.5	$[\pm 45_3 / 90_4 / \pm 45 / 90_4]_s$	22	$4.344 \times 10^4$	0.1990	0.1940
0/7.5/2.5	$[90_4 / \pm 45 / 90_4 / \pm 45_2 / 90_2]_s$	18	$1.938 \times 10^3$	0.2580	0.3214
2.5/0/2.5	$[\pm 45 / 0_2 / \pm 45_4 / 0_2 / \pm 45]_s$	22	$6.738 \times 10^5$	0.1592	0.1079
2.5/2.5/2.5	$[\pm 45_8]_s$	1	$1.023 \times 10^7$	0.1885	0.2137
5/0/2.5	$[(\pm 45 / 0_2)_4]_s$	19	$4.344 \times 10^4$	0.1990	0.1940
5/2.5/2.5	$[(0_2 / \pm 45)_2 / \pm 45_4]_s$	14	$2.642 \times 10^5$	0.2491	0.3838
5/5/2.5	$[\pm 45_8]_s$	1	$8.551 \times 10^4$	0.2814	0.5651
5/0/5	$[0_2 / \pm 45_2 / 0_4 / \pm 45_3]_s$	21	46	0.3157	0.4352
5/2.5/5	$[\pm 45 / 0_2 / \pm 45_5 / 0_2]_s$	11	932	0.3734	0.7102
5/5/5	$[\pm 45_8]_s$	1	962	0.3770	0.8550
7.5/0/2.5	$[0_2 / \pm 45 / 0_2 / (0_2 / \pm 45)_2 / 0_2]_s$	19	$1.938 \times 10^3$	0.2580	0.3214
7.5/2.5/2.5	$[\pm 45_4 / 0_2 / \pm 45 / 0_4]_s$	23	$1.090 \times 10^4$	0.2959	0.5538
10/0/2.5	$[(0_4 / \pm 45)_2 / 0_4]_s$	14	73	0.3565	0.5709

Table 7.5. Optimum stacking sequence designs and the corresponding fatigue lives for various in-plane tension and compression cyclic loads

Loading $N_{xx}/N_{yy}/N_{xy}$ ( $\times 10^2$ N/mm)	Stacking sequence	No. of global optima	Fatigue life (cycles)	$FI_{fiber}$	$FI_{matrix}$
5/-2.5/0	$[(0_2 / 90_2)_2 / 0_4 / 90_2 / 0_2]_s$	27	$2.833 \times 10^7$	0.1552	0.0903
5/-5/0	$[90_2 / (0_2 / 90_2)_2 / 90_2 / 0_4]_s$	36	$3.987 \times 10^6$	0.1912	0.1196
5/-7.5/0	$[90_4 / (0_2 / 90_2)_2 / 90_2 / 0_2]_s$	20	$2.709 \times 10^5$	0.2479	0.2099
5/-10/0	$[90_4 / 0_4 / 90_4 / 0_2 / 90_2]_s$	22	$1.573 \times 10^4$	0.3103	0.3611
-5/-5/0	$[90_4 / 0_2 / 90_2 / 0_4 / 90_2 / 0_2]_s$	14	$4.660 \times 10^6$	0.1858	0.3350
7.5/-2.5/0	$[(0_4 / 90_2)_2 / 0_4]_s$	23	$3.566 \times 10^6$	0.1963	0.1349
7.5/-5/0	$[0_2 / (0_2 / 90_2)_2 / 0_4 / 90_2]_s$	23	$2.709 \times 10^5$	0.2479	0.2099
10/-2.5/0	$[(0_4 / 90_2)_2 / 0_4]_s$	18	$2.009 \times 10^5$	0.2615	0.2767
10/-5/0	$[0_4 / 90_4 / 0_4 / 90_2 / 0_2]_s$	23	$1.573 \times 10^4$	0.3103	0.3611
10/-7.5/0	$[0_2 / (0_2 / 90_2)_3 / 0_2]_s$	22	751	0.3710	0.5043
10/-10/0	$[0_4 / (0_2 / 90_4)_2]_s$	27	311	0.3824	0.4784
-10/-7.5/0	$[0_2 / \pm 45_7]_s$	2	$2.058 \times 10^3$	0.3823	0.9882

Table 7.6. Comparison of conventional (Con.) and non-conventional (Non-con.) fiber angle optimizations for various in-plane cyclic loadings

Loading $N_{xx}/N_{yy}/N_{xy}$ ( $\times 10^2$ N/mm)	Angle type	Stacking sequence	Fatigue life (cycles)
5/0/0	Con.	$[0_4 / 90_2 / 0_4 / 90_2 / 0_4]_s$	$1.283 \times 10^8$
	Non-con.	$[0_{16}]_s$	$4.704 \times 10^8$
5/2.5/0	Con.	$[0_4 / \pm 45_3 / 0_2 / \pm 45_2]_s$	$5.503 \times 10^7$
	Non-con.	$[\pm 35_8]_s$	$6.373 \times 10^7$
5/5/0	Con.	$[(0_2 / 90_2)_2 / 90_2 / 0_4 / 90_2]_s$	$4.660 \times 10^6$
	Non-con.	$[0_2 / \pm 55 / \pm 63 / \pm 12 / 90_2 / \pm 27 / \pm 35 / \pm 78]_s$	$4.660 \times 10^6$
5/7.5/0	Con.	$[90_2 / 0_2 / (0_2 / 90_4)_2]_s$	$2.979 \times 10^5$
	Non-con.	$[\pm 51_8]_s$	$4.959 \times 10^5$
5/10/0	Con.	$[90_2 / \pm 45 / 90_4 / \pm 45_4]_s$	$3.175 \times 10^4$
	Non-con.	$[\pm 55]_s$	$8.230 \times 10^4$
5/0/2.5	Con.	$[(\pm 45 / 0_2)_4]_s$	$4.344 \times 10^4$
	Non-con.	$[\pm 49 / 0_2 / \pm 49_2 / 0_2 / \pm 49 / 0_4]_s$	$6.946 \times 10^4$
5/2.5/2.5	Con.	$[(0_2 / \pm 45)_2 / \pm 45_4]_s$	$2.642 \times 10^5$
	Non-con.	$[\pm 35_8]_s$	$6.311 \times 10^5$
5/5/2.5	Con.	$[\pm 45_8]_s$	$8.551 \times 10^4$
	Non-con.	$[\pm 45_8]_s$	$8.551 \times 10^4$
5/2.5/5	Con.	$[\pm 45 / 0_2 / \pm 45_5 / 0_2]_s$	932
	Non-con.	$[\pm 36_8]_s$	3243
5/-2.5/0	Con.	$[(0_2 / 90_2)_2 / 0_4 / 90_2 / 0_2]_s$	$2.833 \times 10^7$
	Non-con.	$[0_2 / 90_2 / 0_4 / (90_2 / 0_2)_2]_s$	$2.833 \times 10^7$
5/-7.5/0	Con.	$[90_4 / (0_2 / 90_2)_2 / 90_2 / 0_2]_s$	$2.709 \times 10^5$
	Non-con.	$[(90_2 / 0_2)_3 / 90_4]_s$	$2.709 \times 10^5$
7.5/2.5/0	Con.	$[0_2 / (0_2 / \pm 45_2)_2 / 0_2]_s$	$6.667 \times 10^6$
	Non-con.	$[\pm 29_8]_s$	$1.580 \times 10^7$
7.5/5/0	Con.	$[(90_2 / 0_2)_2 / 0_2 / 90_2 / 0_4]_s$	$2.979 \times 10^5$
	Non-con.	$[\pm 39_8]_s$	$4.959 \times 10^5$
10/2.5/0	Con.	$[(0_4 / \pm 45)_2 / 0_2 / \pm 45]_s$	$7.752 \times 10^5$
	Non-con.	$[\pm 26_8]_s$	$3.953 \times 10^6$

Table 7.3 shows the results for only tension cyclic loads. As the results indicate, the fatigue life is found to be sensitive to the level of stress. For each  $N_{xx}$  loading levels of 5, 7.5, 10 ( $\times 10^2$  N/mm), fatigue life of the optimum designs decreases with the increase of  $N_{yy}$  loading as may be expected. Maximum fatigue lives of the optimum designs are achieved between  $10^6$  and  $10^8$  cycles. However, fatigue lives in the range of  $10^3$ - $10^4$  cycles are able to be reached for the designs of 5/10/0, 10/5/0 and 10/7.5/0 critical loadings. Unpredictably, in the design cases for 7.5/2.5/0 and 10/2.5/0 loadings, the designs with more fatigue life are obtained compared to the 7.5/0/0 and 10/0/0 loading cases, respectively. It is also noted that the same fatigue lives are obtained with different stacking sequence designs for 5/10/0-10/5/0 and 7.5/10/0-10/7.5/0 loadings. Furthermore, failure indexes indicate that all the laminate configurations are reliable against static failure.

Table 7.4 shows the effect of the existence of shear stress on the optimum designs. It is seen that fatigue life dramatically decreases in the presence of shear load. For instance, the fatigue lives of the designs obtained for 5/0/2.5, 5/2.5/2.5 and 5/5/2.5 loadings are less than the ones for 5/0/0, 5/2.5/0 and 5/5/0 loadings in Table 7.3. In the same manner, a considerable decrease occurs when the applied shear load is increased. For instance, the designs found for 5/0/5, 5/2.5/5 and 5/5/5 loadings have quite less fatigue lives than those for 5/0/2.5, 5/2.5/2.5 and 5/5/2.5 loadings. The increase of  $N_{xx}$  also decreases the fatigue life of composites. This decrease can be seen in 2.5/0/2.5, 5/0/2.5, 7.5/0/2.5 and 10/0/2.5 loadings. It is also noted that for 0/5/2.5-5/0/2.5 and 0/7.5/2.5-7.5/0/2.5 loadings different stacking sequences are obtained with the same fatigue life values. All the laminates are safe against static loading even if they have short fatigue lives. In general, it can be said that fatigue life dramatically changes and mostly decreases according to the shear load level and its applied combination.

In Table 7.5, the optimum results for tension-compression (T-C) and compression-compression (C-C) loadings are given. It is seen that the optimum stacking sequence designs for T-C loading yield less fatigue life than the previous designs for tension-tension (T-T) loading. For instance, the optimum design found for 5/-2.5/0 loading has a fatigue life of  $2.833 \times 10^7$  cycles whereas it is  $5.503 \times 10^7$  cycles for 5/2.5/0 loading. However, it is found that the stacking sequence designs for C-C loading have longer fatigue lives than the designs for T-C loading. For instance, the design for -5/-5/0 loading has 16.88% higher fatigue life than the design for 5/-5/0 loading. Also, when C-C loading cases are compared to T-T loading cases, it is seen that the same fatigue lives

are obtained in different stacking sequences (e.g., -5/-5/0 – 5/5/0 and -10/-7.5/0 – 10/7.5/0). This is due to the assumption that tension fatigue failure stress equals to compression fatigue failure stress in the FTF prediction model as stated earlier.

Table 7.6 shows the comparison results of the optimization using conventional fiber angles (Con.) and the optimization using non-conventional fiber angles (Non-con.) for selected in-plane cyclic loadings. Stacking sequences and fatigue lives corresponds to related loadings and angle types are given in the table. Optimum results obtained by non-conventional angles are superior or at least comparable to the results obtained by conventional angles. For example, in 5/2.5/2.5 loading,  $[\pm 35_8]_s$  design with a fatigue life of  $6.311 \times 10^5$  cycles is found by non-conventional lamination while  $[(0_2 / \pm 45)_2 / \pm 45_4]_s$  design with a fatigue life of  $2.642 \times 10^5$  cycles is found by conventional lamination. This corresponds to an increase of 58.14% in fatigue life. As in 10/2.5/0 loading case, the increase in fatigue life can even be up to 80.39%. Nevertheless, in 5/5/0, 5/5/2.5, 5/-2.5/0 and 5/-7.5/0 loading cases, fatigue lives are the same values even if their stacking sequences are different.

As the fatigue optimization results show in general, fatigue life of composites changes dramatically according to type of loading, loading combination and level of stress. Most of the designs are obtained within fatigue life range of  $10^5$ - $10^7$ . However, in design cases of high loading, fatigue life can only be increased to  $10^2$  and  $10^3$  cycle levels. Especially in the presence of shear and compressive loads, fatigue life significantly decreases. These unsatisfactory results indicate the most critical cases that restrict to develop reasonable fatigue-resistant designs.

## **7.2. Fatigue Life Maximization using Different Models**

### **7.2.1. Validation of the Proposed Fatigue Optimization Strategy**

In this fatigue optimization study, multidirectional laminate derivations are produced to increase the fatigue life theoretically using different fatigue life prediction models and the proposed PSA-GPSA hybrid algorithm. It is obvious that the optimum stacking sequences giving maximum fatigue lives require a validation supporting the proposed fatigue optimization strategy. In this regard, a pre-optimization study is performed to justify the theoretical derivation procedure using experimental data from

the literature. The prediction and optimization procedures are applied to different multidirectional composite laminates [24-27]. For each laminate, first, estimated fatigue life is determined. Then, the optimum laminate configurations to be replaced with the tested laminate are investigated and the stacking sequences with increased fatigue lives are obtained. The results are presented with the stacking sequences and experimental fatigue lives of the reference (Ref.) materials in Table 7.7. In the table, the maximized result for each case is shown, and the corresponding fatigue life values are given as logarithmic. It should also be noted that the fatigue life prediction models are used in their original equation forms (linear or nonlinear) for both estimation and optimization studies.

It can be seen in the table that the predicted fatigue life values obtained by each one of the models are found to be very close to the experimental fatigue life values. The optimization results show that longer fatigue lives can be obtained with mostly same stacking sequences of the laminates; however, fatigue life values show differences according to the model.

For example, while an approximated fatigue life of 5.98 is reached experimentally and predictively for the  $[45/90/-45/0]_s$  sequence [26] for each model, different fatigue lives are achieved by the same optimum  $[0_3/45]_s$  sequence. ST method maximized the life up to  $10^{15}$  cycles. Considering that the fatigue lives of the laminates in [24-27] are accurately predicted by all the models and the optimization results corresponds to final failure as in the experiments, it can be concluded that the optimum results obtained theoretically will be acceptable.

Table 7.7. Fatigue life prediction and optimization using different models for various experimental data

Ref.	Stacking sequence	Experimental fatigue life	Model	Predicted fatigue life	Optimized stacking sequence	Maximized fatigue life
[26]	$[0/90/90/0]_s$	6.2871	FTPF	6.2809	$[0_3/90]_s$	7.4888
			FWE	6.2871	$[0_3/90]_s$	7.2922
			SB	6.2910	$[0_3/90]_s$	7.5410
			ST	6.2871	$[0_3/90]_s$	7.4862
	$[45/0/0/-45]_s$	5.8845	FTPF	5.8831	$[0_3/45]_s$	7.9712
			FWE	5.8845	$[0_3/45]_s$	9.7389
			SB	5.8859	$[0_3/45]_s$	8.0564
			ST	5.8845	$[0_3/45]_s$	13.2903
	$[45/90/-45/0]_s$	5.9772	FTPF	5.9745	$[0_3/45]_s$	8.0152
			FWE	5.9772	$[0_3/45]_s$	10.0686
			SB	5.9789	$[0_3/45]_s$	8.0843
			ST	5.9772	$[0_3/45]_s$	15.1647
[25]	$[0/90_4]_s$	5.9804	FTPF	5.9939	$[0_4/90]_s$	16.2972
			FWE	5.9934	$[0_4/90]_s$	8.9651
			SB	5.9933	$[0_4/90]_s$	10.9360
			ST	5.9934	$[0_4/90]_s$	13.2630
	$[0_2/90_2]_s$	5.5941	FTPF	5.9900	$[0_3/90]_s$	11.6336
			FWE	5.9895	$[0_3/90]_s$	7.3045
			SB	5.9894	$[0_3/90]_s$	10.2460
			ST	5.9895	$[0_3/90]_s$	8.2480
[24]	$[0/90]_{4s}$	6.1121	FTPF	6.1299	$[0_4/(90/0)_2]_s$	6.5118
			FWE	5.8960	$[0_4/(90/0)_2]_s$	6.7819
			SB	6.1117	$[0_4/(90/0)_2]_s$	6.4879
			ST	-	-	-
	$[0/\pm 45/90]_{2s}$	6.0486	FTPF	6.3835	$[0_2/45/0_2/90/0_2]_s$	6.5777
			FWE	6.3413	$[(0_2/90)_2/0_2]_s$	7.2682
			SB	6.3400	$[0_2/90/0_3/45/0]_s$	6.5598
			ST	-	-	-
[27]	$[0/45/90/-45]_{2s}$	6.1058	FTPF	6.1161	$[0_3/45]_{2s}$	11.5239
			FWE	6.1058	$[0_3/90]_{2s}$	7.4988
			SB	6.1159	$[0_3/45]_{2s}$	11.2096
			ST	6.1058	$[0_3/90]_{2s}$	9.3919
	$[0/90]_{4s}$	6.1125	FTPF	6.1230	$[0_3/90]_{2s}$	10.4296
			FWE	6.1125	$[0_3/90]_{2s}$	6.9675
			SB	6.1206	$[0_3/90]_{2s}$	10.8691
			ST	6.1125	$[0_3/90]_{2s}$	7.8599

## 7.2.2. Optimization Problems and Results

In this optimization study, the aim is to investigate the optimum fiber stacking sequences of the laminated composites for maximum fatigue life using FTPF, FWE, SB, and ST fatigue life prediction models and is thus to determine the potential usability on my thesis and fatigue design for future applications by evaluating the feasibility of the results. The stacking sequence of the laminate and fatigue life  $N$  are determined for each design case in the optimization. The number of distinct laminae  $n$  and the thickness of the laminae  $t_0$  of the laminates are predefined in the design. The orientation angles are considered as the discrete values of  $0^\circ$ ,  $45^\circ$ ,  $-45^\circ$ ,  $90^\circ$  which are conventional in industry. The composite material used in this study is taken from the study of Hashin and Rotem [5]. The laminated composite material is a unidirectional 32-layer E-glass/epoxy. The ply thickness  $t_0$  is 0.127 mm. Stress ratio  $R$  is 0.1 and frequency  $\nu$  is 19 Hz. The material, strength and fatigue properties are presented in Table 7.8. We have considered several problems including in-plane cyclic loadings  $N_{xx}$ ,  $N_{yy}$ ,  $N_{xy}$  (load per unit length) applied in combinations of tension, compression and shear loads. The PSA-GPSA hybrid algorithm is used to solve the optimization problems. The same problem with the previous optimization study is chosen, however different models and hybrid algorithm are used in this optimization study.

Table 7.8. Properties of the laminates used in the study [5]

Material Properties	Strength Properties	Fatigue Properties
$E_{11} = 181$ GPa	$X_t = -X_c = 1235.64$ MPa	$X = 1414.98 - 138.60 \log N$
$E_{22} = 10.3$ GPa	$Y_t = -Y_c = 28.44$ MPa	$Y = 36.11 - 3.26 \log N$
$G_{12} = 7.17$ GPa	$S_{21} = 37.95$ MPa	$S = 35.95 - 3.65 \log N$
$\nu_{12} = 0.28$		

Optimum stacking sequence designs of composite laminates are searched for maximum fatigue life. The laminates are subjected to symmetry and balance geometric constraints to avoid undesirable stiffness coupling effects. Apart from that, in order to decrease the probability of large scale matrix cracking and to provide damage tolerant

structures [44], ply contiguity constraint is applied to the laminates by constraining the maximum number of contiguous plies of the same orientation to four.

Consequently, the optimization problem can be defined as

Maximize:  $\log N(\theta_k)$ ,  $\theta_k \in \{0_2, \pm 45, 90_2\}$ ,  $k = 1, \dots, 32$

Models: FTPF, FWE, SB, ST

Constraints: Symmetry

Balance

Ply contiguity

Tool: MATLAB Optimization Toolbox

where the number of design variables  $\theta_k$  becomes 8 due to balanced and symmetric configuration of the plates. Hence, composite plates are to be arranged in the sequence of  $[\pm\theta_1 / \pm\theta_2 / \pm\theta_3 / \pm\theta_4 / \pm\theta_5 / \pm\theta_6 / \pm\theta_7 / \pm\theta_8]_s$ . The fiber angles will be used as ply stacks of  $0_2$ ,  $\pm 45$ ,  $90_2$  for the design cases. MATLAB Optimization Toolbox [50] is used to constitute the hybrid PSA embedded GPSA with predefined operators.

Regarding the optimization strategy, in order to determine fatigue life of a laminate, first, fatigue life of each lamina is calculated using the equations of each model which are induced to  $\log N$  formulations and then the minimum value among the obtained fatigue lives is chosen as the fatigue life of the laminate. This selection additionally guarantees the first-ply fatigue failure strength. In the optimization, a laminate configuration is accepted to be more fatigue-resistant than other configurations providing that the fatigue life found by the fatigue model is longer than the fatigue lives of the others.

In order to increase the efficiency and reliability of the algorithm, at least 50 independent searches are performed for each case. Different load levels and combinations which allow feasible designs are investigated. The optimum stacking sequences of laminates, the fatigue lives, and the number of global optima found for various in-plane cyclic loads ( $N_{xx}/N_{yy}/N_{xy}$ ) obtained using the four different models are presented in Tables 7.9 – 7.12. Since multiple global optima exist in many loading cases, only one stacking sequence is shown for each loading in the tables. For the global optima in the tables, values outside brackets denote global optima number, and values inside brackets denote the optimum stacking sequences ensuring the ply contiguity constraint.



Table 7.9. Optimum stacking sequence designs and the corresponding fatigue lives for various in-plane tension cyclic loads

Loading	Model	Stacking sequence	Global optima	Fatigue life
5/0/0	FTPF	$[0_2 / (0_2 / 90_2)_2 / 0_4 / 90_2]_s$	21(5)	$5.012 \times 10^7$
	FWE	$[0_2 / (0_2 / 90_2)_2 / 0_4 / 90_2]_s$	28(5)	$1.064 \times 10^6$
	SB	$[(0_4 / 90_2)_2 / 90_2 / 0_2]_s$	33(5)	$4.787 \times 10^7$
	ST	$[0_2 / (0_2 / 90_2)_2 / 0_4 / 90_2]_s$	27(5)	$3.437 \times 10^6$
5/2.5/0	FTPF	$[(0_2 / \pm 45)_2 / \pm 45_3 / 0_2]_s$	23(18)	$5.503 \times 10^7$
	FWE	$[(0_4 / 90_2)_2 / 0_2 / 90_2]_s$	30(4)	$1.929 \times 10^5$
	SB	$[(0_2 / \pm 45)_2 / \pm 45_3 / 0_2]_s$	17(15)	$9.964 \times 10^6$
	ST	$[(0_4 / 90_2)_2 / 0_2 / 90_2]_s$	30(4)	$3.592 \times 10^5$
5/5/0	FTPF	$[90_2 / 0_2 / \pm 45_4 / 90_2 / 0_2]_s$	23(20)	$4.660 \times 10^6$
	FWE	$[0_2 / 90_2 / 0_2 / (0_2 / 90_2)_2 / 0_2]_s$	43(8)	$3.500 \times 10^4$
	SB	$[(0_2 / \pm 45 / 90_2)_2 / \pm 45_2]_s$	37(32)	$4.754 \times 10^5$
	ST	$[0_2 / 90_2 / 0_2 / (0_2 / 90_2)_2 / 0_2]_s$	38(5)	$5.343 \times 10^4$
5/7.5/0	FTPF	$[90_4 / 0_4 / 90_4 / 0_2 / 90_2]_s$	10(1)	$2.979 \times 10^5$
	FWE	$[(0_2 / 90_2)_2 / 0_4 / 90_2 / 0_2]_s$	42(8)	$6.348 \times 10^3$
	SB	$[(90_2 / 0_2)_2 / 90_4 / 0_2 / 90_2]_s$	13(2)	$1.942 \times 10^4$
	ST	$[(0_2 / 90_2)_2 / 0_4 / 90_2 / 0_2]_s$	38(7)	$1.028 \times 10^4$
5/10/0	FTPF	$[\pm 45_2 / 90_4 / \pm 45_2 / 90_2 / \pm 45]_s$	28(21)	$3.175 \times 10^4$
	FWE	$[0_2 / 90_2 / (0_4 / 90_2)_2]_s$	37(5)	$1.151 \times 10^3$
	SB	$[\pm 45_2 / 90_4 / \pm 45_2 / 90_2 / \pm 45]_s$	14(11)	$1.266 \times 10^3$
	ST	$[0_2 / 90_2 / (0_4 / 90_2)_2]_s$	31(2)	$2.409 \times 10^3$
7.5/0/0	FTPF	$[0_2 / 90_2 / 0_2 / (0_2 / 90_2)_2 / 0_2]_s$	29(4)	$1.284 \times 10^6$
	FWE	$[0_2 / 90_2 / 0_2 / (0_2 / 90_2)_2 / 0_2]_s$	31(5)	$1.594 \times 10^4$
	SB	$[0_2 / 90_2 / 0_2 / (0_2 / 90_2)_2 / 0_2]_s$	21(4)	$1.360 \times 10^6$
	ST	$[(0_4 / 90_2)_2 / 0_2 / 90_2]_s$	32(4)	$2.433 \times 10^4$
7.5/2.5/0	FTPF	$[(\pm 45 / 0_2)_4]_s$	10(5)	$6.667 \times 10^6$
	FWE	$[(0_4 / 90_2)_2 / 90_2 / 0_2]_s$	28(4)	$2.892 \times 10^3$
	SB	$[0_2 / \pm 45_2 / 0_2]_{2s}$	13(6)	$9.185 \times 10^5$
	ST	$[(0_4 / 90_2)_2 / 90_2 / 0_2]_s$	31(5)	$5.158 \times 10^3$
7.5/7.5/0	FTPF	$[(\pm 45 / 90_2)_2 / (\pm 45 / 0_2)_2]_s$	15(11)	$2.826 \times 10^4$
	FWE	-*	-	-
	SB	$[\pm 45_2 / 90_2 / \pm 45 / 0_4 / \pm 45 / 90_2]_s$	45(44)	$1.098 \times 10^3$
	ST	-*	-	-
10/0/0	FTPF	$[(0_4 / 90_2)_2 / 0_2 / \pm 45]_s$	29(5)	$5.242 \times 10^4$
	FWE	-*	-	-
	SB	$[0_2 / 90_2 / (0_4 / 90_2)_2]_s$	23(4)	$3.126 \times 10^4$
	ST	-*	-	-
10/2.5/0	FTPF	$[0_2 / \pm 45 / 0_2 / (0_2 / \pm 45)_2 / 0_2]_s$	18(1)	$7.752 \times 10^5$
	FWE	-*	-	-
	SB	$[(0_4 / \pm 45)_2 / \pm 45 / 0_2]_s$	14(3)	$6.770 \times 10^4$
	ST	-*	-	-

\* The model does not yield any feasible design.

Table 7.10. Optimum stacking sequence designs and the corresponding fatigue lives for various in-plane tension-compression cyclic loads

Loading	Model	Stacking sequence	Global optima	Fatigue life
2.5/-2.5/0	FTPF	$[(0_2 / 90_2)_2 / (90_2 / 0_2)_2]_s$	14(3)	$2.277 \times 10^8$
	FWE	$[(0_2 / \pm 45)_2 / 90_2 / 0_2]_s$	16(4)	$6.421 \times 10^8$
	SB	$[(0_2 / 90_2)_2 / (90_2 / 0_2)_2]_s$	55(20)	$2.472 \times 10^8$
	ST	$[0_2 / 90_2 / 0_4 / (90_2 / 0_2)_2]_s$	33(8)	$9.494 \times 10^{12}$
5/-2.5/0	FTPF	$[0_2 / (0_2 / 90_2)_2 / 0_4 / 90_2]_s$	21(3)	$2.833 \times 10^7$
	FWE	$[0_2 / (0_2 / \pm 45)_3 / \pm 45]_s$	5(3)	$3.079 \times 10^7$
	SB	$[0_2 / (0_2 / 90_2)_2 / 0_4 / 90_2]_s$	36(5)	$7.292 \times 10^7$
	ST	$[0_2 / 90_2 / (0_4 / \pm 45)_2]_s$	36(6)	$1.340 \times 10^9$
5/-5/0	FTPF	$[90_4 / 0_2 / 90_2 / 0_4 / 90_2 / 0_2]_s$	50(20)	$3.987 \times 10^6$
	FWE	$[0_4 / \pm 45 / 0_2 / 90_2 / 0_4 / \pm 45]_s$	19(3)	$8.706 \times 10^7$
	SB	$[90_4 / 0_2 / 90_2 / 0_4 / 90_2 / 0_2]_s$	47(17)	$1.843 \times 10^7$
	ST	$[0_2 / (0_2 / 90_2)_3 / 0_2]_s$	30(5)	$2.004 \times 10^9$
5/-7.5/0	FTPF	$[90_2 / 0_2 / (90_2 / 0_2 / 90_2)_2]_s$	15(4)	$2.709 \times 10^5$
	FWE	$[0_2 / 90_2 / 0_4 / (90_2 / 0_2)_2]_s$	24(4)	$1.424 \times 10^8$
	SB	$[90_2 / 0_2 / (90_2 / 0_2 / 90_2)_2]_s$	12(4)	$1.998 \times 10^6$
	ST	$[0_2 / 90_2 / 0_4 / (90_2 / 0_2)_2]_s$	35(5)	$1.491 \times 10^{11}$
5/-10/0	FTPF	$[90_4 / (0_2 / 90_2)_2 / 90_2 / 0_2]_s$	10(2)	$1.573 \times 10^4$
	FWE	$[0_2 / (0_2 / 90_2)_2 / 0_4 / 90_2]_s$	34(8)	$1.391 \times 10^8$
	SB	$[90_4 / (0_2 / 90_2)_2 / 90_2 / 0_2]_s$	15(3)	$1.534 \times 10^5$
	ST	$[0_2 / (0_2 / 90_2)_2 / 0_4 / 90_2]_s$	32(4)	$1.374 \times 10^{11}$
7.5/-2.5/0	FTPF	$[0_4 / (90_2 / 0_2)_3]_s$	28(5)	$9.721 \times 10^5$
	FWE	$[(0_2 / \pm 45)_2 / 0_4 / \pm 45 / 0_2]_s$	13(3)	$1.494 \times 10^7$
	SB	$[0_4 / (90_2 / 0_2)_3]_s$	34(8)	$3.587 \times 10^6$
	ST	$[(0_4 / \pm 45)_2 / \pm 45]_s$	7(5)	$5.128 \times 10^6$
7.5/-5/0	FTPF	$[(0_2 / 90_2 / 0_2)_2 / 90_2 / 0_2]_s$	14(3)	$2.709 \times 10^5$
	FWE	$[0_4 / 90_2 / 0_4 / \pm 45_2 / 0_2]_s$	16(3)	$6.078 \times 10^6$
	SB	$[(0_2 / 90_2 / 0_2)_2 / 90_2 / 0_2]_s$	14(4)	$1.998 \times 10^6$
	ST	$[0_4 / 90_2 / 0_4 / \pm 45 / 0_2 / 90_2]_s$	43(4)	$5.462 \times 10^6$
7.5/-7.5/0	FTPF	$[90_2 / 0_2 / (0_2 / 90_2)_2 / 90_2 / 0_2]_s$	30(23)	$3.591 \times 10^4$
	FWE	$[0_4 / \pm 45 / 0_4 / 90_2 / 0_2 / \pm 45]_s$	22(4)	$1.180 \times 10^7$
	SB	$[90_2 / 0_2 / (0_2 / 90_2)_2 / 90_2 / 0_2]_s$	42(12)	$3.875 \times 10^5$
	ST	$[(0_4 / 90_2)_2 / 0_2 / 90_2]_s$	22(3)	$1.418 \times 10^7$
10/-2.5/0	FTPF	$[(0_4 / 90_2)_2 / 90_2 / 0_2]_s$	29(5)	$2.565 \times 10^4$
	FWE	$[0_2 / \pm 45 / (0_4 / \pm 45)_2]_s$	16(3)	$2.971 \times 10^6$
	SB	$[(0_4 / 90_2)_2 / 90_2 / 0_2]_s$	29(5)	$9.939 \times 10^4$
	ST	$[0_4 / \pm 45]_2]_s$	16(8)	$1.765 \times 10^6$
10/-5/0	FTPF	$[0_2 / (0_2 / 90_2)_3 / 0_2]_s$	9(2)	$1.573 \times 10^4$
	FWE	$[0_4 / \pm 45_2 / 0_4 / \pm 45 / 0_2]_s$	7(1)	$1.191 \times 10^6$
	SB	$[0_2 / (0_2 / 90_2)_3 / 0_2]_s$	14(4)	$1.534 \times 10^5$
	ST	$[(0_4 / \pm 45)_2 / 0_2 / 90_2]_s$	26(4)	$2.827 \times 10^5$

Table 7.11. Optimum stacking sequence designs and the corresponding fatigue lives for various in-plane tension and shear cyclic loads

Loading	Model	Stacking sequence	Global optima	Fatigue life
0/0/2.5	FTPF	$[\pm 45_8]_s$	1(1)	$2.277 \times 10^8$
	FWE	$[0_2 / 90_2]_{4s}$	47(8)	$4.736 \times 10^9$
	SB	$[\pm 45_8]_s$	1(1)	$2.472 \times 10^8$
	ST	-*	-	-
0/2.5/2.5	FTPF	$[\pm 45_4 / (90_2 / \pm 45)_2]_s$	15(14)	$6.738 \times 10^5$
	FWE	$[0_2 / (90_4 / 0_2)_2 / 90_2]_s$	11(3)	$1.700 \times 10^9$
	SB	$[\pm 45_4 / (90_2 / \pm 45)_2]_s$	23(22)	$1.076 \times 10^6$
	ST	$[0_2 / (90_4 / 0_2)_2 / 90_2]_s$	28(5)	$4.957 \times 10^{17}$
0/5/2.5	FTPF	$[90_4 / (\pm 45 / 90_2)_2 / \pm 45_2]_s$	10(7)	$4.344 \times 10^4$
	FWE	$[(90_4 / 0_2)_2 / 90_2 / 0_2]_s$	19(4)	$6.105 \times 10^8$
	SB	$[90_4 / (\pm 45 / 90_2)_2 / \pm 45_2]_s$	30(15)	$9.105 \times 10^4$
	ST	$[(90_4 / 0_2)_2 / 90_2 / 0_2]_s$	26(4)	$1.046 \times 10^{14}$
0/0/5	FTPF	$[\pm 45_8]_s$	1(1)	$3.987 \times 10^6$
	FWE	$[0_2 / (0_2 / 90_4)_2 / 0_2]_s$	47(7)	$4.736 \times 10^9$
	SB	$[\pm 45_8]_s$	1(1)	$1.843 \times 10^7$
	ST	-*	-	-
0/2.5/5	FTPF	$[\pm 45_7 / 90_2]_s$	4(4)	$2.303 \times 10^3$
	FWE	$[(90_4 / 0_2)_2 / 0_2 / 90_2]_s$	14(1)	$1.700 \times 10^9$
	SB	$[\pm 45_7 / 90_2]_s$	7(7)	$3.801 \times 10^3$
	ST	$[(90_4 / 0_2)_2 / 0_2 / 90_2]_s$	26(3)	$4.957 \times 10^{17}$
2.5/0/2.5	FTPF	$[0_2 / \pm 45_6 / 0_2]_s$	5(5)	$6.738 \times 10^5$
	FWE	$[0_2 / 90_2 / (0_4 / 90_2)_2]_s$	15(2)	$7.097 \times 10^7$
	SB	$[\pm 45_3 / 0_2]_{2s}$	7(7)	$1.076 \times 10^6$
	ST	$[0_2 / 90_2 / (0_4 / 90_2)_2]_s$	29(5)	$1.629 \times 10^{10}$
2.5/2.5/2.5	FTPF	$[\pm 45_8]_s$	1(1)	$1.023 \times 10^7$
	FWE	$[(0_2 / 90_2 / 0_2)_2 / 90_2 / 0_2]_s$	38(5)	$1.287 \times 10^7$
	SB	$[\pm 45_8]_s$	1(1)	$1.032 \times 10^7$
	ST	$[(0_2 / 90_2 / 0_2)_2 / 90_2 / 0_2]_s$	38(5)	$2.532 \times 10^8$
2.5/2.5/5	FTPF	$[\pm 45_8]_s$	1(1)	$9.101 \times 10^4$
	FWE	$[(0_2 / 90_2)_2 / 0_4 / 90_2 / 0_2]_s$	43(6)	$1.287 \times 10^7$
	SB	$[\pm 45_8]_s$	1(1)	$2.644 \times 10^5$
	ST	$[(0_2 / 90_2)_2 / 0_4 / 90_2 / 0_2]_s$	42(5)	$2.532 \times 10^8$
5/0/2.5	FTPF	$[0_2 / \pm 45]_{4s}$	16(9)	$4.344 \times 10^4$
	FWE	$[(0_2 / 90_2)_2 / 0_4 / 90_2 / 0_2]_s$	30(4)	$1.064 \times 10^6$
	SB	$[(0_2 / \pm 45)_2 / (\pm 45 / 0_2)_2]_s$	32(14)	$9.105 \times 10^4$
	ST	$[(0_2 / 90_2)_2 / 0_4 / 90_2 / 0_2]_s$	27(5)	$3.437 \times 10^6$
5/2.5/2.5	FTPF	$[\pm 45 / 0_2 / \pm 45]_{2s}$	4(3)	$2.642 \times 10^5$
	FWE	$[0_4 / 90_2 / 0_2 / (0_2 / 90_2)_2]_s$	29(6)	$1.929 \times 10^5$
	SB	$[0_2 / \pm 45_3]_{2s}$	7(7)	$2.465 \times 10^5$
	ST	$[0_4 / 90_2 / 0_2 / (0_2 / 90_2)_2]_s$	29(5)	$3.592 \times 10^5$

(Cont. on next page)

Table 7.11 (cont.)

5/5/2.5	FTPF	$[\pm 45_8]_s$	1(1)	$8.551 \times 10^4$
	FWE	$[(90_2 / 0_4)_2 / 90_2 / 0_2]_s$	39(6)	$3.500 \times 10^4$
	SB	$[\pm 45_8]_s$	1(1)	$2.918 \times 10^4$
	ST	$[(90_2 / 0_4)_2 / 90_2 / 0_2]_s$	38(6)	$5.343 \times 10^4$
7.5/2.5/2.5	FTPF	$[\pm 45 / 0_2 / \pm 45_2 / (0_2 / \pm 45)_2]_s$	34(29)	$1.090 \times 10^4$
	FWE	$[(0_4 / 90_2)_2 / 0_2 / 90_2]_s$	31(3)	$2.892 \times 10^3$
	SB	$[\pm 45 / 0_2 / \pm 45_2 / (0_2 / \pm 45)_2]_s$	26(22)	$9.431 \times 10^3$
	ST	$[(0_4 / 90_2)_2 / 0_2 / 90_2]_s$	35(4)	$5.158 \times 10^3$

\* The model does not yield any feasible design.

Table 7.12. Optimum stacking sequence designs and the corresponding fatigue lives for various in-plane tension-compression-shear cyclic loads

Loading	Model	Stacking sequence	Global optima	Fatigue life
1/-1/1	FTPF	$[\pm 45 / (\pm 45 / 90_2)_2 / 0_4 / \pm 45]_s$	37(35)	$5.492 \times 10^7$
	FWE	$[(0_4 / 90_2)_2 / 0_2 / 90_2]_s$	37(6)	$1.747 \times 10^9$
	SB	$[\pm 45 / (\pm 45 / 90_2)_2 / 0_4 / \pm 45]_s$	66(59)	$6.087 \times 10^7$
	ST	$[(0_4 / 90_2)_2 / 0_2 / 90_2]_s$	25(5)	$6.860 \times 10^{17}$
1/-2.5/1	FTPF	$[\pm 45 / 0_2 / \pm 45 / 90_4 / \pm 45 / 90_2 / 0_2]_s$	36(31)	$6.615 \times 10^6$
	FWE	$[0_4 / 90_4 / 0_4 / 90_2 / 0_2]_s$	37(7)	$2.328 \times 10^9$
	SB	$[\pm 45 / 0_2 / \pm 45 / 90_4 / \pm 45 / 90_2 / 0_2]_s$	33(25)	$8.363 \times 10^6$
	ST	$[0_4 / 90_4 / 0_4 / 90_2 / 0_2]_s$	39(7)	$4.335 \times 10^{19}$
1/-5/1	FTPF	$[0_2 / 90_2 / (90_2 / \pm 45 / 90_2)_2]_s$	13(1)	$3.764 \times 10^5$
	FWE	$[0_2 / (0_2 / 90_2)_2 / 0_4 / 90_2]_s$	27(2)	$2.274 \times 10^9$
	SB	$[0_2 / 90_2 / (90_2 / \pm 45 / 90_2)_2]_s$	51(10)	$5.184 \times 10^5$
	ST	$[0_2 / 90_2]_{4s}$	41(15)	$2.418 \times 10^{18}$
1/-1/2.5	FTPF	$[0_2 / \pm 45_6 / 90_2]_s$	48(48)	$1.211 \times 10^6$
	FWE	$[(0_2 / 90_2)_2 / 0_4 / 90_2 / 0_2]_s$	23(5)	$1.747 \times 10^9$
	SB	$[0_2 / \pm 45_6 / 90_2]_s$	46(46)	$1.679 \times 10^6$
	ST	$[(0_2 / 90_2)_2 / 0_4 / 90_2 / 0_2]_s$	27(5)	$6.860 \times 10^{17}$
1/-2.5/2.5	FTPF	$[\pm 45 / 0_2 / \pm 45 / 90_2 / \pm 45_3 / 90_2]_s$	41(41)	$1.571 \times 10^5$
	FWE	$[90_2 / (0_4 / 90_2)_2 / 0_2]_s$	34(2)	$2.328 \times 10^9$
	SB	$[\pm 45 / 0_2 / \pm 45 / 90_2 / \pm 45_3 / 90_2]_s$	21(21)	$2.698 \times 10^5$
	ST	$[90_2 / (0_4 / 90_2)_2 / 0_2]_s$	38(6)	$4.335 \times 10^{19}$
1/-5/2.5	FTPF	$[(90_2 / \pm 45)_2 / \pm 45_2 / 0_2 / 90_2]_s$	18(13)	$4.315 \times 10^3$
	FWE	$[0_2 / 90_2 / (0_4 / 90_2)_2]_s$	22(2)	$2.274 \times 10^9$
	SB	$[(90_2 / \pm 45)_2 / \pm 45_2 / 0_2 / 90_2]_s$	15(12)	$8.102 \times 10^3$
	ST	$[0_2 / 90_2]_{4s}$	46(11)	$2.418 \times 10^{18}$
2.5/-2.5/1	FTPF	$[90_2 / \pm 45 / 0_2 / 90_4 / 0_4 / \pm 45]_s$	58(51)	$1.211 \times 10^6$
	FWE	$[(0_4 / 90_2)_2 / 0_2 / 90_2]_s$	25(4)	$3.913 \times 10^8$
	SB	$[90_2 / \pm 45 / 0_2 / 90_4 / 0_4 / \pm 45]_s$	91(66)	$1.679 \times 10^6$
	ST	$[(0_4 / 90_2)_2 / 0_2 / 90_2]_s$	26(4)	$9.494 \times 10^{12}$
2.5/-5/1	FTPF	$[90_2 / \pm 45 / (90_4 / 0_2)_2]_s$	29(6)	$3.857 \times 10^4$
	FWE	$[0_2 / (0_2 / 90_2)_3 / 0_2]_s$	27(3)	$8.117 \times 10^8$
	SB	$[90_2 / \pm 45 / (90_4 / 0_2)_2]_s$	63(8)	$6.617 \times 10^4$
	ST	$[0_2 / (0_2 / 90_2)_3 / 0_2]_s$	30(6)	$6.508 \times 10^{14}$
2.5/-2.5/2.5	FTPF	$[(0_2 / \pm 45)_2 / (90_2 / \pm 45)_2]_s$	22(22)	$2.540 \times 10^4$
	FWE	$[0_2 / 90_2 / 0_4 / (90_2 / 0_2)_2]_s$	36(5)	$3.913 \times 10^8$
	SB	$[90_2 / 0_2 / \pm 45_2]_{2s}$	60(55)	$4.846 \times 10^4$
	ST	$[0_2 / 90_2 / 0_4 / (90_2 / 0_2)_2]_s$	24(5)	$9.494 \times 10^{12}$

Table 7.9 shows the results for only tension cyclic loads. As the results indicate, the fatigue life is found to be sensitive to the level of stress. For each  $N_{xx}$  loading levels of 5, 7.5, 10 ( $\times 10^2$  N/mm), fatigue life of the optimum designs decreases with the increase of  $N_{yy}$  loading as may be expected. The optimum stacking sequence designs are obtained in fatigue life values from  $10^3$  to  $10^7$  cycles. However, this range varies according to the model. FWE and ST models does not yield any feasible optimum design solution for 7.5/7.5/0, 10/0/0 and 10/2.5/0 loading cases. The same optimum designs can be found with different fatigue life values by the models for specific loadings except 7.5/7.5/0, 10/0/0 and 10/2.5/0. Generally, FTPF-SB and FWE-ST model pairs find the same stacking sequences. For some loading cases, the number of same stacking sequence found is three (e.g., 5/0/0, 7.5/0/0). Maximum values of fatigue life are mostly obtained by the FTPF.

Table 7.10 shows the results for tension-compression cyclic loads. FTPF and SB models find same stacking sequences with different fatigue lives in all the loading cases. Between FTPF and SB, the maximum fatigue lives are obtained by SB model. However, FWE and ST does not give the same optimum designs in the loading cases except 5/-10/0. In general, ST and FWE models find the maximum fatigue life valued designs (e.g., 2.5/-2.5/0, 5/-5/0, 5/-7.5/0, 5/-10/0, etc.) and FTPF model finds the lower fatigue life valued designs among the others.

Table 7.11 shows the results for tension and shear cyclic loads. Here, optimum designs and fatigue lives show changes according to the model and the loading type. For instance, while ST model finds optimum stacking sequences having fatigue life values more than  $10^{10}$  cycles for the loading cases of 0/2.5/2.5, 0/5/2.5, 0/2.5/5 and 2.5/0/2.5, any reasonable design cannot be obtained by the ST for 0/0/2.5 and 0/0/5 pure shear loading cases. Similarly, also here, usually FTPF-SB and FWE-ST model pairs find the same stacking sequences with different fatigue lives. In general, optimum designs with their fatigue life values seem reasonable for all the models in the loadings of 2.5/0/2.5, 2.5/2.5/2.5, 2.5/2.5/5, 5/0/2.5, 5/2.5/2.5, 5/5/2.5 and 7.5/2.5/2.5. However, it may not be said that reasonable fatigue lives are obtained for the ST model's loading cases of 0/2.5/2.5, 0/5/2.5 and 0/2.5/5 even if the same stacking sequences are obtained with the FWE model.

Table 7.12 shows the results for tension-compression-shear cyclic loading cases. In many loading cases, similarly as in the previous loading types, FTPF-SB and FWE-ST

model pairs find the same stacking sequences with different fatigue lives. FTPF and SB models find the optimum designs with an acceptable life range between  $10^3$ - $10^8$ . However, FWE and ST models find the optimum designs with the fatigue lives of  $10^8$ - $10^9$  and  $10^{12}$ - $10^{19}$ , respectively, which does not seem reasonable considering the loading cases all together.

## CHAPTER 8

### EXPERIMENTAL STUDIES

#### 8.1. Background

There are different methods of production of polymer matrix composites with thermoset matrix materials such as epoxy, unsaturated polyester, and vinyl ester. The oldest and simplest manufacturing methods of the composite materials with polymer matrix can be accepted to be hand layup and spray methods. Basically, in the procedure, first, fibers are laid onto a mold by hand and then, the resin is brushed on or sprayed onto surface. In spray method, generally, resin and chopped fibers are sprayed together onto the mold surface. The deposited layers are usually densified with rollers in both techniques. Accelerators and catalysts are typically used for curing in the procedure [52]. Hand layup is a reliable process. However, it is also a very slow and labor-intensive method by nature [2].

In recent years, there is a growing interest of the automotive industry on the development of manufacturing methods that can support mass production rates. Compression molding, pultrusion, and filament winding are the three well known manufacturing methods for many years. However, research on their basic characteristics and process optimization started mostly in the mid-1970s. Another manufacturing method is resin transfer molding (RTM). It takes significant attention in aerospace and automotive industries due to its ability to produce composite parts with complex shapes at relatively high production rates. Especially, with the improvement in automation, fast-curing resins, new fiber forms, high-resolution quality control tools, the fabrication technology for fiber reinforced polymer composites has advanced at a remarkably rapid pace [2].

Most common used manufacturing methods in industry are bag molding, compression molding, filament winding, pultrusion, auto-clave based and liquid composite molding processes.



## 8.2. Liquid Composite Molding Processes

The manufacturing methods other than Liquid Composite Molding processes may offer disadvantages rather than advantages. For example, hand layup method provides flexibility for different layup configurations since it is an open molds process. However, the final product obtained from this method is not in a good quality since compaction and air suction are unavailable during the laying-up process. In another common method, autoclave molding process that uses laying-up either by hand or by tape laying machine, the quality of composite parts is very good as the impregnation of the fibers is done off-line and vacuum, pressure and temperature controls are used. Nevertheless, the autoclave molding method has disadvantages such as cost of application and shelf life limitation of prepregs. The methods like filament winding and pultrusion are for the parts in special shapes such as those having surfaces of revolutions, or those having constant cross section along their length [53].

On the other hand, in liquid composite molding (LCM) methods, generally, a premixed thermoset resin is injected into fiber fabrics placed in a closed mold. The liquid resin spreads through the fabrics, fills the space between the fibers, and expels the air. Finally, the resin forms the composite part as it cures and transforms to a solid state [2]. Liquid composite molding (LCM) is a process that may reduce the drawbacks to be faced in other methods. The main steps of the general process are presented schematically in Figure 8.1.

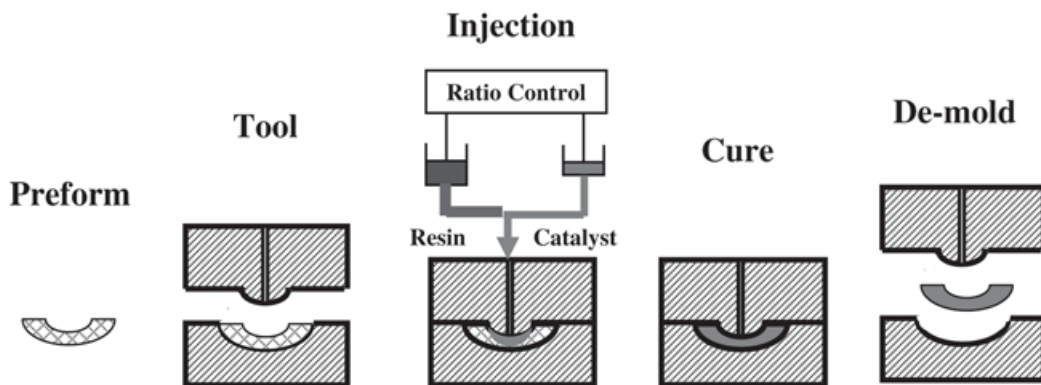


Figure 8.1. General representation of the LCM process  
(Source: Hoa, 2009)

LCM was initially developed for low-cost applications such as in the injection molding of ordinary plastic components. However, LCM has widely accepted as a reliable process for manufacturing of composites in automotive applications due to its relatively fast production rate, low cost, and its ability to provide closed and preserved mold conditions [53].

There are several types of the LCM process depending on the fiber volume fraction and the end-use applications and given as follows:

1. Injection molding (IM)
2. Structural reaction injection molding (SRIM)
3. Resin transfer molding (RTM)
4. Vacuum-assisted resin transfer molding (VARTM)
5. Seaman composite resin infusion molding process (SCRIMP)
6. Resin film infusion molding (RFIM)

In this study, we have used vacuum-assisted resin transfer molding method to produce our carbon/epoxy composite laminates.

### **8.2.1. Resin Transfer Molding (RTM)**

RTM is a low pressure closed molding process that consists of several layers including two-part mold, strand mat, woven roving, or cloth. In the RTM process, a catalyzed resin obtained by mixing is injected into a closed mold with the aid of a centrally located sprue. The resin can be injected in the pressures varying from 69 to 690 kPa. The resins such as epoxy, polyester, vinyl ester, methyl methacrylate or phenolic flow and spread throughout the mold. Thus, they fill the space between the fibers placed in the mold as dry fabric form, transfer the entrapped air via the air vents in the mold to the outside, and coat the fibers. After that the curing step starts to form the final product. The curing step depends on to type of the resin catalyst system that specifies the necessary temperature and time conditions to cure the composite. In order to conform to the exact dimensions after the cured part is removed from the mold, it is necessary to trim the outer part.

RTM method involves simple mold clamping process and it has very low tooling cost when compared to the compression molding method for example. In the process, molding materials such as metal inserts, stiffeners and washers are encapsulated within the molded laminate. The RTM method has been typically used in producing of the parts such as cabinet walls, bench seats, hoppers, water tanks, bathtubs and boat hulls.

RTM can be applied with different types of production methods: vacuum assisted resin transfer molding (VARTM) and Seemann's Composite Resin Infusion Molding Process (SCRIMP). In VARTM, the resin is injected into the stacked fiber fabrics or preforms by using vacuum in addition to the resin injection system. SCRIMP also uses vacuum to pull the resin into the dry fiber preform, however a porous layer is placed on the preform to provide an easy flow path to the resin. In both VARTM and SCRIMP methods, a single-sided rigid mold is used. The preform is placed on the rigid mold surface and covered with a vacuum bag. Figure 8.2 represents the illustration of VARTM process [2].

For the experimental studies of this thesis, carbon/epoxy polymer matrix composites are produced using the VARTM method. The VARTM process prepared and applied in Composite Production Laboratory at İYTE Department of Mechanical Engineering is shown in Figure 8.3. The right side is the injection point (input) for the epoxy resin.

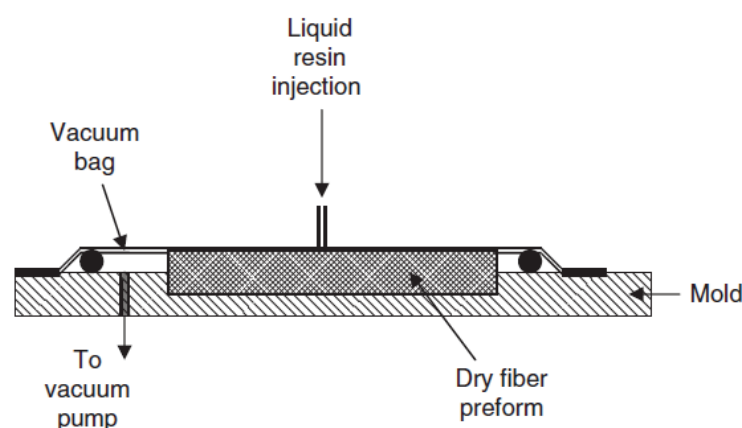


Figure 8.2. Vacuum-assisted resin transfer molding (VARTM)  
(Source: Mallick, 2007)

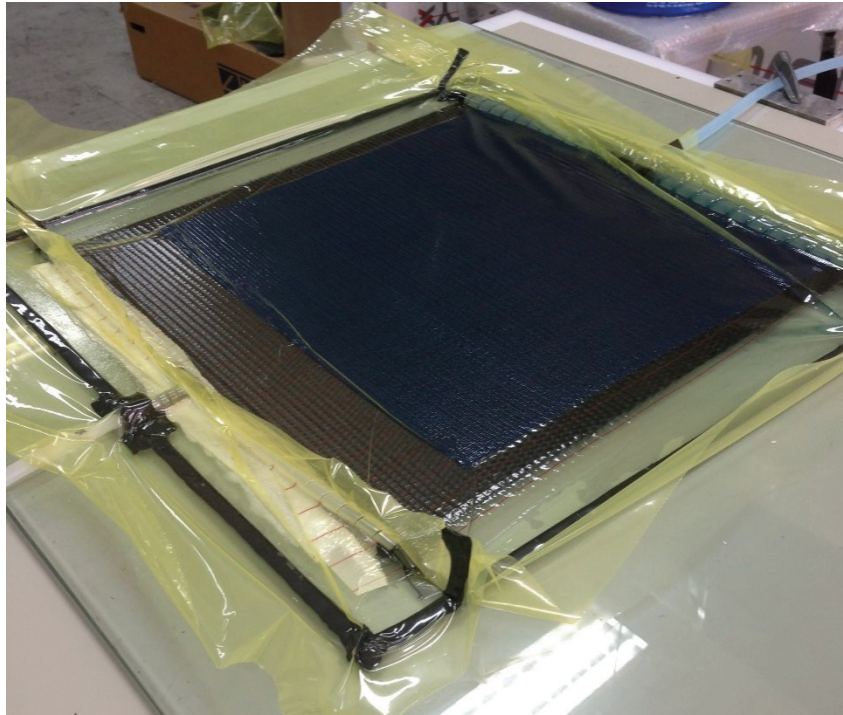


Figure 8.3. VARTM process application in the laboratory

### **8.3. Material Characterization of the Carbon/Epoxy Composites**

The analysis and design of a composite structure require the determination of the specified material properties of the laminated composite to be used as input data.

In general, it can be said that composite materials are tested for three main objectives:

- a) determination of essential material properties of the unidirectional laminate for use as input in structural design and analysis of composites,
- b) verification purposes of analytical predictions for mechanical behavior of the laminates,
- c) independent experimental studies for the characterization of newly-developed composite materials or structures.

In the present thesis, in order to be able to design fatigue-resistant composite laminates, quasi-static mechanical properties and fatigue strength properties of the carbon/epoxy composite laminates have been obtained by experimental procedure.

### 8.3.1. Quasi-static Mechanical Properties

Uniaxial tensile tests are conducted on unidirectional carbon/epoxy laminates to determine the longitudinal and transverse Young's moduli,  $E_1$ ,  $E_2$ , and shear modulus,  $G_{12}$ ; tensile strength in longitudinal, transverse and shear directions,  $X_t$ ,  $Y_t$ ,  $S_{21}$ ; and Poisson's ratio,  $\nu_{12}$  properties. The formulas used in calculations can be expressed basically as follows:

$$\begin{aligned} \sigma_1 &= \frac{P}{A}, E_1 = \frac{\sigma_1}{\varepsilon_1} \\ \sigma_2 &= \frac{P}{A}, E_2 = \frac{\sigma_2}{\varepsilon_2} \end{aligned} \quad \nu_{12} = -\frac{\varepsilon_2}{\varepsilon_1} \quad X_t = \frac{P_{ult}}{A}, Y_t = \frac{P_{ult}}{A}, S = \frac{P_{ult}}{A} \quad (8.1)$$

The carbon fabric is selected as CWUD300 UD, 300 gr/m<sup>2</sup> and 12k, from Metyx Composites and the epoxy is selected as MGS L160 from Dost Kimya. Carbon/epoxy laminated composite material is characterized in terms of tensile properties [54] experimentally. The static strength properties of  $X_t$ ,  $Y_t$ ,  $S_{21}$  and elastic properties of  $E_1$ ,  $E_2$  are obtained.

Quasi-static tests are performed in İYTE Center for Materials Research using Shimadzu AG1 250 kN (Figure 8.4) mechanical testing machine and computer for data acquisition. In determination of tensile properties, at least five specimens per test are used. Longitudinal and transverse properties are determined using  $[0_4]$  and  $[90_6]$  unidirectional specimens, respectively. Shear properties are determined using  $[\pm 45]_{2s}$  specimens. The geometry of the tensile test specimens used to obtain longitudinal, transverse and shear properties are given in Figures 8.5, 8.6 and 8.7 respectively.



Figure 8.4. Shimadzu AG1 250 kN mechanical testing machine

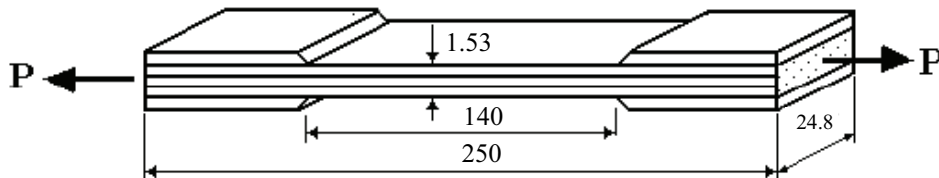


Figure 8.5. Specimen geometry and dimensions for longitudinal properties in test

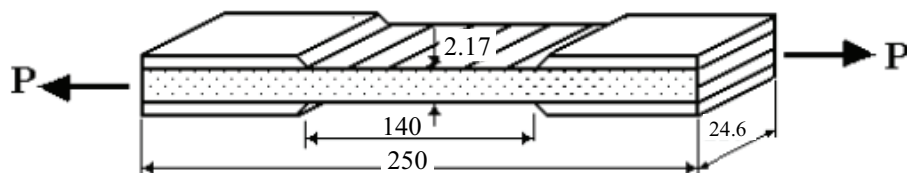


Figure 8.6. Specimen geometry and dimensions for transverse properties in test

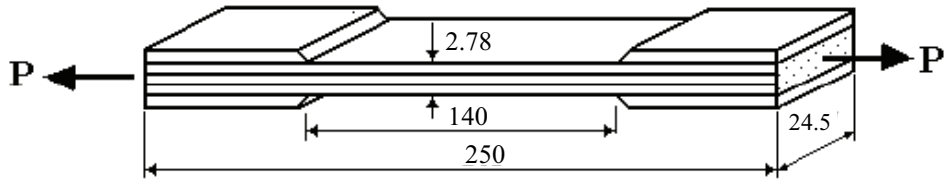


Figure 8.7. Specimen geometry and dimensions for shear properties in test

Poisson's ratio,  $\nu_{12}$  is found by a separate test performed at İnoMa Company in İzmir Institute of Technology Technopark. The test is performed using Shimadzu AG-IC 100-kN mechanical testing machine. Micro-Measurements® strain gauges are attached to the specimens to measure the strain in transverse direction. Axial strains are measured by a video extensometer. A sample specimen is given in Figure 8.8.

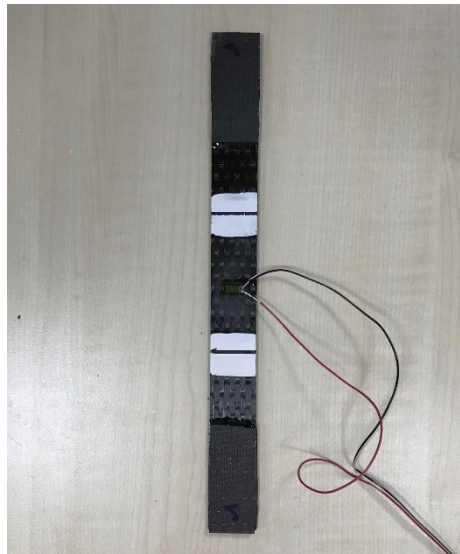


Figure 8.8. The specimen for Poisson's ratio test

The test is performed according to ASTM E132 standard [55]. A picture during the application of the test is shown in Figure 8.9. The complete test setup can be seen in this figure.





Figure 8.9. The representation of the Poisson's ratio test

Shear modulus is obtained by the formula from reference [56]. It is reported that shear modulus can be found with great approximation. The formula to calculate the shear modulus,  $G_{12}$  is expressed as follows:

$$G_{12} = \frac{1}{\left( \frac{4}{E_x} - \frac{1}{E_1} - \frac{1}{E_2} + \frac{2\nu_{12}}{E_1} \right)} \quad (8.2)$$

where  $E_x$  is longitudinal modulus of elasticity of the shear test specimens.

All the results of mechanical properties of carbon/epoxy specimens under static tensile loading are given in Table 8.1.



Table 8.1. Quasi-static material properties of carbon/epoxy composite

$E_1$ (GPa)	$E_2$ (GPa)	$G_{12}$ (GPa)	$\nu_{12}$	$X_t$ (MPa)	$Y_t$ (MPa)	$S_{21}$ (MPa)
102.19	5.90	6.19	0.31	1409.47	24.10	104.22

### 8.3.2. Fatigue Strength Properties

Fatigue tests are conducted in Composite Research Laboratory at İYTE Department of Mechanical Engineering using MTS 100-kN servohydraulic fatigue test machine in order to determine fatigue strength properties of the carbon/epoxy composite laminate. These properties are specified with S-N curves for the  $[0_4]$ ,  $[90_6]$  and  $[\pm 45]_{2s}$  laminates. Four specimens for each of the  $[0_4]$ ,  $[90_6]$  and  $[\pm 45]_{2s}$  laminates are shown in the Figure 8.10.

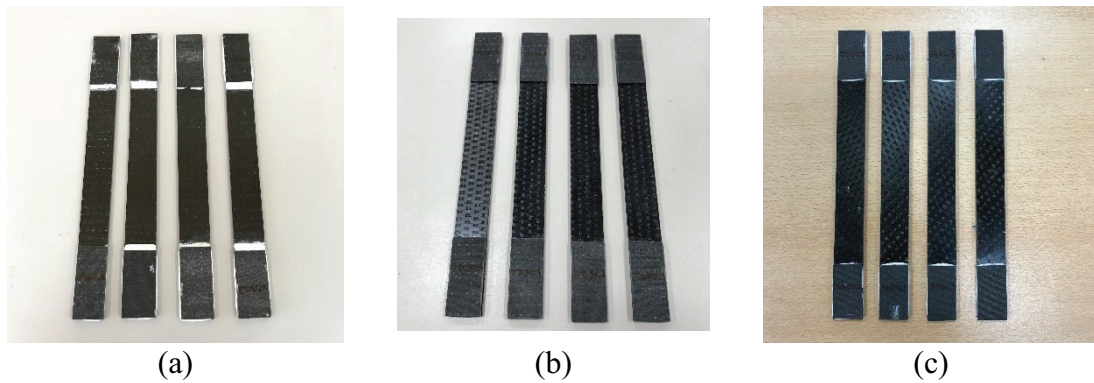


Figure 8.10. Fatigue test specimens for the (a) $[0_4]$ , (b) $[90_6]$  and (c) $[\pm 45]_{2s}$  laminates

Fatigue behavior for the  $[0_4]$ ,  $[90_6]$  and  $[\pm 45]_{2s}$  laminates are given by the S-N curves in Figure 8.11, 8.12 and 8.13, respectively.

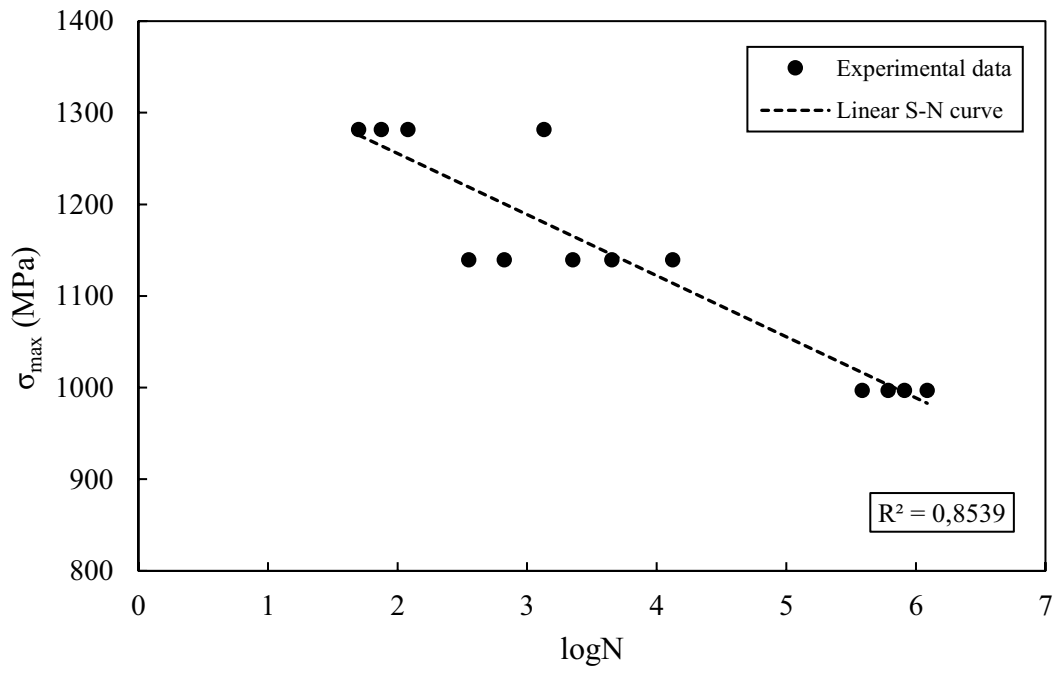


Figure 8.11. S-N curve of the  $[0_4]$  laminate

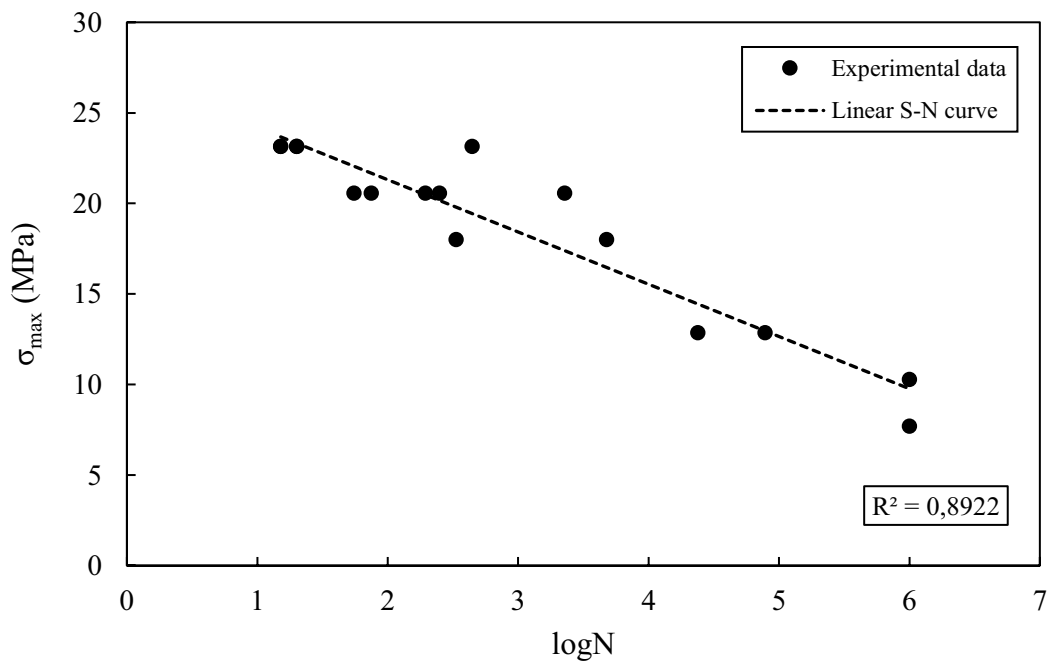


Figure 8.12. S-N curve of the  $[90_6]$  laminate

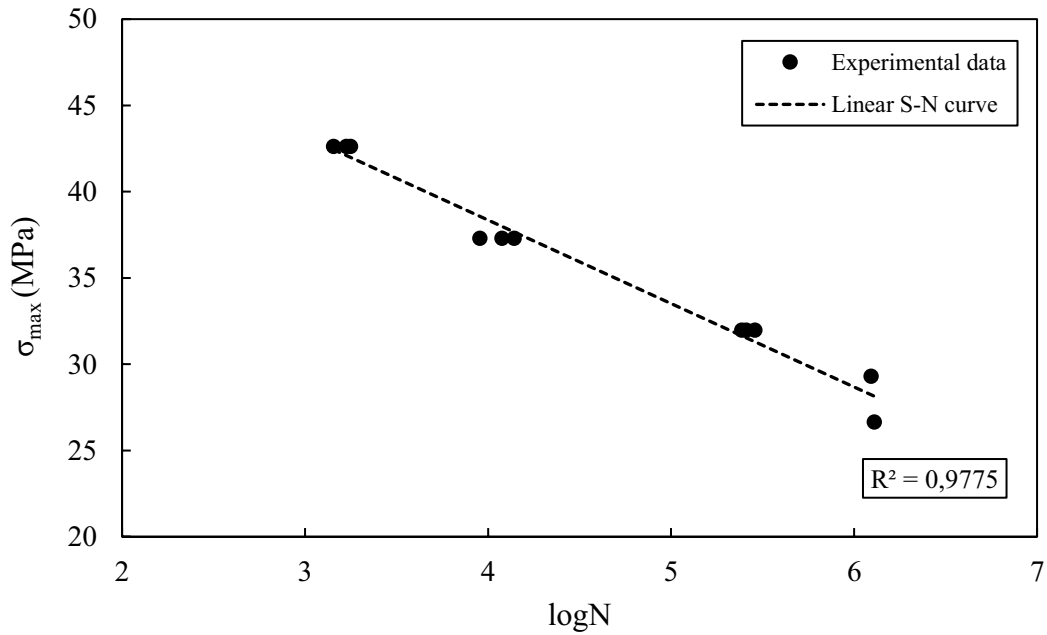


Figure 8.13. S-N curve of the  $[\pm 45]_{2s}$  laminate

The fatigue failure stress equations in linear form that are obtained from the corresponding S-N curves with regression analysis (Figs. 8.11-13) can be given as:

$$\begin{aligned}
 X &= 1389 - 66.694 \log N \\
 Y &= 27.075 - 2.885 \log N \\
 S &= 57.7 - 4.836 \log N
 \end{aligned}
 \tag{8.3}$$

Coefficient of determination ( $R^2$ ) values are specified in the figures to show how close the data are to the fitted regression line. It is seen from the values that the linear regression lines (S-N curves) generally fit well to the experimental data. However,  $R^2$  values of the fitness of the curves are lower for the  $[0_4]$  and  $[90_6]$  laminates due to the scattering of the experimental data.

The fatigue failure stress equations are to use as fatigue strength parameters in the FTPF fatigue life prediction model for the optimization problem of carbon/epoxy laminates.

## CHAPTER 9

# OPTIMUM FATIGUE-RESISTANT DESIGN OF CARBON/EPOXY COMPOSITE LAMINATES

### 9.1. Problem Definition

In this study, the objective is to find optimum stacking sequence designs of carbon/epoxy composite laminates subjected to various constant in-plane cyclic loadings for maximum fatigue life using the FTPF fatigue life prediction model. The orientation angles in each lamina  $\theta_k$ , thus stacking sequences of the laminates, and fatigue life  $N$  are determined in design process. The number of distinct laminae  $n$  and the thickness of the laminae  $t_0$  of the laminates are predefined in the design. The orientation angles are firstly considered as the discrete values of  $0^\circ$ ,  $45^\circ$ ,  $-45^\circ$ ,  $90^\circ$  which are conventional in industry. Then, the angles between  $-90^\circ$  and  $90^\circ$  with  $5^\circ$  intervals are used in the design to investigate how these non-conventional angles affect the fatigue life. The optimum fatigue-resistant carbon/epoxy composite is designed for several in-plane cyclic loadings in 8-, 16- and 32-ply laminates. The ply thickness  $t_0$  is prescribed as 0.3475 mm according to the experimental practice. Stress ratio ( $R$ ) is 0.1 and the test frequency ( $\nu$ ) is taken as 5 Hz. The material and strength properties obtained from the experimental procedure are presented together in Table 9.1.

Table 9.1. Properties of the carbon/epoxy composite

Material Properties	Strength Properties	Fatigue Properties
$E_{11} = 102.19$ GPa	$X_t = 1409.47$ MPa	$X = 1389 - 66.694 \log N$
$E_{22} = 5.90$ GPa	$Y_t = 24.10$ MPa	$Y = 27.075 - 2.885 \log N$
$G_{12} = 6.19$ GPa	$S_{21} = 104.22$ MPa	$S = 115.4 - 9.673 \log N$
$\nu_{12} = 0.31$		

The objective function for the optimization problem is formulated with the same procedure as in section 7.1.1.1. Accordingly, the optimization problem can be defined as

$$\text{Maximize: } \log N(\theta_{k_i}), \theta_{k_i} \in \{0_2^\circ, \pm 45^\circ, 90_2^\circ\}, k_1 = 1, \dots, 8; k_2 = 1, \dots, 16; k_3 = 1, \dots, 32$$

$$\theta_{k_i} \in \{0_2^\circ, \pm 5^\circ, \dots, \pm 85^\circ, 90_2^\circ\}$$

Model: FTPF

Constraints: Symmetry

Balance

Ply contiguity (max. 4 contiguous plies in a sequence)

Tool: MATLAB Optimization Toolbox

where the number of design variables  $\theta_k$  becomes 2, 4 and 8 for  $k_1$ ,  $k_2$  and  $k_3$ , respectively due to balanced and symmetric configuration of the plates. Hence, composite plates are to be arranged in the sequence of  $[\pm\theta_1 / \pm\theta_2]_s$ ,  $[\pm\theta_1 / \pm\theta_2 / \pm\theta_3 / \pm\theta_4]_s$  and  $[\pm\theta_1 / \pm\theta_2 / \pm\theta_3 / \pm\theta_4 / \pm\theta_5 / \pm\theta_6 / \pm\theta_7 / \pm\theta_8]_s$ , respectively. The fiber angles will be used as ply stacks of  $0_2^\circ$ ,  $\pm 45^\circ$ ,  $90_2^\circ$  or  $0_2^\circ, \pm 5^\circ, \dots, \pm 85^\circ, 90_2^\circ$  for the design cases. MATLAB Optimization Toolbox [50] is used to constitute the hybrid PSA embedded GPSA with predefined operators.

In the study, we have considered several problems including in-plane cyclic loadings  $N_{xx}$ ,  $N_{yy}$ ,  $N_{xy}$  applied in various combinations of tension, compression and shear loads. These loading cases are given in result tables. The hybrid PSA-GPSA algorithm proposed in section 6.5 is used to solve the optimization problems. The programming codes of the objective function and the run command are given in Appendix B. Representative composite plate geometry showing the coordinates and constant in-plane cyclic loads can be seen in Figure 4.1.

## 9.2. Fatigue Optimization and Results

As similar to the previous optimization studies, to determine fatigue life of a laminate, first, fatigue life of each layer is calculated using the  $\log N$  equation of the FTFP model and then, the minimum value among the obtained fatigue lives of the layers is chosen as the fatigue life of the laminate. This selection can also be considered as the guarantee of the first-ply fatigue failure strength. In the optimization, a laminate configuration is accepted to be more fatigue-resistant than other configurations providing that the fatigue life found by the fatigue model is longer than the fatigue lives of the others.

Before the proceed of the main optimization scheme, a number of fatigue optimization problems selected from the literature [14] are solved to test the performance of the hybrid PSA-GPSA algorithm. FWE prediction model is implemented to the optimization in the reference study. In the same manner, FWE model is used in our solutions. The reference loading conditions, optimum lay-ups and fatigue lives are presented together with our obtained optimum lay-up and fatigue life results in Table 9.2.

Table 9.2. Performance results of the PSA-GPSA algorithm in fatigue optimization

Loading ( $\times 10^5$ N/m) $N_{xx}/N_{yy}/N_{xy}$	Optimum lay-up <sup>[14]</sup>	Fatigue life <sup>[14]</sup> (cycles)	Optimum lay-up <sup>present</sup>	Fatigue life <sup>present</sup> (cycles)
5/0/0	$[0_{16}]_s$	$5.633 \times 10^8$	$[0_{16}]_s$	$5.633 \times 10^8$
5/3/0	$[-38_8 / 38_8]_s$	$2.842 \times 10^5$	$[-7_4 / 15_4 / -7_4 / 90_4]_s$	$2.109 \times 10^5$
5/5/0	$[-10_4 / 80_4 / -30_4 / 60_4]_s$	$1.119 \times 10^4$	$[0_4 / 90_4 / 16_4 / -16_4]_s$	$4.498 \times 10^4$
5/7/0	$[49_8 / -50_8]_s$	1291	$[-20_4 / 10_4 / -20_8]_s$	$6.869 \times 10^4$
5/-5/0	$[0_8 / 90_8]_s$	$9.725 \times 10^5$	$[0_{12} / 90_4]_s$	$2.502 \times 10^8$
5/-7/0	$[0_8 / 90_8]_s$	$2.593 \times 10^4$	$[0_4 / 90_4 / 0_8]_s$	$2.465 \times 10^8$

As seen in Table 9.2, in almost all the loading cases, better stacking sequence designs of higher fatigue life are achieved by the PSA-GPSA hybrid algorithm as compared to the reference results. Nevertheless, an under-optimum result is obtained for only the 5/3/0 loading case. As a result, it can be said that the proposed hybrid algorithm outperforms in fatigue optimization problems.

In fatigue optimization of carbon/epoxy composite laminates, at least 100 independent searches are performed for each case to increase the efficiency and reliability of the algorithm. Different load levels and combinations which allow feasible designs are investigated. The optimum stacking sequence designs, the fatigue lives, and the number of global optima found for various in-plane cyclic loads ( $N_{xx}/N_{yy}/N_{xy}$ ) obtained using the  $0_2^\circ$ ,  $\pm 45^\circ$ ,  $90_2^\circ$  angle stacks for 8-, 16- and 32-ply laminates are presented in Tables 9.3 – 9.9. The results for the angles with  $5^\circ$  increment ( $0_2^\circ, \pm 5^\circ, \dots, \pm 85^\circ, 90_2^\circ$ ) are shown in Tables 9.10 – 9.12. Since multiple global optima exist in many loading cases, only one stacking sequence is shown for each loading in the tables. For the global optima in the tables, values outside brackets denote global optima number, and values inside brackets denote the optimum stacking sequences ensuring the ply contiguity constraint. Tables 9.3 – 9.5 represent the optimum 8-ply stacking sequence design results.

Table 9.3. Optimum 8-ply design results for various in-plane tension cyclic loads

Loading ( $\times 10^2$ N/mm) $N_{xx}/N_{yy}/N_{xy}$	Stacking sequence	Number of global optima	Fatigue life (cycles)
1/1/0	$[0_2 / 90_2]_s$	3	$5.277 \times 10^7$
1/2.5/0	$[\pm 45 / 90_2]_s$	2	$3.233 \times 10^6$
1/5/0	$[90_2 / \pm 45]_s$	2	$2.370 \times 10^5$
2.5/0/0	$[0_2 / \pm 45]_s$	2	$1.364 \times 10^8$
2.5/0.625/0	$[0_2 / \pm 45]_s$	2	$1.681 \times 10^7$
2.5/1.25/0	$[0_2 / 90_2]_s$	2	$4.841 \times 10^5$
2.5/2.5/0	$[\pm 45]_{2s}$	1	$2.289 \times 10^5$
2.5/3.75/0	$[0_2 / 90_2]_s$	2	5661
3.75/0/0	$[0_2 / \pm 45]_s$	2	$7.865 \times 10^6$
5/0/0	$[0_2 / \pm 45]_s$	2	$3.010 \times 10^5$

Table 9.4. Optimum 8-ply design results for various in-plane tension and compression cyclic loads

Loading ( $\times 10^2$ N/mm) $N_{xx}/N_{yy}/N_{xy}$	Stacking sequence	Number of global optima	Fatigue life (cycles)
1/-1/0	$[0_2 / 90_2]_s$	2	$2.385 \times 10^8$
1/-2.5/0	$[0_2 / 90_2]_s$	2	$1.864 \times 10^6$
1/-5/0	$[0_2 / 90_2]_s$	2	644
2.5/-0.625/0	$[0_2 / 90_2]_s$	2	$1.486 \times 10^6$
2.5/-1.25/0	$[0_2 / 90_2]_s$	2	$2.169 \times 10^6$
2.5/-2.5/0	$[0_2 / 90_2]_s$	2	$4.701 \times 10^6$
2.5/-3.75/0	$[0_2 / 90_2]_s$	2	$7.125 \times 10^4$
2.5/-5/0	$[0_2 / 90_2]_s$	2	1155

Table 9.5. Optimum 8-ply design results for various in-plane tension, compression and shear cyclic loads

Loading ( $\times 10^2$ N/mm) $N_{xx}/N_{yy}/N_{xy}$	Stacking sequence	Number of global optima	Fatigue life (cycles)
0/2.5/1	$[90_2 / \pm 45]_s$	2	$2.522 \times 10^6$
1/-0.5/1	$[0_2 / \pm 45]_s$	2	$3.277 \times 10^6$
1/1/1	$[\pm 45]_{2s}$	1	$4.843 \times 10^6$
1/-1/1	$[\pm 45 / 90_2]_s$	1	$3.809 \times 10^4$
1/2.5/1	$[\pm 45 / 90_2]_s$	2	$6.275 \times 10^4$
1/-2.5/1	$[90_2 / \pm 45]_s$	1	6494
1/5/1	$[90_2 / \pm 45]_s$	1	4884
2.5/0/1	$[0_2 / \pm 45]_s$	2	$2.522 \times 10^6$
2.5/0/2.5	$[0_2 / \pm 45]_s$	2	3347
2.5/1/1	$[0_2 / \pm 45]_s$	2	$6.275 \times 10^4$
2.5/2.5/1	$[\pm 45]_{2s}$	1	$2.051 \times 10^4$

Table 9.3 shows the results for only tension cyclic loads. Maximum fatigue lives of the optimum designs are achieved up to  $1.36 \times 10^8$  cycles depending on the loads applied. Many stacking sequence design alternatives cannot be found since the number of design variables is only 2. The loadings of 1/5/0, 2.5/2.5/0, 2.5/3.75/0 and 5/0/0 are the



critical design cases in which the fatigue lives are obtained in cycle range of  $10^3$  and  $10^5$ . Table 9.4 shows the results for several tension and compression cyclic loads. The stacking sequence  $[0_2 / 90_2]_s$  is obtained in all loading cases. Fatigue lives can be maximized to the values of  $10^8$  cycles. However, the loadings of 1/-5/0 and 2.5/-5/0 are fatigue life critical cases. Tension-compression loading cases mostly yield higher fatigue lives when compared to the tension-tension loading cases in Table 9.3 (e.g., 1/1/0 and 1/-1/0, 2.5/2.5/0 and 2.5/-2.5/0). Table 9.5 shows the optimization results for various combinations of tension (T), compression (C) and shear (S) cyclic loads. As seen, maximum fatigue lives are obtained in  $10^6$  cycles level. It can be noted that fatigue life significantly decreases in the presence of shear load (e.g., 1/-1/0 and 1/-1/1, 1/2.5/0 and 1/2.5/1, etc.). T/C/S loading is the most critical design case. For example, 1/1/1 loading yields the  $[\pm 45]_{2s}$  design with  $4.843 \times 10^6$  life while 1/-1/1 loading gives the  $[\pm 45 / 90_2]_s$  design with a much lower life,  $3.809 \times 10^4$ .

Tables 9.6 – 9.8 represent the optimum 16-ply stacking sequence design results. In 16-ply design case, there are 4 design variables due to balance and symmetry constraints.

Table 9.6. Optimum 16-ply design results for various in-plane tension cyclic loads

Loading ( $\times 10^2$ N/mm) $N_{xx}/N_{yy}/N_{xy}$	Stacking sequence	Number of global optima	Fatigue life (cycles)
2.5/2.5/0	$[(0_2 / 90_2)_2]_s$	5(5)	$2.085 \times 10^7$
5/0/0	$[0_4 / \pm 45 / 0_2]_s$	4(1)	$3.348 \times 10^8$
5/2.5/0	$[0_2 / \pm 45_3]_s$	4(4)	$3.103 \times 10^6$
5/5/0	$[0_2 / \pm 45 / 90_2 / \pm 45]_s$	5(5)	$2.289 \times 10^5$
5/7.5/0	$[90_2 / 0_2 / 90_2 / \pm 45]_s$	10(8)	$2.065 \times 10^4$
7.5/2.5/0	$[(0_2 / \pm 45)_2]_s$	6(5)	$4.260 \times 10^5$
7.5/5/0	$[0_2 / 90_2 / 0_2 / \pm 45]_s$	9(9)	$2.065 \times 10^4$
10/0/0	$[0_4 / \pm 45 / 0_2]_s$	4(1)	$7.531 \times 10^6$
10/2.5/0	$[(\pm 45 / 0_2)_2]_s$	6(5)	$1.179 \times 10^5$

Table 9.7. Optimum 16-ply design results for various in-plane tension and compression cyclic loads

Loading ( $\times 10^2$ N/mm) $N_{xx}/N_{yy}/N_{xy}$	Stacking sequence	Number of global optima	Fatigue life (cycles)
2.5/-2.5/0	$[0_2 / 90_2]_{2s}$	6(4)	$1.272 \times 10^8$
2.5/-5/0	$[0_2 / 90_4 / \pm 45]_s$	10(8)	$5.636 \times 10^6$
5/-5/0	$[0_2 / 90_4 / 0_2]_s$	5(3)	$4.701 \times 10^6$
5/-7.5/0	$[90_2 / 0_2]_{2s}$	5(3)	$7.125 \times 10^4$
7.5/-2.5/0	$[0_4 / 90_2 / 0_2]_s$	4(1)	$3.339 \times 10^6$
7.5/-5/0	$[0_2 / 90_2]_{2s}$	6(4)	$7.125 \times 10^4$
10/-2.5/0	$[0_4 / 90_2 / 0_2]_s$	4(1)	$1.890 \times 10^5$
10/-5/0	$[0_4 / 90_2 / 0_2]_s$	4(1)	6058

Table 9.8. Optimum 16-ply design results for various in-plane tension, compression and shear cyclic loads

Loading ( $\times 10^2$ N/mm) $N_{xx}/N_{yy}/N_{xy}$	Stacking sequence	Number of global optima	Fatigue life (cycles)
2.5/2.5/2.5	$[\pm 45]_{4s}$	1(1)	$1.021 \times 10^6$
2.5/-2.5/2.5	$[0_2 / 90_2 / \pm 45_2]_s$	9(9)	$2.990 \times 10^6$
2.5/2.5/5	$[\pm 45]_{4s}$	1(1)	$3.881 \times 10^4$
2.5/-2.5/5	$[0_2 / \pm 45_2 / 90_2]_s$	12(12)	$1.045 \times 10^4$
5/0/2.5	$[0_4 / \pm 45_2]_s$	6(5)	$8.921 \times 10^5$
5/2.5/2.5	$[0_2 / \pm 45_3]_s$	4(4)	$7.148 \times 10^4$
5/-2.5/2.5	$[0_2 / \pm 45 / 0_2 / 90_2]_s$	9(8)	$1.203 \times 10^5$
5/5/2.5	$[\pm 45]_{4s}$	1(1)	$1.098 \times 10^4$
5/-5/2.5	$[\pm 45_2 / 90_2 / 0_2]_s$	12(12)	$1.045 \times 10^4$
7.5/0/2.5	$[0_2 / \pm 45]_{2s}$	6(5)	$9.337 \times 10^4$
7.5/2.5/2.5	$[\pm 45 / 0_2 / \pm 45_2]_s$	4(4)	8092
7.5/-2.5/2.5	$[\pm 45 / 0_4 / 90_2]_s$	9(8)	6630

Table 9.6 shows the optimization results for only tension cyclic loads. Different stress levels varying from  $N_{xx} = 2,5$  to  $10$  ( $\times 10^2$  N/mm) are tested. Multiple global optima are found. Feasible stacking sequence designs are achieved in many loading cases.

However, low fatigue life cases have occurred in the 5/7.5/0 and 7.5/5/0 loadings. Table 9.7 shows the results for several tension and compression cyclic loads. Mostly, the designs are obtained in the range of  $10^5$  and  $10^8$  cycles. The same sequences are found in some loading cases (e.g.,  $[0_4 / 90_2 / 0_2]_s$  in 7.5/-2.5/0, 10/-2.5/0 and 10/-5/0 loadings). It can be noted that fatigue lives are higher in T/C loadings compared to the T/T loadings in Table 9.6 considering that the same amount of load are applied (e.g., 2.5/2.5/0 and 2.5/-2.5/0, 5/5/0 and 5/-5/0, etc.). Table 9.8 shows the results for various combinations of tension, compression and shear cyclic loads. Many global optima are found. It is seen that fatigue life significantly decreases in the presence of shear load (e.g., 2.5/2.5/0 and 2.5/2.5/2.5, 5/0/0 and 5/0/2.5, etc.). The loadings of 2.5/-2.5/5, 5/5/2.5, 5/-5/2.5, 7.5/2.5/2.5, 7.5/-2.5/2.5 are the critical cases in which the fatigue lives can be maximized only up to  $10^3$ - $10^4$  cycles.

Table 9.9 shows the optimum stacking sequence design results for 32-ply laminates under various in-plane cyclic load combinations. As seen in the table, multiple global optima are obtained for almost each loading case. Feasible designs with fatigue life of  $10^5$ - $10^8$  cycles are achieved in most of the loading cases. Designs with low fatigue life are found in the Tension-(Tension/Compression)-Shear loadings such as 10/5/5, 10/-5/5 and 10/10/2.5, which is a similar trend to the previous design problems with fewer plies. It is also seen that fatigue lives are higher in T/C loadings compared to the T/T loadings (e.g.,  $3.103 \times 10^6$  cycles for 10/5/0 loading and  $1.263 \times 10^7$  cycles for 10/-5/0 loading). This is also a similar trend as in the previous optimum design problems performed using fewer plies.

Table 9.9. Optimum 32-ply stacking sequence design results for various in-plane cyclic loads

Loading ( $\times 10^2$ N/mm) $N_{xx}/N_{yy}/N_{xy}$	Stacking sequence	Number of global optima	Fatigue life (cycles)
10/0/0	$[(0_2 / \pm 45)_2 / 0_4 / \pm 45 / 0_2]_s$	11(1)	$2.442 \times 10^8$
10/0/2.5	$[0_4 / \pm 45_2 / 0_4 / \pm 45 / 0_2]_s$	22(5)	$1.216 \times 10^7$
10/2.5/0	$[(0_2 / \pm 45)_3 / \pm 45_2]_s$	21(14)	$1.714 \times 10^7$
10/5/0	$[\pm 45_4 / (\pm 45 / 0_2)_2]_s$	6(6)	$3.103 \times 10^6$
10/-5/0	$[0_2 / (0_2 / 90_2)_3 / 0_2]_s$	39(6)	$1.263 \times 10^7$
10/5/2.5	$[\pm 45_2 / 0_2 / \pm 45]_{2s}$	11(10)	$4.924 \times 10^5$
10/5/5	$[\pm 45_3 / 0_2 / \pm 45_4]_s$	8(8)	$7.253 \times 10^4$
10/-5/5	$[\pm 45 / 0_2 / 90_2 / 0_4 / \pm 45_3]_s$	50(40)	$1.415 \times 10^5$
10/10/0	$[0_2 / 90_2 / 0_2 / \pm 45_4 / 90_2]_s$	68(43)	$2.289 \times 10^5$
10/-10/0	$[0_2 / 90_2]_{4s}$	48(21)	$4.701 \times 10^6$
10/10/2.5	$[\pm 45]_{8s}$	1(1)	$5.151 \times 10^4$
10/-10/2.5	$[(0_2 / 90_2 / \pm 45)_2 / 0_2 / 90_2]_s$	73(51)	$3.861 \times 10^5$

In Tables 9.10 – 9.12, the results of optimum stacking sequence design with  $5^\circ$  incremental fiber angles ( $0_2^\circ, \pm 5^\circ, \dots, \pm 85^\circ, 90_2^\circ$ ) for the cases in which low fatigue life is obtained are presented together with the results of the designs with the conventional  $0_2^\circ, \pm 45^\circ, 90_2^\circ$  angles.

Table 9.10. Optimum 8-ply design results with 5° incremental fiber angles for the low fatigue life cases

Loading ( $\times 10^2$ N/mm) $N_{xx}/N_{yy}/N_{xy}$	Stacking sequence	Number of global optima	Fatigue life (cycles)
1/-1/1	$[\pm 25 / \pm 65]_s$	4(4)	$7.835 \times 10^6$
	$[\pm 45 / 90_2]_s$	1(1)	$3.809 \times 10^4$
1/2.5/1	$[\pm 55]_{2s}$	1(1)	$1.135 \times 10^6$
	$[\pm 45 / 90_2]_s$	2(2)	$6.275 \times 10^4$
1/-2.5/1	$[\pm 35 / 90_2]_s$	2(2)	$6.940 \times 10^5$
	$[90_2 / \pm 45]_s$	1(1)	6494
1/5/0	$[\pm 60 / \pm 65]_s$	2(2)	$8.146 \times 10^6$
	$[90_2 / \pm 45]_s$	2(2)	$2.370 \times 10^5$
1/-5/0	$[\pm 35 / 90_2]_s$	2(2)	7528
	$[0_2 / 90_2]_s$	2(2)	644
1/5/1	$[\pm 60 / \pm 65]_s$	2(2)	$2.003 \times 10^5$
	$[90_2 / \pm 45]_s$	1(1)	4884
2.5/0/2.5	$[\pm 20 / \pm 40]_s$	2(2)	$2.752 \times 10^4$
	$[0_2 / \pm 45]_s$	2(2)	3347
2.5/2.5/0	$[\pm 65 / \pm 25]_s$	4(4)	$2.289 \times 10^5$
	$[\pm 45]_{2s}$	1(1)	$2.289 \times 10^5$
2.5/2.5/1	$[\pm 45]_{2s}$	1(1)	$2.051 \times 10^4$
	$[\pm 45]_{2s}$	1(1)	$2.051 \times 10^4$
2.5/3.75/0	$[\pm 50]_{2s}$	1(1)	$4.235 \times 10^4$
	$[0_2 / 90_2]_s$	2(2)	5661
2.5/-5/0	$[\pm 20 / 90_2]_s$	2(2)	1534
	$[0_2 / 90_2]_s$	2(2)	1155
5/0/0	$[\pm 5]_{4s}$	1(1)	$1.279 \times 10^9$
	$[0_2 / \pm 45]_s$	2(2)	$3.010 \times 10^5$

Table 9.11. Optimum 16-ply stacking sequence design results with 5° incremental fiber angles for the low fatigue life cases

Loading ( $\times 10^2$ N/mm) $N_{xx}/N_{yy}/N_{xy}$	Stacking sequence	Number of global optima	Fatigue life (cycles)
2.5/2.5/5	$[\pm 45]_{4s}$	1(1)	$3.881 \times 10^4$
	$[\pm 45]_{4s}$	1(1)	$3.881 \times 10^4$
2.5/-2.5/5	$[\pm 25 / \pm 60 / \pm 65 / \pm 30]_s$	1(1)	$3.196 \times 10^4$
	$[0_2 / \pm 45_2 / 90_2]_s$	12(12)	$1.045 \times 10^4$
5/2.5/2.5	$[\pm 35 / \pm 40]_{2s}$	4(4)	$1.949 \times 10^5$
	$[0_2 / \pm 45_3]_s$	4(4)	$7.148 \times 10^4$
5/5/2.5	$[\pm 45]_{4s}$	1(1)	$1.098 \times 10^4$
	$[\pm 45]_{4s}$	1(1)	$1.098 \times 10^4$
5/-5/2.5	$[\pm 5 / \pm 85 / \pm 25 / \pm 65]_s$	8(8)	$3.220 \times 10^4$
	$[\pm 45_2 / 90_2 / 0_2]_s$	12(12)	$1.045 \times 10^4$
5/7.5/0	$[\pm 45 / \pm 55 / \pm 50_2]_s$	2(2)	$3.196 \times 10^4$
	$[90_2 / 0_2 / 90_2 / \pm 45]_s$	10(8)	$2.065 \times 10^4$
7.5/0/2.5	$[0_2 / \pm 5 / \pm 30_2]_s$	12(12)	$5.447 \times 10^5$
	$[0_2 / \pm 45]_{2s}$	6(5)	$9.337 \times 10^4$
7.5/2.5/2.5	$[\pm 30 / \pm 35_3]_s$	4(4)	$8.147 \times 10^4$
	$[\pm 45 / 0_2 / \pm 45_2]_s$	4(4)	8092
7.5/-2.5/2.5	$[0_2 / \pm 70 / \pm 30 / \pm 15]_s$	9(9)	$2.853 \times 10^4$
	$[\pm 45 / 0_4 / 90_2]_s$	9(8)	6630
7.5/5/0	$[\pm 40_2 / \pm 35 / \pm 45]_s$	1(1)	$3.196 \times 10^4$
	$[0_2 / 90_2 / 0_2 / \pm 45]_s$	9(9)	$2.065 \times 10^4$
10/2.5/0	$[\pm 30]_{4s}$	1(1)	$3.356 \times 10^6$
	$[(\pm 45 / 0_2)_2]_s$	6(5)	$1.179 \times 10^5$
10/-5/0	$[0_2 / 90_2 / 0_2 / \pm 40]_s$	12(10)	7374
	$[0_4 / 90_2 / 0_2]_s$	4(1)	6058

Table 9.12. Optimum 32-ply stacking sequence design results with 5° incremental fiber angles for the low fatigue life cases

Loading ( $\times 10^2$ N/mm) $N_{xx}/N_{yy}/N_{xy}$	Stacking sequence	Number of global optima	Fatigue life (cycles)
10/0/0	$[\pm 5]_{8s}$	1(1)	$3.551 \times 10^{19}$
	$[(0_2 / \pm 45)_2 / 0_4 / \pm 45 / 0_2]_s$	11(1)	$2.442 \times 10^8$
10/0/2.5	$[\pm 5_3 / \pm 35_3 / \pm 5_2]_s$	13(13)	$5.936 \times 10^7$
	$[0_4 / \pm 45_2 / 0_4 / \pm 45 / 0_2]_s$	22(5)	$1.216 \times 10^7$
10/2.5/0	$[\pm 30]_{8s}$	1(1)	$1.287 \times 10^8$
	$[(0_2 / \pm 45)_3 / \pm 45_2]_s$	21(14)	$1.714 \times 10^7$
10/5/0	$[(\pm 35 / \pm 40)_2 / \pm 40 / \pm 35]_s$	15(15)	$5.079 \times 10^6$
	$[\pm 45_4 / (\pm 45 / 0_2)_2]_s$	6(6)	$3.103 \times 10^6$
10/-5/0	$[0_2 / \pm 55 / 0_4 / (90_2 / 0_2)_2]_s$	11(2)	$1.584 \times 10^7$
	$[0_2 / (0_2 / 90_2)_3 / 0_2]_s$	39(6)	$1.263 \times 10^7$
10/5/2.5	$[(\pm 35 / \pm 40)_3 / \pm 40_2]_s$	40(40)	$1.028 \times 10^6$
	$[\pm 45_2 / 0_2 / \pm 45]_{2s}$	11(10)	$4.924 \times 10^5$
10/5/5	$[\pm 35_3 / \pm 40_5]_s$	38(38)	$1.953 \times 10^5$
	$[\pm 45_3 / 0_2 / \pm 45_4]_s$	8(8)	$7.253 \times 10^4$
10/-5/5	$[\pm 30_2 / 90_4 / \pm 10 / \pm 5 / \pm 30_2]_s$	1(1)	$2.755 \times 10^5$
	$[\pm 45 / 0_2 / 90_2 / 0_4 / \pm 45_3]_s$	50(40)	$1.415 \times 10^5$
10/10/0	$[\pm 15 / \pm 30 / \pm 60 / (0_2 / 90_2)_2 / \pm 75]_s$	53(29)	$2.289 \times 10^5$
	$[0_2 / 90_2 / 0_2 / \pm 45_4 / 90_2]_s$	68(43)	$2.289 \times 10^5$
10/-10/0	$[0_2 / 90_2]_{4s}$	19(11)	$4.701 \times 10^6$
	$[0_2 / 90_2]_{4s}$	48(21)	$4.701 \times 10^6$
10/10/2.5	$[\pm 45]_{8s}$	1(1)	$5.151 \times 10^4$
	$[\pm 45]_{8s}$	1(1)	$5.151 \times 10^4$
10/-10/2.5	$[\pm 30 / 90_4 / 0_4 / \pm 60 / 90_2 / 0_2]_s$	5(2)	$4.961 \times 10^5$
	$[(0_2 / 90_2 / \pm 45)_2 / 0_2 / 90_2]_s$	73(51)	$3.861 \times 10^5$

Table 9.10 shows the 8-ply stacking sequence design results. Optimum results obtained by the non-conventional angles are superior or at least comparable to the results obtained by the conventional angles. For example, in 1/-1/1 loading,  $[\pm 25/\pm 65]_s$  design with a fatigue life of  $7.835 \times 10^6$  cycles is found using  $5^\circ$  incremental fiber angles while  $[\pm 45/90_2]_s$  design with a fatigue life of  $3.809 \times 10^4$  cycles is found by conventional lamination. This corresponds to a serious increase of approximately 20470% in fatigue life. Considering the 5/0/0 loading case, the increase in fatigue life can even be up to 424817%. However, in 2.5/0/2.5, 2.5/2.5/0, 2.5/2.5/1 and 2.5/-5/0 loading cases, the same optimum designs are obtained.

Table 9.11 shows the optimization results for 16-ply laminate design. As seen in the table, in many loading cases, optimum designs with higher fatigue lives are found when compared to the designs with the conventional angles (e.g., 5/2.5/2.5, 7.5/0/2.5). Nevertheless, for almost all loading cases, the designs optimized by the non-conventional angles cannot reach practicable fatigue lives (e.g., 5/-5/2.5, 7.5/2.5/2.5, etc.). This situation shows that the applied cyclic loadings are too large to obtain feasible stacking sequence designs.

Table 9.12 shows the results for the optimum 32-ply stacking sequence designs. It can be seen from the table that considerable increase in various ratios in fatigue life are achieved by the design with the  $5^\circ$  incremental angles in many cases when compared to the conventional angle design. However, the same fatigue lives with the conventional design are found in the loadings of 10/10/0, 10/-10/0 and 10/10/2.5 even though different stacking sequences are obtained.

When all these fatigue optimization results are considered, it is seen that the research on fatigue optimization of carbon/epoxy composite laminates is a necessary practice to be able to increase the fatigue life, thus durability of the carbon/epoxy composite structures in critical applications.



## CHAPTER 10

### CONCLUSION

In this thesis study, the optimum stacking sequence design of carbon/epoxy composite laminates under various cyclic loading conditions for maximum fatigue life are achieved using different fatigue life prediction models and hybrid algorithms.

Firstly, the fatigue behavior of unidirectional E-glass/epoxy composite laminate is predicted using the FTPF, FWE, SB and ST models for various fiber off-axis angle specimens. The predictions of all models are shown to be in a good agreement with the experimental data, and consistent with the literature. After the off-axis angle laminate estimations, fatigue life prediction of multidirectional graphite/epoxy, glass/epoxy, carbon/epoxy and carbon/PEEK composites in different multidirectional configurations are obtained. It is seen in general that the models can successfully simulate the fatigue behavior of multidirectional composite laminates with different materials and configurations. Besides, while FTPF, FWE and SB methods mostly make the same estimations, ST somewhat underestimates the experimental data according to them. Hence, these positive results showed that the fatigue life prediction methods can be used in the optimization study.

Secondly, the algorithms and strategy to be used in the optimization are verified. Two different hybrid algorithms are used to solve the model problems. The first hybrid algorithm is constituted from GA and GPSA. A buckling optimization problem with different design cases is selected as a test problem and solved to evaluate the performance of the hybrid algorithm. The results are compared with the published data in the literature. It is seen that the GA-GPSA hybrid algorithm has the capability to find better results than the other algorithms compared. The second algorithm is constituted from PSA and GPSA. The same buckling problem is selected to test its performance and compare to the results in the literature. It is seen that the PSA-GPSA hybrid algorithm finds the best results in a shorter time than all the other algorithms compared. After the reliability of the algorithm is ensured, the fatigue optimization strategy is also validated for all the models through comparisons of their prediction and fatigue life maximization results with the

experimental data that belongs to different composite materials and multidirectional laminate configurations from the literature.

Then, the optimization studies are performed. Here, first, a number of fatigue design problems that include stacking sequence design cases for various in-plane cyclic loadings are solved by the GA-GPSA hybrid algorithm using only the FTPF model. The results show in general that fatigue life of composites changes dramatically according to type of loading, loading combination and level of stress. Most of the designs are obtained within fatigue life range of  $10^5$ - $10^7$ . However, in design cases of high loading, fatigue life can only be increased to  $10^2$  and  $10^3$  cycle levels. Especially in the presence of shear and compressive loads, fatigue life significantly decreases. These unsatisfactory results indicate the most critical cases that restrict to develop reasonable fatigue-resistant designs. Secondly, similar fatigue design problems with the first optimization study are solved by PSA-GPSA hybrid algorithm using the FTPF, FWE, SB and ST models. The results of the optimization study for maximum fatigue life imply that FTPF and SB models produce more reliable fatigue-resistant designs than FWE and ST models considering that the fatigue life values reached by the FTPF and SB are more reasonable compared to the life values found by the FWE and ST. This situation possibly arises from that FTPF and SB use the S-N curve equations of  $[0]$ ,  $[\pm 45]$  and  $[90]$  laminates to constitute their models, which guarantees a more robust mechanical model. However, the FWE and ST models use only one S-N curve equation to constitute their models, and these off-axis S-N curves should be selected wisely as they directly affect the accuracy of the predictions. It is also understood that even if one S-N curved fatigue life prediction models give accurate fatigue life predictions, this does not mean that they will give feasible optimum stacking sequence results.

As the final study of this thesis, the proposed fatigue-resistant design methodology is applied to carbon/epoxy composite laminates. After obtaining material properties from experimental procedure, the optimum stacking sequence designs of symmetric and balanced carbon/epoxy composite laminates subjected to various in-plane cyclic loads are investigated using the FTPF fatigue life prediction model and PSA-GPSA hybrid algorithm. The designs are constituted with both the conventional  $0_2^\circ, \pm 45^\circ, 90_2^\circ$  and the  $5^\circ$  incremental  $0_2^\circ, \pm 5^\circ, \dots, \pm 85^\circ, 90_2^\circ$  fiber angle stacks. The results show that fatigue life of composites significantly changes according to type of loading, loading combination and level of stress. Most of the designs are obtained within fatigue life range of  $10^5$ - $10^7$  cycles.

However, in design cases of high loading, and the combination of tension, compression and shear loadings, fatigue life can be increased to  $10^4$  cycles level at maximum. These unsatisfactory results indicate the most critical cases that restrict to develop reasonable fatigue-resistant designs. For these optima with low fatigue life, the results of optimization with the non-conventional  $0_2^\circ, \pm 5^\circ, \dots, \pm 85^\circ, 90_2^\circ$  angles show that the fatigue strength are enhanced in many loading cases when compared to the design with the conventional angles.

In conclusion, all the outcomes of this thesis study demonstrate the necessity and importance of design optimization practice of laminated composites for fatigue life advance in the structures where fatigue is critical. In this manner, the study shows in general that fatigue strength of laminated composites can be seriously improved by appropriate fiber stacking sequence designs along with reliable fatigue life prediction methods and powerful hybrid optimization algorithms.

## REFERENCES

1. Kaw, Autar K. *Mechanics of Composite Materials*. London: CRC, 2006.
2. Mallick, P. K. *Fiber-reinforced composites: materials, manufacturing, and design*. Boca Raton, FL: CRC Press, 2008.
3. Vassilopoulos, Anastasios P., and Thomas Keller. *Fatigue of fiber-reinforced composites*. London: Springer-Verlag, 2011.
4. Quaresimin, Marino, Luca Susmel, and Ramesh Talreja. "Fatigue behaviour and life assessment of composite laminates under multiaxial loadings." *International Journal of Fatigue* 32, no. 1 (2010): 2-16.
5. Hashin Z., and Rotem A. "A fatigue failure criterion for fiber reinforced materials." *Journal of Composite Materials* 7, 1973, 448-64.
6. Rotem, Assa. "Fatigue Failure of Multidirectional Laminate." *AIAA Journal* 17, no. 3 (1979): 271-77.
7. Sims D. F., and Brogdon V. H. "Fatigue Behavior of Composites under Different Loading Modes." In: Reifsnider KL, Lauraitis KN, editors. *Fatigue of filamentary materials*. *ASTM STP* 636 (1977): 185-205.
8. Fawaz, Z., and F. Ellyin. "Fatigue Failure Model for Fibre-Reinforced Materials under General Loading Conditions." *Journal of Composite Materials* 28, no. 15 (1994): 1432-451.
9. Philippidis, T. P., and A. P. Vassilopoulos. "Fatigue Strength Prediction under Multiaxial Stress." *Journal of Composite Materials* 33, no. 17 (1999): 1578-599.
10. Kawai, M. "A phenomenological model for off-axis fatigue behavior of unidirectional polymer matrix composites under different stress ratios." *Composites Part A: Applied Science and Manufacturing* 35, no. 7-8 (2004): 955-63.
11. Shokrieh, M. M., and F. Taheri-Behrooz. "A unified fatigue life model based on energy method." *Composite Structures* 75, no. 1-4 (2006): 444-50.
12. Adali, S. "Optimisation of Fibre Reinforced Composite Laminates Subject to Fatigue Loading." *Composite Structures* 3, 1985, 43-55.
13. Walker, M. "A method for optimally designing laminated plates subject to fatigue loads for minimum weight using a cumulative damage constraint." *Composite Structures* 48, no. 1-3 (2000): 213-18.
14. Ertas A. H., and F. O. "Sonmez. Design optimization of fiber-reinforced laminates for maximum fatigue life." *Journal of Composite Materials* 48, no. 20 (2014):2493-2503.
15. Muc, A., and M. Muc-Wierzgoń. "Discrete optimization of composite structures under fatigue constraints." *Composite Structures* 133 (2015): 834-39.
16. Deveci, H. Arda, and H. Seçil Artem. "Optimum design of fatigue-resistant composite laminates using hybrid algorithm." *Composite Structures* 168 (2017): 178-88.
17. Vassilopoulos, A. P. *Fatigue life prediction of composites and composite structures*. Cambridge, UK: Woodhead Publishing Limited, 2010.
18. Vinson, J. R., and R. L. Sierakowski. *The Behavior of Structures Composed of*

*Composite Materials*. Kluwer Academic Publishers, 2004.

19. ASTM D 3479/D 3479M – 96 (Reapproved 2002), "Standard Test Method for Tension-Tension Fatigue of Polymer Matrix Composite Materials."
20. ISO 13003:2003, "Fibre-reinforced plastics – Determination of fatigue properties under cyclic loading conditions."
21. Tsai S. W., and H. T. Hahn. *Introduction to Composite Materials*. Lancaster: Technomic, 1980.
22. Sandhu R. S., Gallo R. L., and G. P. Sendeckyj. "In Initiation and Accumulation of Damage in Composite Laminates." In: Daniel IM editor. *ASTM STP 787* (1982): 163-182.
23. Kadi, H. El, and F. Ellyin. "Effect of stress ratio on the fatigue of unidirectional glass fibre/epoxy composite laminae." *Composites* 25, no. 10 (1994): 917-24.
24. Rotem A., and H. G. Nelson. "Residual Strength of Composite Laminates Subjected to Tensile-Compressive Fatigue Loading." *Journal of Composites Technology and Research* 12, no. 2 (1990): 76-84.
25. Naderi, M., and A. R. Maligno. "Fatigue life prediction of carbon/epoxy laminates by stochastic numerical simulation." *Composite Structures* 94, no. 3 (2012): 1052-059.
26. Lian, Wei, and Weixing Yao. "Fatigue life prediction of composite laminates by FEA simulation method." *International Journal of Fatigue* 32, no. 1 (2010): 123-33.
27. Jen, M. H. R., and C. H. Lee. "Strength and life in thermoplastic composite laminates under static and fatigue loads. Part I: Experimental." *International Journal of Fatigue* 20, no. 9 (1998): 605-15.
28. Yang, Xin-She. *Engineering optimization: an introduction with metaheuristic applications*. Hoboken, NJ: John Wiley, 2010.
29. Rao, S. S. *Engineering optimization: theory and practice*. Hoboken, NJ: John Wiley, 2009.
30. Blum, Christian, and Günther R. Raidl. *Hybrid metaheuristics powerful tools for optimization*. Cham: Springer international publishing AG, 2016.
31. Yogeswaran M., Ponnambalam S. G., and M. K. Tiwari. "An efficient hybrid evolutionary heuristic using genetic algorithm and simulated annealing algorithm to solve machine loading problem in FMS." *International Journal of Production Research* 47, no. 19 (2009): 5421-48.
32. Alarifi, Abdulaziz, Zhefu Liu, Fatih Safa Erenay, Ali Elkamel, and Eric Croiset. "Dynamic Optimization of Lurgi Type Methanol Reactor Using Hybrid GA-GPS Algorithm: The Optimal Shell Temperature Trajectory and Carbon Dioxide Utilization." *Industrial & Engineering Chemistry Research* 55, no. 5 (2016): 1164-173.
33. Deveci, H. Arda, Levent Aydin, and H. Seçil Artem. "Buckling optimization of composite laminates using a hybrid algorithm under Puck failure criterion constraint." *Journal of Reinforced Plastics and Composites* 35, no. 16 (2016): 1233-247.
34. Holland, J. H. *Adaptation in natural and artificial systems: An introductory analysis with applications to biology, control, and artificial intelligence*. Oxford: U Michigan Press, 1975.

35. Torczon, Virginia. "On the Convergence of Pattern Search Algorithms." *SIAM Journal on Optimization* 7, no. 1 (1997): 1-25.
36. Nicosia, Giuseppe, and Giovanni Stracquadanio. "Generalized Pattern Search Algorithm for Peptide Structure Prediction." *Biophysical Journal* 95, no. 10 (2008): 4988-999.
37. MATLAB Optimization Toolbox. Computer software. Version R2016a. The Mathworks, Inc., 2016.
38. Vassilopoulos, A., E. Georgopoulos, and T. Keller. "Comparison of genetic programming with conventional methods for fatigue life modeling of FRP composite materials." *International Journal of Fatigue* 30, no. 9 (2008): 1634-645.
39. Al-Assaf, Y., and H. El Kadi. "Fatigue life prediction of unidirectional glass fiber/epoxy composite laminae using neural networks." *Composite Structures* 53, no. 1 (2001): 65-71.
40. Junior, R., A. Neto, and E. Aquino. "Building of constant life diagrams of fatigue using artificial neural networks." *International Journal of Fatigue* 27, no. 7 (2005): 746-51
41. Vassilopoulos, A., E. Georgopoulos, and V. Dionysopoulos. "Artificial neural networks in spectrum fatigue life prediction of composite materials." *International Journal of Fatigue* 29, no. 1 (2007): 20-29.
42. Xiang, Ke-Lu, Pu-Yu Xiang, and You-Ping Wu. "Prediction of the fatigue life of natural rubber composites by artificial neural network approaches." *Materials & Design* 57 (2014): 180-85.
43. Salmalian, K., Soleimani, M., and S. Rouhi. "Fatigue life Modeling and Prediction of GRP Composites Using Multi-objective Evolutionary Optimized Neural Networks." *MMMAS* 1, no. 6 (2012): 1-10.
44. Riche, Rodolphe Le, and Raphael T. Haftka. "Optimization of laminate stacking sequence for buckling load maximization by genetic algorithm." *AIAA Journal* 31, no. 5 (1993): 951-56.
45. Soremekun, G., Z. Gürdal, R. T. Haftka, and L. T. Watson. "Composite laminate design optimization by genetic algorithm with generalized elitist selection." *Computers & Structures* 79, no. 2 (2001): 131-43.
46. Rao, A. Rama Mohan, and N. Arvind. "A scatter search algorithm for stacking sequence optimisation of laminate composites." *Composite Structures* 70, no. 4 (2005): 383-402.
47. Rao, A. Rama Mohan, and N. Arvind. "Optimal stacking sequence design of laminate composite structures using tabu embedded simulated annealing." *Structural Engineering and Mechanics* 25, no. 2 (2007): 239-68.
48. Rao, A. Rama Mohan, and K. Lakshmi. "Optimal design of stiffened laminate composite cylinder using a hybrid SFL algorithm." *Journal of Composite Materials* 46, no. 24 (2012): 3031-055.
49. Rao, A. Rama Mohan. "Lay-up sequence design of laminate composite plates and a cylindrical skirt using ant colony optimization." *Proceedings of the Institution of Mechanical Engineers, Part G: Journal of Aerospace Engineering* 223, no. 1 (2008): 1-18.

50. MATLAB Optimization Toolbox. Computer software. Version R2016b, The Mathworks, Inc., 2016.
51. Global Optimization Toolbox User's Guide, MATLAB computer software in version R2016b, The Mathworks, Inc., 2016; 384-95.
52. Chawla, Krishan K. *Composite materials: science and engineering*. New York: Springer, 2013.
53. Hoa, S. V. *Principles of the manufacturing of composite materials*. Lancaster, PA: DEStech Publications, Inc., 2009.
54. ASTM D 3039/D 3039M – 14, "Standard Test Method for Tensile Properties of Polymer Matrix Composite Materials."
55. ASTM E 132, "Test Method for Poisson's Ratio at Room Temperature."
56. Jones, Robert M. *Mechanics of composite materials*. Tokyo: McGraw-Hill, 1998.

## APPENDIX A

### MATLAB PROGRAM CODE FOR EXPERIMENTAL CORRELATION

#### Sample code for 30° off-axis angle predictions

```
hold off
clc;clear;

Xt = 1235.64; %[MPa]
Xc = -1235.64;
Yt = 28.44;
Yc = -28.44;
S12 = 37.95;

grafik1=1;
grafik2=1;
grafik3=1;
grafik4=1;

for sigma1 = 30:1:56
a=30; %[degrees]
sigma=[sigma1;0;0]; %[MPa]

r=cos((a*pi)/180);
s=sin((a*pi)/180);
sigma1 = r^2*sigma(1,1)+s^2*sigma(2,1)+2*r*s*sigma(3,1);
sigma2 = s^2*sigma(1,1)+r^2*sigma(2,1)-2*r*s*sigma(3,1);
sigma6 = -r*s*sigma(1,1)+r*s*sigma(2,1)+(r^2-s^2)*sigma(3,1);
n=sym('n');

logN1 = solve(sigma6^2/((73*n)/20 - 719/20)^2 + sigma2^2/((163*n)/50 - 3611/100)^2
+ sigma1^2/((693*n)/5 - 70749/50)^2 -(sigma1*sigma2)/(((163*n)/50 -
3611/100)*((693*n)/5 - 70749/50)) - 1 == 0, n); % FTPF

logN1=double(logN1);

logN2 = solve(sigma6^2/((73*n)/20 - 719/20)^2 + sigma2^2/((163*n)/50 - 3611/100)^2
- 1 == 0, n); % Matrix failure (Hashin-Rotem)

logN3 = solve(sigma6^2/(sigma1^2*((73*n)/20 - 719/20)^2) - 1/sigma1^2 +
sigma2^2/(sigma1^2*((163*n)/50 - 3611/100)^2) + ...
sigma1^2/(sigma1^2*((693*n)/5 - 70749/50)^2) -
(sigma1*sigma2)/(sigma1^2*((693*n)/5 - 70749/50)^2) == 0,n); % Sims - Brogdon
```



```

%%%%%%%% Shokrieh-Taheri %%%%%%%%%
R = 0.1;

k = 8.18;
alfa = -0.1638;

sigma_r = 2*sigmax1;

W = ((1+R)/(1-R))*(sigma_r^2)*(((cosd(a)^4)/Xt^2) + ((sind(a)^4)/Yt^2) +
(((sind(a)^2)*(cosd(a)^2))/S12^2));

Nf(grafik4) = (W/k)^(1/alfa);
grafik4=grafik4+1;

%%%%%%%%%

counterreal=1; nfindex=1;
while counterreal<=size(logN1,1)
    if isreal(logN1(counterreal,1))==1
        Nf1(nfindex,1)=logN1(counterreal,1);
        nfindex=nfindex+1;
    end
    counterreal=counterreal+1;
end

counterreal1=1; nfindex1=1;
while counterreal1<=size(logN3,1)
    if isreal(logN3(counterreal1,1))==1
        Nf11(nfindex1,1)=logN3(counterreal1,1);
        nfindex1=nfindex1+1;
    end
    counterreal1=counterreal1+1;
end

minNf1(grafik1) = min(Nf1);
grafik1=grafik1+1;

minNf2(grafik2) = min(real(logN2));
grafik2=grafik2+1;

minNf3(grafik3) = min(Nf11);
grafik3=grafik3+1;

end

hold on

```

%%%%%%%% Fawaz - Ellyin (FWE) %%%%%%%%%

Xr = 142.98; %[MPa] Reference angle --> 15 degree

mr = -15.31;

br = 148.13;

R = 0.1;

Rr= 0.1;

i=1;

S = 30:1:56; %(31.1688 : 55.0649)

Sr = 57.4026:1.748246:102.856996; % reference stress

for j = 1:27

SS=S(1,j);

SSr=Sr(1,j);

sigma\_max = (2\*SS)/(1-R);

sigma\_max\_r = (2\*SSr)/(1-Rr); % 15 deg reference maximum stress

% Stress Ratio Correlation Factor %

%g = (sigma\_max/sigma\_max\_r)\*((1-R)/(1-Rr));

g=1;

sigma = [SS;0;0];

sigma\_x = sigma(1,1);

sigma\_y = sigma(2,1);

sigma\_xy = sigma(3,1);

% The first & second biaxial ratios %

a1 = sigma\_y/sigma\_x;

a2 = sigma\_xy/sigma\_x;

%%%%%%%% Static Strength Correlation Factor %%%%%%%%%

m=cosd(30);

n=sind(30);

f = (Xt/Xr)\*(((m^2 + a1\*(n^2) + 2\*a2\*m\*n)^2) - ((m^2) + a1\*(n^2) +  
2\*a2\*m\*n)\*((n^2) + a1\*(m^2) - 2\*a2\*m\*n) + ((Xt^2)/(Yt^2))\*((n^2) + a1\*(m^2) -  
2\*a2\*m\*n)^2) + ((Xt^2)/(S12^2))\*(((a1-1)\*m\*n) + a2\*((m^2) + (n^2)))^2)^(-0.5);

% Logarithmic Fatigue life %

logN4(i)=((SS/f)-br)/(mr\*g);

i=i+1;

end

```
%%%%%%%%%
```

```
exp_data=xlsread('30deg.xls');
```

```
sigma_grafik = 30:1:56; % 31.1688:55.0649
```

```
plot(minNf1,sigma_grafik,minNf2,sigma_grafik,minNf3,sigma_grafik,logN4,sigma_grafik,log10(Nf),sigma_grafik,exp_data(:,1),exp_data(:,2),'o','LineWidth',1)
```

```
xlabel('logN');
```

```
ylabel('\sigma_{a}');
```

```
legend('FTPF','HR','SB','FWE','ST');
```

### Sample code for multidirectional [0/90]4s Graphite/Epoxy laminate

```
hold off
```

```
clc;clear;
```

```
Nplies = 16; %--> number of layers
```

```
h_ply = 2/16; %--> thickness of a layer[mm]
```

```
E1 = 129*10^3; %[MPa]
```

```
E2 = 11*10^3; %[MPa]
```

```
% G12 = 5.886*10^3; %[MPa]
```

```
G12 = 22*10^3; %[MPa]
```

```
NU12 = 0.27;
```

```
NU21 = (NU12*E2)/E1;
```

```
Q11 = E1/(1 - NU12*NU21);
```

```
Q12 = (NU21*E1)/(1 - NU12*NU21);
```

```
Q22 = E2/(1 - NU12*NU21);
```

```
Q66 = G12;
```

```
t = Nplies * h_ply ; % total thickness
```

```
for j = 1:(Nplies+1)
```

```
h(j) = -(t/2-((j-1)*(t/Nplies)));
```

```
end
```

```
% Stacking sequence %
```

```
x_half = [0 90 0 90 0 90 0 90];
```

```
x = [x_half fliplr(x_half)];
```

```
%%%%%%%%%
```

```
% ABD matrisinin hesaplanması%
```

```
A=zeros(3,3);
```

```
% B=zeros(3,3);
```

```
% D=zeros(3,3);
```

```
for k=1:Nplies
```

```
    c=cos((x(k)*pi)/180);
```

```
    s=sin((x(k)*pi)/180);
```

```

Qbar11 = Q11*c^4 + 2*(c^2)*(s^2)*(Q12+2*Q66) + Q22*s^4;
Qbar12 = Q12*(c^4 + s^4) + (Q11+Q22-4*Q66)*(c^2)*(s^2);
Qbar22 = Q11*s^4 + 2*(Q12+2*Q66)*(c^2)*(s^2) + Q22*c^4;
Qbar16 = (Q11-Q12-2*Q66)*s*(c^3) + (Q12-Q22+2*Q66)*c*(s^3);
Qbar26 = (Q11-Q12-2*Q66)*c*(s^3) + (Q12-Q22+2*Q66)*s*(c^3);
Qbar66 = (Q11+Q22-2*Q12-2*Q66)*(c^2)*(s^2) + Q66*(c^4+s^4);
eval(['Qbar_' num2str(k) ']=[Qbar11 Qbar12 Qbar16;Qbar12 Qbar22 Qbar26;Qbar16
Qbar26 Qbar66;']);

```

```

A(1,1)=A(1,1)+Qbar11*(h(1,k+1)-h(1,k));
A(1,2)=A(1,2)+Qbar12*(h(1,k+1)-h(1,k));
A(1,3)=A(1,3)+Qbar16*(h(1,k+1)-h(1,k));
A(2,2)=A(2,2)+Qbar22*(h(1,k+1)-h(1,k));
A(3,3)=A(3,3)+Qbar66*(h(1,k+1)-h(1,k));
A(2,3)=A(2,3)+Qbar26*(h(1,k+1)-h(1,k));

```

end

```

A(2,1)=A(1,2);
A(3,2)=A(2,3);
A(3,1)=A(1,3);

```

%%%%%%%% Calculation of Inverse A matrix

```

a11=A(2,2)*A(3,3)-(A(3,2)*A(2,3));
a12=A(1,3)*A(3,2)-(A(3,3)*A(1,2));
a13=A(1,2)*A(2,3)-(A(2,2)*A(1,3));
a21=A(2,3)*A(3,1)-(A(3,3)*A(2,1));
a22=A(1,1)*A(3,3)-(A(3,1)*A(1,3));
a23=A(1,3)*A(2,1)-(A(2,3)*A(1,1));
a31=A(2,1)*A(3,2)-(A(3,1)*A(2,2));
a32=A(1,2)*A(3,1)-(A(3,2)*A(1,1));
a33=A(1,1)*A(2,2)-(A(2,1)*A(1,2));

```

```
aa=[a11,a12,a13;a21,a22,a23;a31,a32,a33];
```

```
detA=A(1,1)*A(2,2)*A(3,3) + A(1,2)*A(2,3)*A(3,1) + A(1,3)*A(2,1)*A(3,2) -
A(1,3)*A(2,2)*A(3,1) - A(1,2)*A(2,1)*A(3,3) - A(1,1)*A(2,3)*A(3,2);
```

```
Ainv=(1/detA)*aa;
```

%%%%%%%% FTPF %%%%%%%%%

```
clear c s
```

```
grafik1=1;
```

```
for Nx = 595.1244:15.76378:1556.71498 % 595.1244 : 1556.7150
```

```
    Ny = 0; %[N/mm]
```

```
    Nxy = 0;
```

```
    N=[Nx;Ny;Nxy];
```

```
    eps=Ainv*N;
```

```

sigma=Qbar_1*eps; %[MPa]

a=0; %[degrees]
r=cos((a*pi)/180);
s=sin((a*pi)/180);
sigma1 = r^2*sigma(1,1)+s^2*sigma(2,1)+2*r*s*sigma(3,1);
sigma2 = s^2*sigma(1,1)+r^2*sigma(2,1)-2*r*s*sigma(3,1);
sigma6 = -r*s*sigma(1,1)+r*s*sigma(2,1)+(r^2-s^2)*sigma(3,1);

n=sym('n');

logN=solve(sigma6^2/((411292995188215*n)/35184372088832 - 189/2)^2 +
sigma2^2/((6417*n)/625 - 72)^2 + sigma1^2/((94703*n)/1000 - 1630)^2 - ...
(sigma1*sigma2)/(((6417*n)/625 - 72)*((94703*n)/1000 - 1630)) - 1 == 0, n);
logN=double(logN);

counterreal=1; nfindex=1;
while counterreal<=size(logN,1)
    if isreal(logN(counterreal,1))==1
        Nf(nfindex,1)=logN(counterreal,1);
        nfindex=nfindex+1;
    end
    counterreal=counterreal+1;
end

minNf1(grafik1)=min(Nf);
grafik1=grafik1+1;
end

%%%% HASHIN-ROTEM (HR) %%%

clear Nx eps sigma sigma1 sigma2 sigma6 r s

grafik2=1;
for Nx = 516.1570:23.0925:1924.7995 % 516.1570 : 1924.8
    Ny = 0; %[N/mm]
    Nxy = 0;
    N=[Nx;Ny;Nxy];
    eps=Ainv*N;
    sigma=Qbar_1*eps; %[MPa]

a=0; %[degrees]
r=cos((a*pi)/180);
s=sin((a*pi)/180);
sigma1 = r^2*sigma(1,1)+s^2*sigma(2,1)+2*r*s*sigma(3,1);
sigma2 = s^2*sigma(1,1)+r^2*sigma(2,1)-2*r*s*sigma(3,1);
sigma6 = -r*s*sigma(1,1)+r*s*sigma(2,1)+(r^2-s^2)*sigma(3,1);

n=sym('n');

```

```

logN2=solve(sigma6^2/((411292995188215*n)/35184372088832 - 189/2)^2 +
sigma2^2/((6417*n)/625 - 72)^2 - 1 == 0, n);

minNf2(grafik2)=min(real(logN2));
grafik2=grafik2+1;
end

%%%%%%%%% Sims - Brogdon (SB) %%%%%%%%%%%%%%

clear Nx eps sigma sigma1 sigma2 sigma6 r s

grafik3=1;
for Nx = 470.9753:10.8922:1135.3995 % 470.9753 : 1135.4
    Ny = 0; %[N/mm]
    Nxy = 0;
    N=[Nx;Ny;Nxy];
    eps=Ainv*N;
    sigma=Qbar_1*eps; %[MPa]

a=0; %[degrees]
r=cos((a*pi)/180);
s=sin((a*pi)/180);
sigma1 = r^2*sigma(1,1)+s^2*sigma(2,1)+2*r*s*sigma(3,1);
sigma2 = s^2*sigma(1,1)+r^2*sigma(2,1)-2*r*s*sigma(3,1);
sigma6 = -r*s*sigma(1,1)+r*s*sigma(2,1)+(r^2-s^2)*sigma(3,1);

    n=sym('n');

    logN3=solve(sigma6^2/(sigma(1,1)^2*((411292995188215*n)/35184372088832 -
189/2)^2) - 1/sigma(1,1)^2 + sigma2^2/(sigma(1,1)^2*((6417*n)/625 - 72)^2) ...
+ sigma1^2/(sigma(1,1)^2*((94703*n)/1000 - 1630)^2) -
(sigma1*sigma2)/(sigma(1,1)^2*((94703*n)/1000 - 1630)^2) == 0, n);
    logN3=double(logN3);

counterreal=1; nfindex=1;
while counterreal<=size(logN3,1)
    if isreal(logN3(counterreal,1))==1
        Nf(nfindex,1)=logN3(counterreal,1);
        nfindex=nfindex+1;
    end
    counterreal=counterreal+1;
end

minNf3(grafik3)=min(Nf);
grafik3=grafik3+1;
end

%%%%%%%%% FWE %%%%%%%%%%%%%%

clear Nx eps sigma

```

```

Xt = 1630;
Yt = 74;
S12 = 205;
Xr = 205; %[MPa] Reference angle --> 45 degree
mr = -18.87;
br = 167.6;
R = -1;
Rr = -1;

i=1;

S = 485.791:4.99275:790.34875; % 485.791 : 790.349
Sr = 49.4125:1.81614:160.19704; % reference 49.4125 : 160.197 (45 deg)

for j = 1:62
    SS=S(1,j);
    SSr=Sr(1,j);
    sigma_max = (2*SS)/(1-R);

    sigma_max_r = (2*SSr)/(1-Rr); % 45 deg reference maximum stress

    % Stress Ratio Correlation Factor %
    %g = (sigma_max/sigma_max_r)*((1-R)/(1-Rr));
    g=1;

    sigma = [SS;0;0];

    sigma_x = sigma(1,1);
    sigma_y = sigma(2,1);
    sigma_xy = sigma(3,1);

    % The first & second biaxial ratios %
    a1 = sigma_y/sigma_x;
    a2 = sigma_xy/sigma_x;

    % Static Strength Correlation Factor %
    m=cosd(0);
    n=sind(0);

    f = (Xt/Xr)*(((m^2 + a1*(n^2) + 2*a2*m*n)^2) - ((m^2) + a1*(n^2) +
    2*a2*m*n)*((n^2) + a1*(m^2) - 2*a2*m*n) + ((Xt^2)/(Yt^2))*(((n^2) + a1*(m^2) -
    2*a2*m*n)^2) + ((Xt^2)/(S12^2))*(((a1-1)*m*n) + a2*((m^2) + (n^2)))^2)^(-0.5);

    % Logarithmic Fatigue life %
    logN4(i) = ((SS/f)-br)/(mr*g);

    i=i+1;

```

```

end

%%%%%%%%%%%%%%%%%%%%%%%%%%%%%%%%%%%%%%%%%%%%%%%%%%%%%%%%%%%%%%%%%%%%%%%%
%%%%%%%%%%%%%%%%%%%%%%%%%%%%%%%%%%%%%%%%%%%%%%%%%%%%%%%%%%%%%%%%%%%%%%%%

hold on
x1=3.6:.1:6.1;
plot(x1,-91.61*x1 + 740.7,'--')

x2=3.6:.1:6.1;
plot(x2,-156.9*x2 + 1262,'-.')

exp_data=xlsread('Plot_data_cross_ply.xls');
sigma_grafik = 485.5:5:790.5; % (range = 61) % 485.791 : 790.349
plot(minNf1,sigma_grafik,minNf2,sigma_grafik,minNf3,sigma_grafik,logN4,sigma_grafik,exp_data(:,1),exp_data(:,2),'o','LineWidth',1)
xlabel('logN');
ylabel('\sigma_{a} (MPa)');
legend('First ply failure(FWE-Sonmez)','Final failure(FWE-Sonmez)','FTPF','HR','SB','FWE');

```



## APPENDIX B

### MATLAB PROGRAM CODE FOR OPTIMIZATION

#### Sample code for the objective function

```
function f = FTPF_objfunc(x)

Nplies = 32; %--> number of layers
n4=Nplies/4;
n2=Nplies/2;
h_ply = 0.3475; %--> thickness of a layer [mm]
E1 = 102.19*10^3; %[MPa]
E2 = 5.90*10^3; %[MPa]
G12 = 6.19*10^3; %[MPa]
NU12 = 0.31;
NU21 = (NU12*E2)/E1;
Q11 = E1/(1 - NU12*NU21);
Q12 = (NU21*E1)/(1 - NU12*NU21);
Q22 = E2/(1 - NU12*NU21);
Q66 = G12;

t = Nplies * h_ply ; % total thickness
for j = 1:(Nplies+1)
    h(j) = -(t/2-((j-1)*(t/Nplies)));
end

% 0-45-90 fiber angles %

j=1;
for i=1:n4

    if x(i)>=30
        x1(j)=90;
        x1(j+1)=90;
        j=j+2;

    elseif x(i)>=-30
        x1(j)=45;
        x1(j+1)=-45;
        j=j+2;
    else

        x1(j)=0;
        x1(j+1)=0;
        j=j+2;
    end
end
```

```

end
end

% balance & symmetry

for i=1:n4
x1(j)=x(i);
x1(j+1)=-x(i);
j=j+2;
end
for i=1:n2
x(i)=x1(i);
end

for i=1:n2
x(n2+i)=x(n2-i+1);
end

% ABD matrisinin hesaplanması%

A=zeros(3,3);
for k=1:Nplies
c=cos((x(k)*pi)/180);
s=sin((x(k)*pi)/180);
Qbar11 = Q11*c^4 + 2*(c^2)*(s^2)*(Q12+2*Q66) + Q22*s^4;
Qbar12 = Q12*(c^4 + s^4) + (Q11+Q22-4*Q66)*(c^2)*(s^2);
Qbar22 = Q11*s^4 + 2*(Q12+2*Q66)*(c^2)*(s^2) + Q22*c^4;
Qbar16 = (Q11-Q12-2*Q66)*s*(c^3) + (Q12-Q22+2*Q66)*c*(s^3);
Qbar26 = (Q11-Q12-2*Q66)*c*(s^3) + (Q12-Q22+2*Q66)*s*(c^3);
Qbar66 = (Q11+Q22-2*Q12-2*Q66)*(c^2)*(s^2) + Q66*(c^4+s^4);
eval(['Qbar_' num2str(k) '= [Qbar11 Qbar12 Qbar16; Qbar12 Qbar22 Qbar26; Qbar16
Qbar26 Qbar66];']);

A(1,1)=A(1,1)+Qbar11*(h(1,k+1)-h(1,k));
A(1,2)=A(1,2)+Qbar12*(h(1,k+1)-h(1,k));
A(1,3)=A(1,3)+Qbar16*(h(1,k+1)-h(1,k));
A(2,2)=A(2,2)+Qbar22*(h(1,k+1)-h(1,k));
A(3,3)=A(3,3)+Qbar66*(h(1,k+1)-h(1,k));
A(2,3)=A(2,3)+Qbar26*(h(1,k+1)-h(1,k));

end

A(2,1)=A(1,2);
A(3,2)=A(2,3);
A(3,1)=A(1,3);

%%%%%%%%%% Calculation of Inverse A matrix

a11=A(2,2)*A(3,3)-(A(3,2)*A(2,3));
a12=A(1,3)*A(3,2)-(A(3,3)*A(1,2));

```

```

a13=A(1,2)*A(2,3)-(A(2,2)*A(1,3));
a21=A(2,3)*A(3,1)-(A(3,3)*A(2,1));
a22=A(1,1)*A(3,3)-(A(3,1)*A(1,3));
a23=A(1,3)*A(2,1)-(A(2,3)*A(1,1));
a31=A(2,1)*A(3,2)-(A(3,1)*A(2,2));
a32=A(1,2)*A(3,1)-(A(3,2)*A(1,1));
a33=A(1,1)*A(2,2)-(A(2,1)*A(1,2));

aa=[a11,a12,a13;a21,a22,a23;a31,a32,a33];

detA=A(1,1)*A(2,2)*A(3,3) + A(1,2)*A(2,3)*A(3,1) + A(1,3)*A(2,1)*A(3,2) -
A(1,3)*A(2,2)*A(3,1) - A(1,2)*A(2,1)*A(3,3) - A(1,1)*A(2,3)*A(3,2);

Ainv=(1/detA)*aa;

%%%%%%%%%% In-Plane LOADS %%%%%%%%%%%

Nx = 10*10^2; %[N/mm]
Ny = 2.5*10^2; %[N/mm]
Nxy = 2.5*10^2;
N=[Nx;Ny;Nxy];

%%%%%%%%%% Stresses %%%%%%%%%%%

for k=1:Nplies
    eps=Ainv*N;
    Qbar_ =eval(['Qbar_' int2str(k)]);
    eval(['sigma' num2str(k) '=Qbar_*eps;']);
end

%%%%%%%%%% Principal Material System Stresses (sigma1, sigma2 & sigma6)

clear c s
for k=1:Nplies
    c=cos((x(k)*pi)/180);
    s=sin((x(k)*pi)/180);
    sigma=eval(['sigma' int2str(k)]);
    eval(['sigma1_' num2str(k) '=c^2*sigma(1,1)+s^2*sigma(2,1)+2*c*s*sigma(3,1);'])
    eval(['sigma2_' num2str(k) '=s^2*sigma(1,1)+c^2*sigma(2,1)-2*c*s*sigma(3,1);'])
    eval(['sigma6_' num2str(k) '=-c*s*sigma(1,1)+c*s*sigma(2,1)+(c^2-
s^2)*sigma(3,1);'])
end

%%%%%%%%%% Fatigue Life Objective Function %%%%%%%%%%%

for k=1:Nplies

    sigma1_ =eval(['sigma1_' int2str(k)]);
    sigma2_ =eval(['sigma2_' int2str(k)]);
    sigma6_ =eval(['sigma6_' int2str(k)]);

```

```

p = [(5.36523*10^164),...
      (-4.52195*10^166),...
      (1.54928*10^168 - (1.20619*10^161)*sigma1_^2 +
      (2.78841*10^162)*sigma1_*sigma2_ - (6.4461*10^163)*sigma2_^2 -
      (2.2936*10^163)*sigma6_^2),...
      (-2.76382*10^169 + (5.14192*10^162)*sigma1_^2 -
      (1.50772*10^164)*sigma1_*sigma2_ + (4.22303*10^165)*sigma2_^2 +
      (1.38585*10^165)*sigma6_^2),...
      (2.71221*10^170 - (8.18083*10^163)*sigma1_^2 +
      (2.95185*10^165)*sigma1_*sigma2_ - (1.01198*10^167)*sigma2_^2 -
      (2.98998*10^166)*sigma6_^2),...
      (-1.39082*10^171 + (5.75689*10^164)*sigma1_^2 -
      (2.49932*10^166)*sigma1_*sigma2_ + (1.04925*10^168)*sigma2_^2 +
      (2.70865*10^167)*sigma6_^2),...
      2.91706*10^171 - (1.51196*10^165)*sigma1_^2 +
      (7.75665*10^166)*sigma1_*sigma2_ - (3.97931*10^168)*sigma2_^2 -
      (8.7618*10^167)*sigma6_^2];

```

```
logN = roots(p);
```

```

counterreal=1; nfindex=1;
while counterreal<=size(logN,1)
    if isreal(logN(counterreal,1))==1
        Nf(nfindex,1)=logN(counterreal,1);
        nfindex=nfindex+1;
    end
    counterreal=counterreal+1;
end
minNf=min(Nf);

```

```
objfunc(1,k)=minNf;
```

```
end
```

```
f = -min(objfunc);
```

### Code of the optimization run command

```

clc;clear;
delete('fatigueopt.mat','fatigueopt.xlsx','converted.mat','converted.xlsx');

```

```

iteration=101;
counter=1
tic
while counter<iteration

```

```

hybridopts =
psoptimset('UseParallel',true,'SearchMethod',{@GPSPositiveBasis2N},'CompleteSearch',
'on','CompletePoll','on','PollingOrder','Consecutive',...

'InitialMeshSize',1.0,'InitialPenalty',10,'MeshExpansion',2.0,'MeshContraction',0.5,'Max
Iter',100*16);

options =
optimoptions('particleswarm','UseParallel',true,'UseVectorized',false,'ObjectiveLimit',5,'
HybridFcn',{@patternsearch,hybridopts});

[x,fval] = particleswarm(@FTPF_objfunc,2,[-90 -90 -90 -90 -90 -90 -90 -90],[90 90
90 90 90 90 90],options);

ans(counter,:)= [fval x];
counter=counter+1

end
toc
disp('Bitti.')
beep

save('fatigueopt.mat')
filename = 'fatigueopt.xlsx';
xlswrite(filename,ans)

load fatigueopt.mat
b=sortrows(ans,1);
i=1;
j=2;
c=b;
while i<=size(b,1)
    while j<=size(b,2)

        if b(i,j)<-30
            c(i,j)=0;
        else if b(i,j)>=30
            c(i,j)=90;
        else
            c(i,j)=45;
        end
    end
    j=j+1;
end
j=2;
i=i+1;
end
save('converted.mat')
filename = 'converted.xlsx';
xlswrite(filename,c

```

# VITA

## PERSONAL

**Date of Birth** : 21/08/1985  
**Place of Birth** : Turgutlu / Manisa, Turkey

## EDUCATION

**2017** İzmir Institute of Technology, Mechanical Engineering, PhD  
**2011** İzmir Institute of Technology, Mechanical Engineering, MSc  
**2008** Dokuz Eylül University, Mechanical Engineering, BSc

## PUBLICATIONS

### Journal Papers

- Deveci H.A., Aydın L. and Artem H.S., “Buckling optimization of composite laminates using a hybrid algorithm under Puck failure criterion constraint”, *J Reinf Plast Comp* 2016;35:1233-47.
- Deveci H.A., Artem H.S., “Optimum design of fatigue-resistant composite laminates using hybrid algorithm”, *Composite Structures* 2017;168:178-88.
- Deveci H.A., Artem H.S., “On the estimation and optimization capabilities of the fatigue life prediction models in composite laminates” (submitted).

### Selected Conference Papers

- Deveci H.A., Aydın L. and Artem H.S., “Optimum Design for Anti-Buckled Laminated Composites considering Puck Failure Criterion by Genetic Algorithm”, *Proceedings of the 4th International Conference on Mathematical and Computational Applications*, 372-381, June 11 - 13, 2013, Celal Bayar University, Manisa, Turkey.
- Deveci H.A., Artem H.S., “Çevrimsel yüklemeye maruz tabakalı kompozitlerin maksimum yorulma ömrü için optimum tasarımı” *Trc-IFTtoMM Symposium on Theory of Machines and Mechanisms*, Elektronik Bildiriler Kitabı, 31-38, June 14 - 17, 2015, İzmir Institute of Technology, İzmir, Turkey.
- Deveci H.A., Artem H.S., “Optimum Design of Laminated Composites for Maximum Fatigue Life”, *10th International Conference on Composite Science and Technology*, September 2 - 4, 2015, Lisbon, Portugal.
- Deveci H.A., Artem H.S., “On the estimation and optimization capabilities of the fatigue life prediction models in composite laminates”, *3rd International Conference on Mechanics of Composites*, Conference Proceedings, 92-93, July 4 - 7, 2017, University of Bologna, Italy.